ADAPTIVE EQUALISATION OF TELEVISION SYSTEMS

by

Stewart Greer Furmage, B.E.(Hons.)

submitted in partial fulfilment of the requirements

for the degree of

Master of Engineering Science, in the

Faculty of Engineering

UNIVERSITY OF TASMANIA

HOBART

APRIL, 1972

ACKNOWLEDGMENTS

The work contained in this thesis was undertaken in the Department of Electrical Engineering, University of Tasmania. I wish to thank the staff of the above Department for their help and co-operation. I also thank my fellow post-graduate students for their helpful discussions.

In particular I wish to express my sincere appreciation to Mr. G. Thé, my supervisor, for his valuable guidance and encouragement.

S.G. Furmage.

I hereby declare that, except as stated herein, this thesis contains no material which has been accepted for the award of any other degree or diploma in any university, and that, to the best of my knowledge this thesis contains no copy of material previously published or written by another person except where due reference is made in the text of this thesis.

INDEX

INTRODUCTION

The introduction of long transmission paths with time varying characteristics, television relay switching facilities and colour television creates the need for high quality adaptive equalisation of television signals.

The purpose of this thesis is to investigate techniques which may be used to provide such an adaptive equalising facility.

An adaptive equaliser is defined as one which can track a time varying transmission channel characteristic.

A discussion of the adaptive equaliser best suited to the requirements of the television system is presented and a detailed theoretical and practical investigation of this equaliser undertaken. The practical investigation was made possible with the construction of an experimental equalising system.

Chapter 1 briefly discusses the problem of linear distortion within a television channel and the methods used for evaluating the performance of the channel. The concept of equalisation and the advantages of an adaptive equaliser are commented on.

Chapter 2 introduces a number of techniques which may be used for the control of adaptive equalisers. These include the control systems proposed by Lucky [11, 12] and Rudin [13] and a variation of the adaptive echo canceller proposed by Sondhi [16]. The control systems employing correlation techniques are chosen for further investigation. To the author's knowledge the use of correlation techniques for adaptive equalisation within a television network has not been presented in the literature.

A detailed theoretical study of equalisers employing correlation techniques is discussed in chapter 3. This includes an investigation of a simplified model and a digital computer simulation.

To allow a comprehensive investigation into the proposed methods of adaptive equalisation to be carried out, an experimental equaliser was built. The design, analysis and performance of circuits used for this experimental equaliser are described in appendix B. The results obtained from the equaliser are presented in chapter 4.

Chapter 5 discusses the results obtained from the experimental equaliser. Considerations in choosing the optimum adaptive equaliser are also presented. An adaptive equaliser for the television network is then proposed on the basis of results obtained from the investigation presented in this thesis.

CHAPTER 1

THE EQUALISATION OF TELEVISION CHANNELS

1.1 General

When transmitting a television picture a perfect reproduction of this picture is possible only if the received waveform is identical to that transmitted. Any distortion of the waveform will result in deterioration of the ultimate picture. One of the major requirements of a television channel, therefore, is that any waveform distortion introduced by it must lie within acceptable limits.

Distortion which may be introduced by the transmission channel can be classified into two classes -

1. Linear distortion.
2. Non-linear distortion.

This thesis is concerned with linear distortions only. Non-linear effects in the practical system are assumed to be negligible and for the purposes of this investigation the television channel is assumed to be a linear system.

The effect of any distortion on the transmitted waveform must ultimately be judged by the subjective effect on the viewer. The performance of a television channel should therefore be measured in some manner related to the subjective degradation of a picture being transmitted by it.

1.2 Testing the Television Channel

The performance of the majority of communication systems is tested by measuring their frequency response. For distortionless transmission the signal must be transmitted with the same gain and time delay over the frequency band of interest. This implies that the amplitude response must

be flat and the phase response must be linear. In an attempt to maintain such a transmission characteristic a number of nonminimum phase networks are invariably used within a television channel. If such a channel is to be evaluated in the frequency domain both the amplitude and phase responses are required to fully describe the channel.

For a number of reasons this method is unsuitable for testing television channels [1].

1. The sine wave is in no way representative of a typical picture waveform, and therefore time domain evaluation is a more direct measure of channel quality.
2. Measurement of the phase versus frequency characteristic is difficult over the required frequency range.
3. No immediate information on the subjective effect of the distortion is obtained from the results of the frequency response. Thus it is necessary to calculate the waveform response from the measured characteristics. This is a very cumbersome and time consuming process.
4. There is no known method which will transform time domain waveform tolerances into steady state frequency response tolerances. Maintaining an acceptable waveform response cannot, therefore, be done by placing practical tolerances on the frequency response.

Measuring the waveform response of the channel is a simple and effective testing method. Providing the test signals used are representative of a typical picture waveform then the distortion of these signals will give immediate information on the distortion of the picture transmitted by the channel.

The requirements of a test waveform are - [2]

1. It should be representative of commonly recurring parts of a television picture signal.
2. The shape should be simple so that the presence or absence of distortion can readily be observed on an oscilloscope.

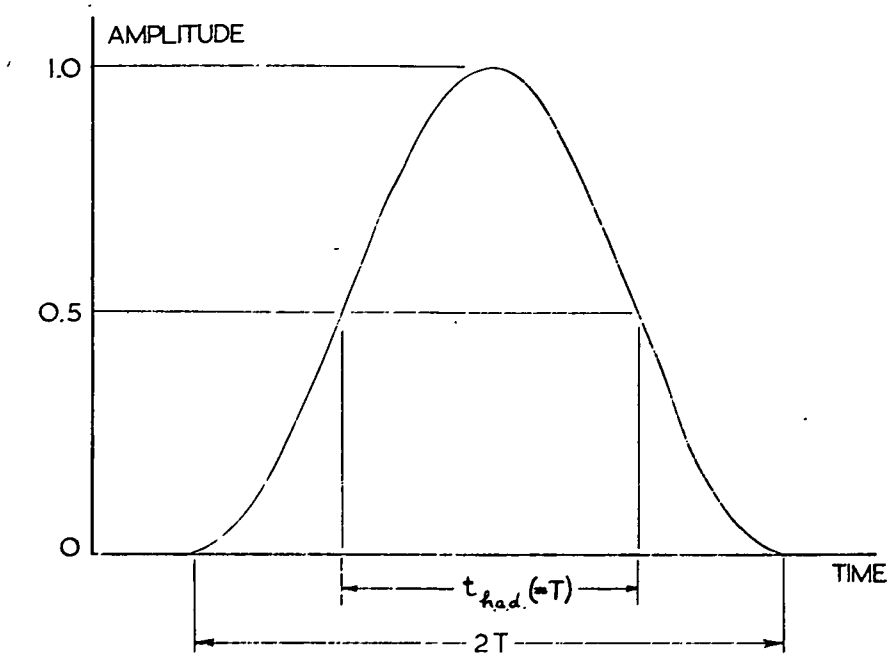

(a) SINE SQUARED PULSE

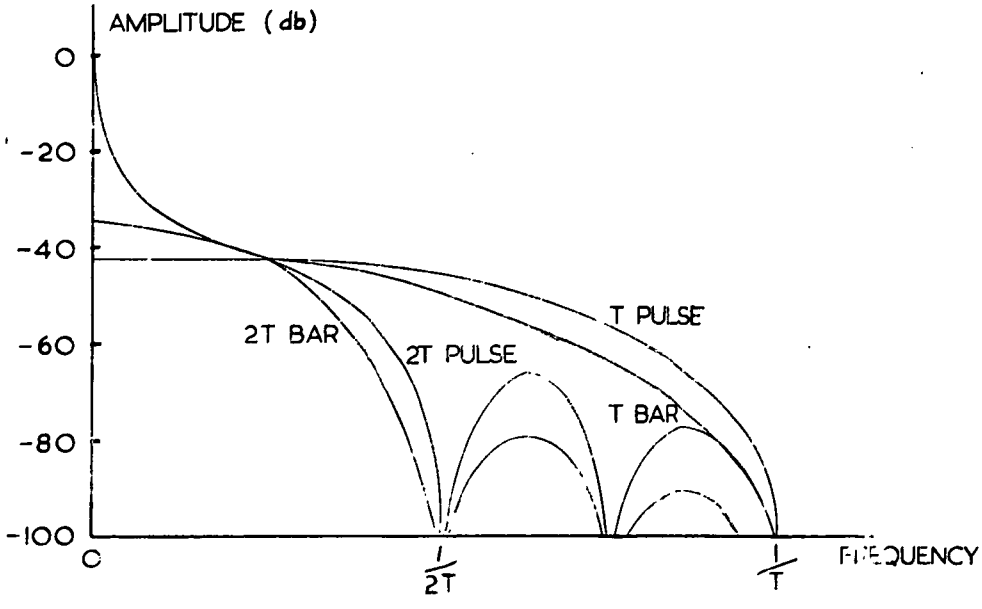

(b) FREQUENCY SPECTRA OF PULSE AND BAR WAVEFORMS

FIG. 1.1

3. The shape should be mathematically simple so that it can be conveniently used for calculations.

4. The spectrum should be confined to the frequency band of interest so that irrelevant information is not obtained from distortions occurring outside this band.

5. It should provide the most sensitive indication of any distortion likely to be encountered in practice so that small amounts of distortion can be detected. This condition can be met by using several waveforms, each sensitive to a particular distortion.

6. The waveform, or an adequate approximation to it, should be capable of being generated in an economical and reproducible manner.

Two waveforms satisfying the above conditions are the sine squared pulse (fig. 1.1(a)) and its time integral known as the "bar" test signal. Approximations of the sine squared pulse and bar pulse are obtained by passing the impulse and step waveforms respectively through a Thomson filter [3]. In practice two sine squared pulses are used, the T pulse and 2T pulse. The T pulse has a half amplitude duration ($t_{h.a.d.}$) of T, where T is the reciprocal of twice the bandwidth of the television channel, and the 2T pulse has a half amplitude duration of 2T.

As shown by fig. 1.1(b), the T pulse has a high energy content at the upper frequency limit of the channel and is therefore sensitive to high frequency distortions. However, it has the drawback of having a large number of frequency components above the band of interest. On the other hand, the spectrum of the 2T pulse falls to zero at the upper limit of the band and therefore it is only sensitive to mid frequency distortions. The bar is used as a low frequency test signal. These waveforms therefore provide a means of testing the complete spectrum of interest for linear distortion.

1.3 Estimating the Channel Performance

To obtain a meaningful result of a performance test a single figure of merit is needed. A rating factor, K, has been defined in order to express the

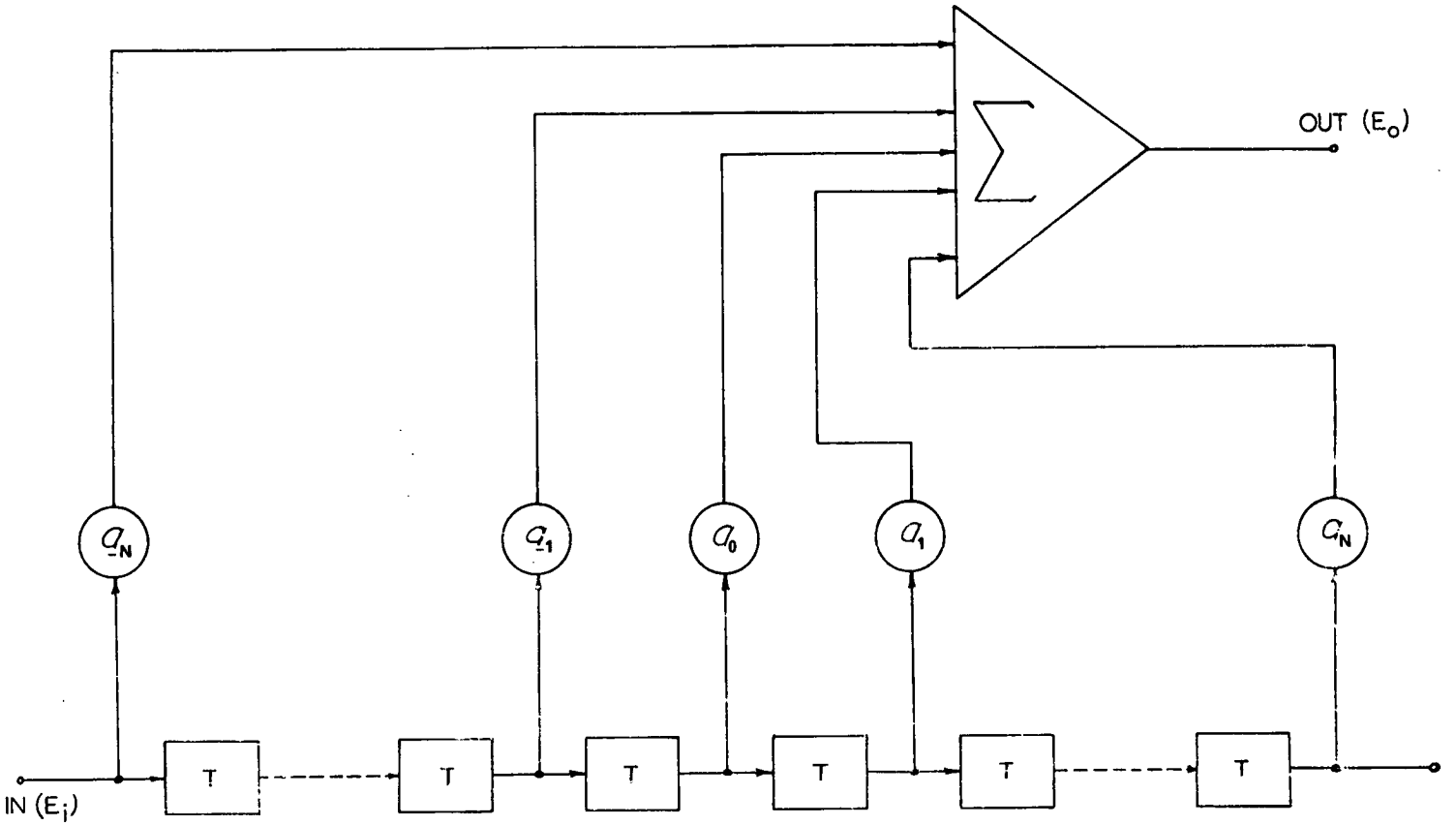

FIG. 1.2 DELAY LINE EQUALISER

subjective severity of the distortion of a picture. This K factor is defined relative to a standard waveform distortion which is a single echo pulse spaced more than 8T from the original pulse. If the distortion of the waveform under test is equally as annoying to an "average" viewer as a standard echo of 1% then the K rating of the distorted waveform is 1%.

The use of pulse and bar test waveforms to determine the K rating of a transmission channel is described in appendix A.

1.4 Equalisation

If the output waveform of a television channel does not meet the required specifications then some form of correction must be applied to the system. For the same reasons leading to the choice of waveform testing of the television channel, it is desirable that equalisation be carried out in the time domain. The purpose of the equaliser within the transmission path is to introduce a linear waveform distortion opposing the distortion produced by the transmission path. Predictable distortions are usually corrected with fixed network equalisers, while time varying and unpredictable distortions require adjustable equalisers.

There are two basic types of adjustable time domain equalisers -

1. The Spectrum Equaliser [4]: Using this equaliser, equalisation is achieved by adding to the channel response successive derivatives with respect to time. This method, mainly because of noise considerations, is not commonly used within television networks.
2. The Delay Line (Transversal) Equaliser [5]: This equaliser is an application of Wheeler's [6] paired echo theory. The signal to be equalised is passed through a multi-tap delay line (fig. 1.2) with an intertap delay of T. The value of T is determined by the Nyquist sampling interval $\frac{1}{2B}$, where B is the bandwidth of the system to be equalised. Equalisation is achieved by adding to the signal a number of its echoes. Both pre-echoes and post-echoes are obtained by tapping the main signal towards the centre of the delay line. The frequency response of the equaliser, neglecting the

constant delay caused by tapping the main signal towards the centre of the delay line, is given by:-

$$\frac{E_o(j\omega)}{E_i(j\omega)} = \sum_{n=-N}^{N} a_n \exp(-jn\omega T) \qquad 1.1$$

If $a_n << a_o$ for $n \neq o$ then the amplitude response of the delay line equaliser may be approximated by:-

$$\left|\frac{E_o(j\omega)}{E_i(j\omega)}\right| \simeq a_o + \sum_{n=1}^{N} (a_n + a_{-n}) \cos n\omega T \qquad 1.2$$

and the phase response may be approximated by:-

$$\arg\left(\frac{E_o(j\omega)}{E_i(j\omega)}\right) \simeq \sum_{n=1}^{N} (a_{-n} - a_n) \sin n\omega T \qquad 1.3$$

Equation 1.1 indicates that the equaliser can be adjusted to approximate any desired linear transfer function. The accuracy of the approximation will depend on the number of taps used. Equations 1.2 and 1.3 show that echoes with an even symmetry about the main signal affect only the amplitude response and echoes with an odd symmetry affect only the phase response of the equaliser.

1.5 Conclusions

Any linear distortions within the transmission channel are readily corrected with a delay line equaliser when transmitting monochrome television signals over relatively short distances. With the introduction of more complex systems, such as longer transmission paths, relay switching facilities and colour television, the problem of equalisation will become much more pronounced.

For the improved equalisation required with the introduction of these systems, manual equalisers have a number of inherent disadvantages.

1. Due to the large number of taps used, adjusting the equaliser is a time consuming process.
2. If accurate equalisation is to be maintained frequent adjustments will be required.
3. Whenever the transmission path is altered the equaliser must be re-adjusted.
4. A break in transmission may be required while the equaliser is adjusted. This can be overcome by transmitting the test signal during the vertical blanking interval (vertical interval testing [7, 8]). Extreme care must be exercised while adjusting the equaliser however, to avoid introducing further distortion.

The introduction of some form of adaptive equalisation would overcome these problems. Such a system would also be very useful for existing monochrome channels which already experience difficult equalisation problems.

CHAPTER 2

ADAPTIVE EQUALISATION

2.1 General

Adaptive equalisation requires the automatic control of an adjustable equaliser's tap settings. Major points to be considered in the design of an adaptive equaliser are -

1. The choice of the adjustable equaliser to be used.
2. The technique required to automatically control the adjustment of the equaliser's tap settings.

2.2 Requirements of an Adaptive Equaliser

An adaptive equaliser used within the television network should satisfy the following requirements -

1. The equalisation of a distorted channel must be accurate. This implies that for any distortion which is likely to be met in practice the K rating after equalisation must be less than 5%.
2. It is desirable that a relatively short settling time be achieved. This will allow picture transmission immediately after the connection or alteration of the transmission path with the viewer unaware of any distortion present.
3. To provide an adaptive facility, with the correction of all time varying linear distortions the control of the equaliser must be continuous. This must be achieved without affecting the programme during programme transmission.
4. The accuracy of the equaliser should not be impaired by noise within the transmission channel. However, this is not expected to be a significant factor as the S/N performance objectives of the Australian television network are very stringent (52 db for continuous random noise and 25 db for impulsive noise [7]).

5. The adaptive equaliser must be economically realisable.

2.3 The Orthogonal Transfer Function Generator

To ensure a maximum rate of convergence the adjustable equaliser must be a variable transfer function generator with no interaction between the adjustable parameters. This is the property of the orthogonal variable transfer function generator [9, 10].

Consider a variable transfer function generator consisting of a linear combination of the linearly independent transfer functions $F_1(s)$, $F_2(s)$, ..., $F_N(s)$ such that the resultant transfer function is given by -

$$F(s) = \sum_{n=1}^{N} a_n F_n(s) \qquad 2.1$$

where the a_n are the adjustable parameters. The required condition for orthogonality, in the frequency domain, is -

$$\frac{1}{2\pi} \int_{-\infty}^{\infty} F_n(j\omega)\, \Phi_{ww}(\omega)\, d\omega = \begin{cases} \text{constant} & n = m \\ 0 & n \neq m \end{cases} \qquad 2.2$$

where $\Phi_{ww}(\omega)$ is the power spectral density of the input signal and the bar indicates the complex conjugate of the function over which it is placed.

The condition for orthogonality in the time domain is -

$$\int_{0}^{\infty} x_n(t)\, \overline{x_m(t)}\, dt = \begin{cases} \text{constant} & n = m \\ 0 & n \neq m \end{cases} \qquad 2.3$$

where $x_n(t)$ and $x_m(t)$ are the signal outputs of the functions $F_n(j\omega)$ and $F_m(j\omega)$ respectively.

From equation 2.2 it can be seen that the orthogonal property is dependent on the spectral density of the input signal. In the case of the

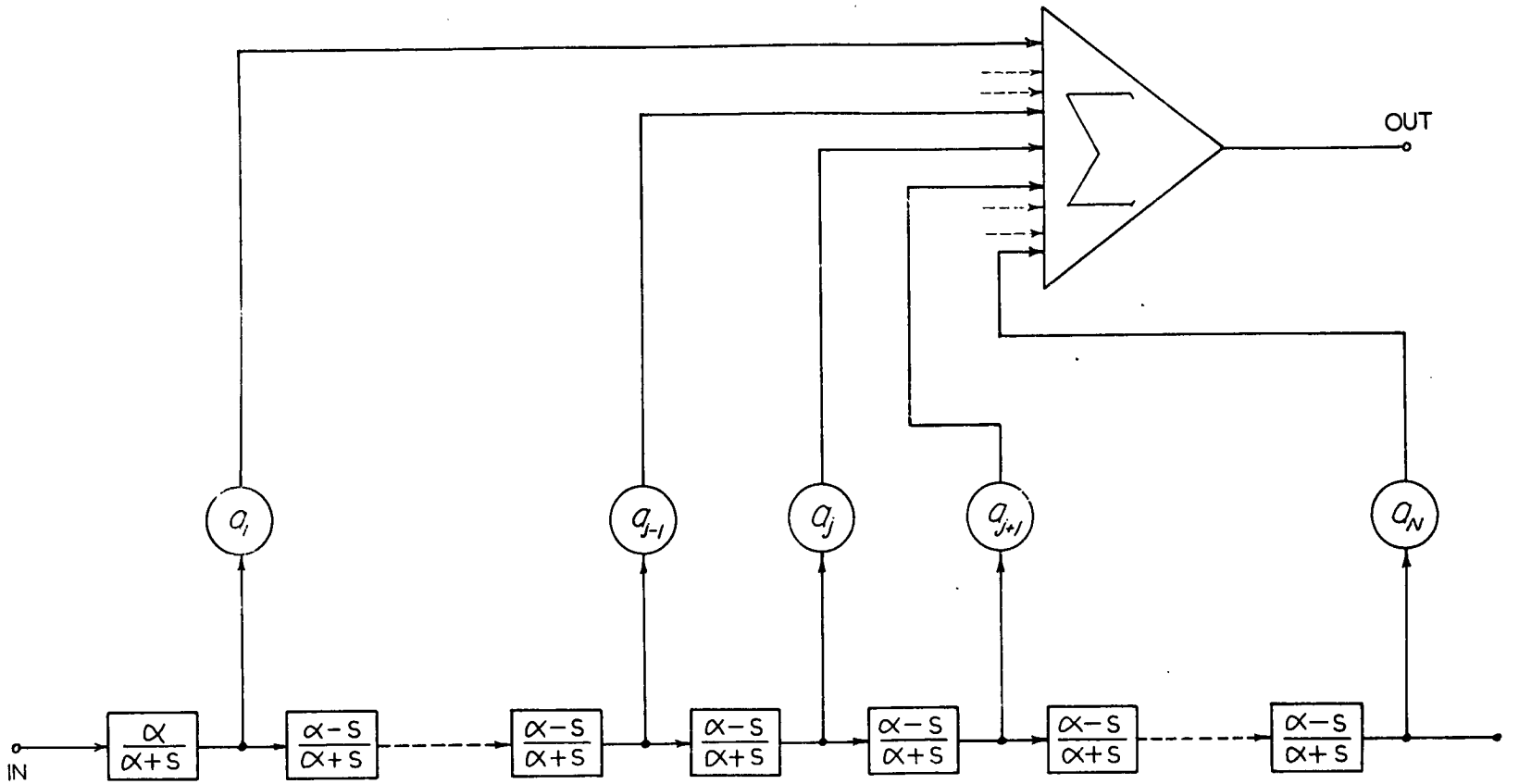

FIG 2.1 ADJUSTABLE EQUALISER USING LAGUERRE FUNCTIONS

delay line, the transfer function for the nth delay is given by -

$$F_n(j\omega) = \exp(-nj\omega T) \qquad 2.4$$

The required conditions for the delay line to be orthogonal are therefore -

$$\frac{1}{2\pi}\int_{-\infty}^{\infty} \exp((m-n)j\omega T)\, \Phi_{ww}(\omega)\, d\omega = 0 \quad \text{for } m \neq n \qquad 2.5$$

$$\frac{1}{2\pi}\int_{-\infty}^{\infty} \Phi_{ww}(\omega)\, d\omega = \text{constant} \quad \text{for } m = n \qquad 2.6$$

Equations 2.5 and 2.6 are satisfied by $\Phi_{ww}(\omega)$ equal to a constant value for all frequencies up to $\frac{1}{2T}$ Hz and zero for all frequencies beyond.

There are also a number of orthogonal systems [9] which could be used in place of the delay line. The most common of these is the set of Laguerre's orthogonal functions. These functions are synthesised with the set of transfer functions -

$$F_n(s) = \frac{\alpha}{s+\alpha}\left(\frac{s-\alpha}{s+\alpha}\right)^n \qquad 2.7$$

where α is a constant. Except at the input, the variable transfer function generator using these functions is similar to the delay line but with each delay replaced by the transfer function $\frac{s-\alpha}{s+\alpha}$ (fig. 2.1).

The condition for orthogonality for this particular system is that $\Phi_{ww}(\omega)$ is a constant. The input signal must therefore be white noise if the orthogonal property is to be retained.

The main advantage of using Laguerre's orthogonal system in preference to the delay line is the simpler circuitry required. For the delay line a more complex transfer function must be realised to provide an adequate

approximation of the delay over the frequency range of interest. The transfer functions $\frac{\alpha}{s+\alpha}$ and $\frac{s-\alpha}{s+\alpha}$ required for the synthesis of the Laguerre functions however, can be realised exactly by a simple RC ladder network and an LC lattice network respectively.

2.4 Basic Principles of Automatic Equalisation

A number of different methods for implementing automatic equalisation have been investigated in the past, most of which are variations of the equalisation principles as described by Lucky [11, 12] and Rudin [13]. The general technique adopted by them involves transmitting a reference signal through the transmission channel plus the equaliser and comparing the received waveform with a locally generated reference or ideal signal. The error between these two waveforms is used to control the adjustable equaliser by means of a steepest descent convergence criterion.

One of two basic criteria may be adopted -

1. Minimisation of the absolute value of the error.

2. Minimisation of the mean square value of the error.

2.4.1 Absolute Error Equalisation

This technique was formulated by Lucky [11] for the particular application of equalising telephone channels for data transmission. The method uses a delay line equaliser and requires a pulse to be transmitted through the distorted channel. The received pulse, after passing through the equaliser is then sampled at discrete time intervals, each interval separated by the Nyquist sampling period T. The values obtained, $h_{-N} \ldots\ldots\ldots h_N$, are then compared with the equivalent values, $g_{-N} \ldots\ldots\ldots g_N$, of the locally generated ideal pulse response. The values h_o and g_o are the values of the equalised and reference pulses at their time origin.

The distortion of the output of the equaliser is defined by

$$D_A = \frac{1}{g_o} \sum_{n=-N}^{N} \left| h_n - g_n \right| \qquad 2.8$$

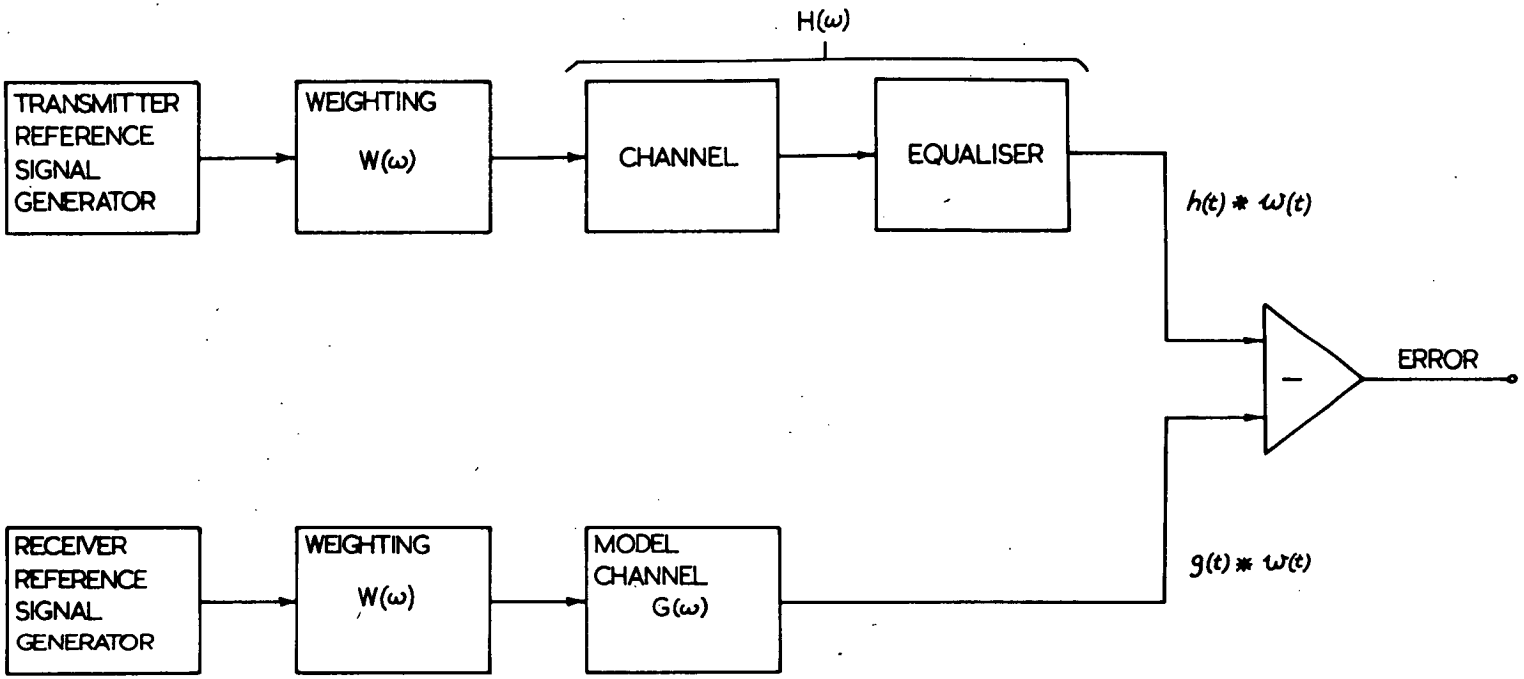

FIG. 2.2 MEAN SQUARE EQUALISATION

Lucky has shown that when using a delay line equaliser with the tap spacing equal to the sampling interval, then:-

$$\frac{\partial D_A}{\partial a_j} = \text{sgn}\ (h_j - g_j) \qquad 2.9$$

where a_j is the value of the j^{th} tap of the delay line and

$$\text{sgn}\ (h_j - g_j) = \begin{cases} +1 & h_j - g_j > 0 \\ -1 & h_j - g_j < 0 \end{cases}$$

Minimisation of the distortion is obtained by forcing the values of these partial derivatives to zero. The implementation of this steepest descent algorithm consists of measuring the sign of the error at each of the sampling instants then incrementing the appropriate tap gains in the opposite direction to the measured sign values. Convergence is assured providing the initial value of D_A is less than one. As only residual distortions are corrected by the equaliser this is not a severe limitation.

2.4.2 Mean Square Error Equalisation

Lucky and Rudin [14] proposed a model adaptive scheme using the delay line equaliser and a mean square error convergence criterion. This criterion was the minimisation of the distortion, defined by -

$$D^1_{MS} = \int_{-\infty}^{\infty} |H(\omega) - G(\omega)|^2\, d\omega \qquad 2.10$$

where $H(\omega)$ is the equalised channel response and $G(\omega)$ the ideal or model channel response (fig. 2.2). This was generalised by adding a frequency weighting function to take into account the relative importance of errors at different frequencies:-

$$D_{MS} = \int_{-\infty}^{\infty} |H(\omega) - G(\omega)|^2\, |W(\omega)|^2\, d\omega \qquad 2.11$$

where $|W(\omega)|^2$ is a non-negative spectral weighting function. Parseval's

theorem is used to obtain the equivalent form of 2.11 in the time domain.

$$D_{MS} = \int_{-\infty}^{\infty} \{(h(t) - g(t)) * w(t)\}^2 \, d(t) \qquad 2.12$$

where h(t), g(t) and w(t) are the impulse responses of the frequency functions H(ω), G(ω) and W(ω) respectively. The symbol * is used to represent the convolution operation. As

$$h(t) = \sum_{n=-N}^{N} a_n \, h_u(t - nT) \qquad 2.13$$

where $h_u(t)$ is the impulse response of the unequalised channel then,

$$D_{MS} = \int_{-\infty}^{\infty} \{ \sum_{n=-N}^{N} a_n \, h_u(t - nT)*w(t) - g(t)*w(t)\}^2 \, dt \qquad 2.14$$

Using the same method described by Lucky [11] it can easily be shown that D_{MS} is a convex function of the tap gains a_n. Thus, there is a single minimum of D_{MS} which occurs when all 2N + 1 derivatives $\frac{\partial D_{MS}}{\partial a_n}$ are zero.

The partial derivative of D_{MS} with respect to a particular tap setting is given by:-

$$\frac{\partial D_{MS}}{\partial a_j} = 2 \int_{-\infty}^{\infty} \{h(t)*w(t) - g(t)*w(t)\}\{h_u(t - jT)*w(t)\}dt \qquad 2.15$$

These equations indicate that the partial derivative of D_{MS} with respect to a particular tap setting is given by the cross-correlation of the error and the output of that tap.

The equation 2.15 contains all the information required for automatic equalisation. Setting all the partial derivatives to zero gives 2N + 1 simultaneous linear equations which can be solved to obtain the equaliser

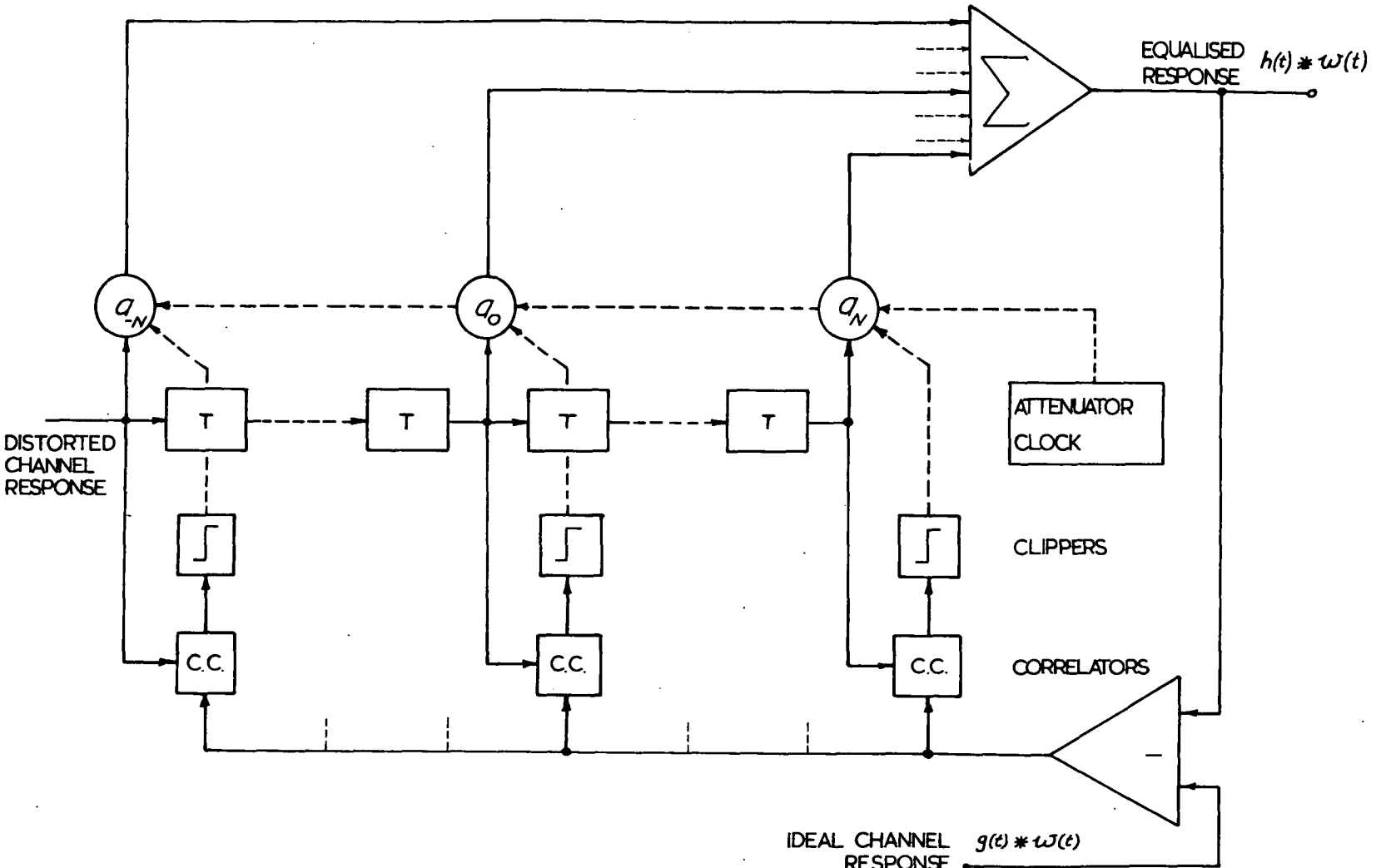

FIG. 2.3 BLOCK DIAGRAM OF AUTOMATIC EQUALISER (LUCKY AND RUDIN)

tap settings required to minimise D_{MS}. On the other hand D_{MS} may be minimised by choosing initial values of a_n then calculating the partial derivatives to indicate the direction in which the coefficients must be adjusted. This is the algorithm for automatic equalisation under the mean square error criterion.

The proposal by Lucky and Rudin (fig. 2.3) for the implementation of this algorithm utilised variable attenuators adjustable in discrete steps of equal magnitude for the tap settings. The polarities of all the cross-correlations were periodically measured and the corresponding taps incremented one step in the opposite direction to the values obtained. The time interval between the measurement of the correlation polarities allowed steady state values to be reached thus avoiding incorrect adjustments due to the transients obtained when the tap settings were altered.

To shorten the settling time of the equaliser the period between tap adjustments was made relatively short during the initial part of the convergence to allow the tap settings to rapidly reach their approximate values. The period was then increased to allow the settings to move slowly to their accurate values.

The steady state output of the j^{th} cross-correlator (fig. 2.3) is given by equation 2.15. Thus any interaction between the j^{th} tap and any of the other taps is given by the following partial derivative -

$$\frac{\partial\left(\frac{\partial D_{MS}}{\partial a_j}\right)}{\partial a_k} = 2 \int_{-\infty}^{\infty} \{h_u(t - kT)*w(t)\}\{h_u(t - jT)*w(t)\}\, dt \qquad \text{for } k \neq j \qquad 2.16$$

Hence the output of the j^{th} cross-correlator is linearly proportional to all the a_k's with the constants of proportionality the cross-correlations between the corresponding outputs of the delay line. This result is to be expected as the right hand side of equation 2.16 is consistent with the algebraic expression used for the definition of the orthogonal property (equation 2.3).

So far the operation of the equaliser with an ideal noiseless distortion channel has been considered. Under this condition the actual steady state signal output of the j^{th} cross-correlator is proportional to ϕ_j where -

$$\phi_j = \left\langle \left(\sum_{n=-N}^{N} a_n x_n(t) - y(t) \right)(x_j(t)) \right\rangle \qquad 2.17$$

where $x_n(t)$ is the output signal of the n^{th} tap and $y(t)$ is the reference signal. The brackets $\langle\ \rangle$ denote a time average. If noise $\eta(t)$, a sample from a stationary random process, is introduced into the channel then the equalised signal is given by -

$$z_n(t) = \sum_{n=-N}^{N} a_n \left(x_n(t) + \eta_n(t)\right) \qquad 2.18$$

where $\eta_n(t)$ is the noise component of the output signal from the n^{th} tap. The output of the j^{th} correlator under noise conditions is then proportional to $\phi_{\eta j}$ where -

$$\phi_{\eta j} = \left\langle \left(\sum_{n=-N}^{N} a_n \left(x_n(t) + \eta_n(t)\right) - y(t) \right)\left(x_j(t) + \eta_j(t)\right) \right\rangle \qquad 2.19$$

Assuming that the noise will be uncorrelated with either the transmitted or the reference signals then -

$$\phi_{\eta j} = \left\langle \left(\sum_{n=-N}^{N} a_n x_n(t) - y(t) \right)(x_j(t)) + \sum_{n=-N}^{N} a_n \eta_n(t) \eta_j(t) \right\rangle \qquad 2.20$$

Comparing this equation with equation 2.17 it can be seen that any noise introduced by the transmission channel will reduce the accuracy of the equalisation of the television signal.

Consideration of the mean square error criterion has so far been confined to the delay line equaliser. This is not the only possibility however, as a more general equaliser using a variable transfer function generator defined by equation 2.1

$$F(s) = \sum_{n=1}^{N} a_n F_n(s)$$

may be employed with the same automatic control system as shown in fig. 2.3.

For such an equaliser equation 2.15 becomes -

$$\frac{\partial D_{MS}}{\partial a_j} = 2 \int_{-\infty}^{\infty} \{h(t)*w(t) - g(t)*w(t)\}\{h_j(t)*w(t)\}dt \qquad 2.21$$

where $h_j(t)$ is the impulse response of the unequalised channel cascaded with $F_j(s)$ and the equalised channel impulse response h(t) is now given by

$$h(t) = \sum_{n=1}^{N} a_n h_n(t) \qquad 2.22$$

If the transfer functions $F_1(s)$, ... $F_N(s)$ are chosen with network responses orthogonal to each other, equation 2.21 reduces to -

$$\frac{\partial D_{MS}}{\partial a_j} = 2 \int_{-\infty}^{\infty} \{a_j h_j(t)*w(t) - g(t)*w(t)\}\{h_j(t)*w(t)\}dt \qquad 2.23$$

Equating this set to zero to obtain the minimum value of D_{MS} with respect to the a_j, then -

$$a_j = \frac{\int_{-\infty}^{\infty} \{g(t)*w(t)\}\{h_j(t)*w(t)\}dt}{\int_{-\infty}^{\infty} \{h_j(t)*w(t)\}\{h_j(t)*w(t)\}dt} \qquad 2.24$$

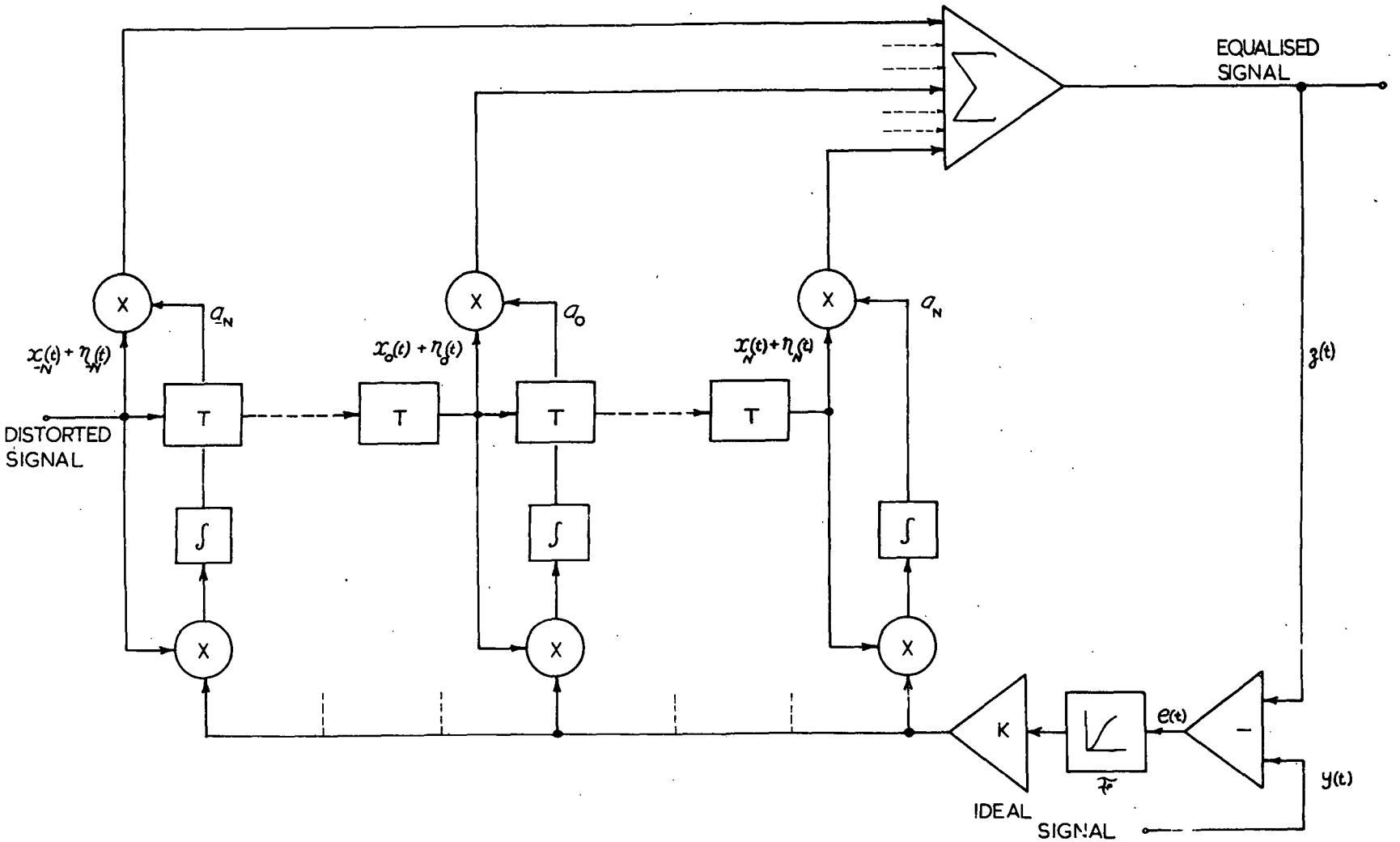

FIG. 2.4 BLOCK DIAGRAM OF AUTOMATIC EQUALISER (SONDHI)

The value of each a_j is then given by the cross-correlation of the reference signal and the output of $F_j(s)$ divided by the auto-correlation of the output of $F_j(s)$.

This technique is identical to the techniques described by Lubbock [15] and Kitamori [10] for self optimising control systems.

Implementation of the control algorithm based on equation 2.24 requires two correlators and a dividing circuit for each tap if all the tap settings are required simultaneously. If each tap setting can be obtained separately then only two correlators and one dividing circuit are required for the complete system.

Unfortunately this control algorithm is not a practical proposition as the orthogonality of the set of functions $F_1(s) \ldots\ldots F_N(s)$ cannot be guaranteed. An orthogonal set of functions can be obtained from a set of linearly independent functions [10] provided the input frequency spectrum is known. However, for television systems the frequency spectrum of the input signal is dependent on the amplitude response of the distorting channel and this is unknown, *a priori*.

Another scheme which may be employed for automatic equalisation which is basically different to Lucky and Rudin's but has a very similar control algorithm is a variation of the adaptive echo canceller described by Sondhi [16]. The basic difference between the two schemes is that the control system employed by Sondhi is not based on a mean square error criterion. The block diagram of this system using a delay line equaliser is shown in fig. 2.4.

The proof of convergence is presented in the following analysis.

If the output of the j^{th} tap is denoted by $x_j(t) + \eta_j(t)$ where $\eta_j(t)$ is the component due to noise within the transmission channel and $x_j(t)$ the signal component then -

$$z(t) = \sum_{j=-N}^{N} a_j(t)(x_j(t) + \eta_j(t)) \qquad 2.25$$

is the equalised signal output. In matrix notation -

$$z(t) = A^T(X + N) \qquad 2.26$$

where A, X etc. refer to vectors which are considered as column matrices with elements $a_{-N}(t)$ .... $a_N(t)$ and $x_{-N}(t)$ .... $x_N(t)$ respectively. The superscript T denotes the transpose of the matrix.

Using Wheelers [6] paired echo theory it may be shown that the ideal signal, y(t), can be assumed to contain echoes of the distorted signal. Thus y(t) is a linear function of the outputs of the delay line -

$$y(t) = L^T X \qquad 2.27$$

where L has elements l_{-N} .... l_N which are assumed fixed (or so slowly varying that their time derivatives may be neglected). Thus,

$$e(t) = y(t) - z(t) \qquad 2.28$$

$$= R^T X - A^T N \qquad 2.29$$

where R = L - A.

Sondhi considers a function C(e) such that C(e) = C(-e) and

$\frac{d^2C(e)}{de^2} \geq 0$. C(e) is therefore a monotonic non-decreasing function of the magnitude of e. The criterion for equalisation is the minimisation of the value of C(e) by varying the coefficients a_j in the opposite direction to its gradient. Now,

$$\text{grad } C(e) = \text{grad } C(A^T X - A^T N)$$

$$= -\mathcal{F}(R^T X - A^T N)(X + N) \qquad 2.30$$

where $\mathcal{F}(.)$ is the derivative of C(.) with respect to its argument. To change A along the negative of the gradient put -

$$\frac{dA}{dt} = K\mathcal{F}(R^T X - A^T N)(X + N) \qquad 2.31$$

where K is a positive constant. Equation 2.31 is the equation that governs the dynamic behaviour of the system shown in fig. 2.4. This system is then a steepest descent control system for the minimisation of C(e).

As R = L - A and L is assumed constant then -

$$\frac{dA}{dt} = -\frac{dR}{dt} \qquad 2.32$$

Thus

$$\frac{dR^T R}{dt} = 2R^T \frac{dR}{dt}$$

$$= -2\, KR^T(X + N)\, \mathcal{F}(R^T X - A^T N) \qquad 2.33$$

For the noiseless case

$$\frac{dR^T R}{dt} = -2\, KR^T X\, \mathcal{F}(R^T X) \qquad 2.34$$

By its definition $\mathcal{F}$ is a monotonic non-decreasing odd function. Thus, the right hand side of equation 2.34 is always negative, hence $R^T R$ the square of the length of the vector R = L - A is non increasing. The system must, therefore, converge with time.

The right hand side of equation 2.33 is negative if and only if $R^T(X + N)$ has the same sign as $R^T X - A^T N$. The convergence of the equaliser is then adversely affected by the presence of a noise component on the received signal. However, providing the noise level is low compared to the received signal then the right hand side of equation 2.33 will be negative for a large percentage of the time and hence convergence will be essentially monotonic as before.

Sondhi considers two different functions for $\mathcal{F}$. These are a linear function $\mathcal{F}(e) = e$ and a nonlinear function $\mathcal{F}(e) = \mathrm{sgn}(e)$. Sondhi found that the use of the nonlinearity led to simplified circuitry and improved convergence properties. The simpler circuitry is obtained as the correlation

multipliers can be replaced with switched modulators. An infinite clipper is used to provide the function $\mathcal{F}(e) = \text{sgn}(e)$.

Although only a delay line equaliser has been considered for this automatic equalising scheme this fact has not been important in the proof of convergence. The only requirement has been that the vector X be derived from all $x_j(t)$ in such a way that the ideal signal may be represented by $L^T X$ with a suitable choice of L. Thus, the circuit of fig. 2.4 may be generalised by replacing the delay line with a general variable transfer function generator.

The similarity between the two automatic equalising techniques discussed so far is evident in figs. 2.3 and 2.4. For $\mathcal{F}(e) = e$ the difference between the two equalisers lies in the method used for adjusting the tap coefficients. Both techniques may also be employed with general variable transfer function generators replacing the delay lines.

With $\mathcal{F}(e) = \text{sgn}(e)$ the basic control of the two equalisers differs. Under this condition the equaliser indicated in fig. 2.4 does not minimise the mean square value of the error.

2.5 The Application of the Proposed Techniques Within the T.V. Network

2.5.1 Method of Operation Within the T.V. Network

The proposed methods of automatic equalisation require a test signal to be transmitted through the distorted channel. To provide an adaptive facility the signal must be transmitted continuously and without affecting the picture information being transmitted. Part of the video signal consists of 18 to 22 horizontal lines during the vertical blanking interval which do not contain any picture information. Thus, it is possible to provide an adaptive operation by inserting the test signals within these horizontal lines.

The automatic adjustment of the equalisers must, therefore, be a gated operation with the control circuitry operational only during the intervals in which the test signals are received.

2.5.2 Absolute Error Equalisation

This criterion has already been used by Arnon [17] for the equalisation of television channels. For his particular system, Arnon uses a band limited 109 nanosecond rectangular pulse as the test waveform which is sampled at 9.2 MHz at the receiver. The errors between the sampled response and stored values of the ideal response are then used to increment wide-band digitally controlled attenuators.

Initial tests of the operation of this equaliser proved very successful with the equalisation of some very large initial distortions.

One disadvantage of this system is the accuracy required of the sampling circuits. The incoming pulse must be sampled accurately and within very stringent timing tolerances because of the high frequencies present.

Another disadvantage is the need for a near perfect delay line. As the absolute error criterion is based on the use of a perfect delay line any approximations made in the realisation of the delay line will result in errors in the equalised waveform.

2.5.3 Mean Square Error Equalisation

The advantage of the mean square error criterion over the absolute error criterion is that it may be employed with any variable equaliser realised with linearly independent functions $F_1(s)$ .... $F_N(s)$. Such an equaliser, by virtue of this property, will automatically adjust the tap settings to correct for any approximations in the realisation of the functions $F_1(s)$ .... $F_N(s)$.

The main disadvantage of this criterion and the reason why it was not adopted by Arnon is the need for correlators, and hence analogue multipliers, which must have a bandwidth of operation compatible with the bandwidth of the television channel.

With the rapid advances in the technological field over the past few years, it appears that the technical problems associated with analogue multipliers are gradually being solved [18, 19, 20]. The analogue multiplier designed by Morton, [20] for example, is capable of operating at video

frequencies to an accuracy of 1%. Also at the time of writing this thesis, a number of integrated circuit analogue multipliers have become commercially available. However, these, as yet, do not have the bandwidth required for video operation.

The correlation multipliers can be replaced with switched modulators thereby simplifying the circuitry required.

2.6 Discussion

The use of the absolute error criterion for equalisation has been extensively covered in the literature. This has been the result of a great deal of research into the use of voice frequency channels for data transmission. This criterion has also been used for the equalisation of television channels.

To the author's knowledge, the use of correlation techniques has not, as yet, been applied to the equalisation of video waveforms. However, the potential of an adaptive equaliser employing these techniques appears to be very good. The automatic equalisers discussed in section 2.4.2 are therefore selected for further investigation.

CHAPTER 3

INVESTIGATION OF THE PROPOSED METHOD OF EQUALISATION

3.1 General

Of the various techniques indicated in section 2.4.2 for implementing an automatic equaliser the technique most suited to the television system must be chosen. This choice must be a compromise between the accuracy of the equalisation, settling time and the economic realisation of the different techniques.

Some points to be considered are:-

1. The type of test signal.
2. The optimum spectral weighting function and model channel filter for the television system.
3. The adjustable equaliser.
4. The automatic control system.

A discussion of these points is presented in this chapter.

3.2 The Test Signal

An ideal test signal used with the proposed method of equalisation should have the following properties:-

1. A flat frequency spectrum up to at least 5 MHz.
2. It must be possible to generate an accurate reproduction of the transmitted waveform at the receiver.
3. It should be a repetitive waveform with no statistical variance so that the correlations may be performed in a finite time.
4. It must be able to be generated simply and economically.

3.2.1 The Sine Squared Pulse

The sine squared pulse would be adequate as a test signal for adaptive television equalisation [21]. However such a signal is unsatisfactory when using an analogue correlation circuit as described in chapter 2. The short duration of the pulse prevents accurate cross-correlation values being obtained using analogue techniques. This may be overcome by sampling both the received and reference waveforms and calculating the cross-correlation values using digital techniques [22]. The cross-correlation value of the j^{th} tap, ϕ_{Dj}, is then given by -

$$\phi_{Dj} = \sum_{n} e_n x_{n-j} \qquad 3.1$$

This method is unsatisfactory, however, because the maximum switching frequencies of modern digital components are not high enough to allow sufficiently accurate sampling of the waveforms at the required sampling frequency (at least 10 MHz).

3.2.2 Pseudo Random Noise

One signal satisfying most of the ideal test signal requirements is pseudo random noise. Pseudo random noise has an energy density spectrum and probability density function similar to that of noise, but has the advantage that it is periodic and reproducible.

Pseudo random noise is generated by filtering a maximal length binary sequence [23], which is generated by a shift register with appropriate feedback. The feedback is obtained by connecting the outputs of two of the flip flops in the shift register to an exclusive or gate, the output of which is then fed to the input of the shift register. The choice of which two flip flops should be used is important to obtain a maximal length sequence. A ten stage shift register with appropriate feedback is shown in fig. B.1 in appendix B.

The length of a maximal length binary sequence is 2^N-1 bits, where N is the number of flip flops in the shift register. The odd number of bits is

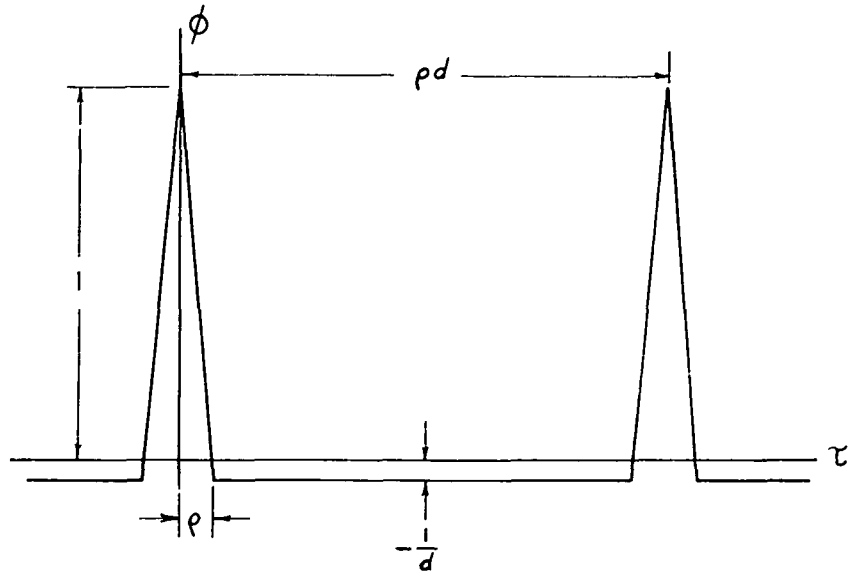

(a) AUTOCORRELATION FUNCTION

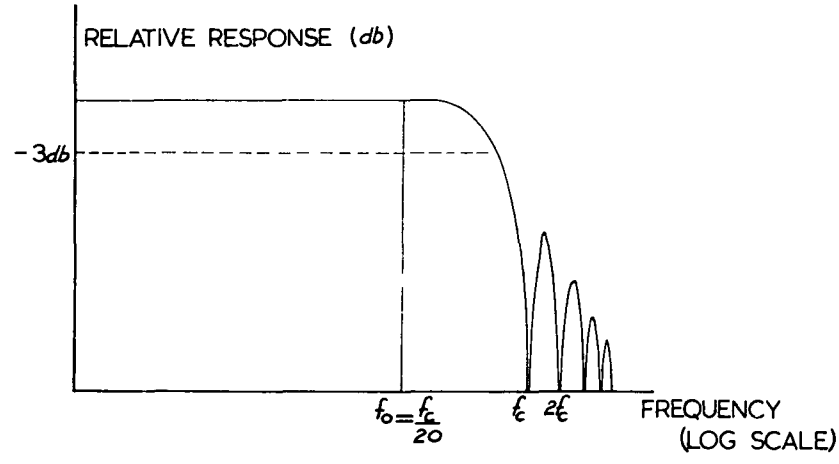

(b) FREQUENCY SPECTRUM

FIG. 3.1 PSEUDO RANDOM NOISE CHARACTERISTICS

produced because the state of all flip flop outputs at zero is forbidden. In this state the output of the exclusive or gate is always zero and the generator will therefore remain in this state.

The auto-correlation function of the maximal length binary sequence, for the output of the generator switching between +1 and -1, is shown in fig. 3.1(a). It is a triangular function, two clock periods in width and repeating itself every 2^N-1 clock periods. The small d.c. value is due to the odd number of bits in the sequence.

The spectral density function of the sequence, obtained by the fourier transform of the autocorrelation function is given by:-

$$\Phi(\omega) = \frac{1}{d^2}\,\delta(\omega-0) + \sum_{\substack{n=-\infty \\ \neq 0}}^{\infty} \frac{1+d}{d^2}\left[\frac{\sin\frac{(n\omega\rho)}{2}}{\frac{n\omega\rho}{2}}\right]\delta(\omega - n\omega_p) \qquad 3.2$$

where $d = 2^N-1$, ρ is the clock period, $\omega_p = \frac{2\pi}{\rho d}$ and $\delta(\omega) = \begin{cases} 1 & \omega = 0 \\ 0 & \omega \neq 0 \end{cases}$

The spectrum is discrete at multiples of ω_p with a normalised envelope defined by -

$$\left[\frac{\sin\left(\frac{n\omega\rho}{2}\right)}{\frac{n\omega\rho}{2}}\right]$$

This is shown in fig. 3.1(b). The bandwidth of the signal is 0.443 times the clock frequency, thus by suitable filtering the spectrum of the test signal can be made flat over the band of interest.

When designing a pseudo random noise generator suitable for a television channel there are three variables, therefore, which must be considered.

1. The length of the shift register. The value of N affects the repetition period of the noise and hence the separation of the discrete spectral elements, but does not affect the shape of

the envelope. An improved signal is obtained for a larger value of N because of the increase in the number of spectral lines within the passband. The value chosen must obviously be a compromise determined by the time interval available within the television signal for the insertion of this test signal.

2. The bandwidth of the filtered pseudo random noise. For the Australian television network the bandwidth of the test signal must be at least 5 MHz. The bandwidth may be increased beyond this value for the reasons discussed in section 5.4.

3. The frequency of the generator clock. The frequency of the clock is usually chosen to be twenty times greater than the bnadwidth required. This achieves the closest approximation to a signal with a Gaussian distribution for a given value of N. The clock frequency of the generator should, under this criterion, be 100 MHz.

   The operation of the generator at 100 MHz conflicts with requirement 4 of the ideal test signal. As a result, it may be necessary to use a lower frequency. A shift register which will operate at this frequency is technically feasible however, as some flop flops are capable of switching at even greater frequencies. The exclusive or operation at this frequency is also possible as logic gates with propagation delays of less than two nanoseconds are available.

   Thus, a pseudo random noise generator can be constructed to operate at 100 MHz. Careful design will be required to eliminate such problems as transport delay and impulse noise, thereby ensuring reliable operation.

3.3 The Weighting Function

The weighting function provides a means of discriminating between the relative importance of the equalisation at different frequencies over the bandwidth of the system. The choice of the weighting function used is therefore dependent upon the subjective effect of the equalisation achieved.

Two main weighting functions are envisaged. The first is a flat characteristic over the full bandwidth of the system and the second is one which falls off at the higher frequencies.

Consideration given to the latter characteristic is due to a particular property of the television signal. It is commonly known that the "average" television signal spectrum falls off at the higher frequencies. It is felt, therefore, that equalising the higher frequencies may not be as important as equalising the lower part of the spectrum.

The ultimate aim of the equalisation process however, is the faithful reproduction of the transmitted waveform as far as is economically feasible. To achieve this goal, assuming that the equaliser can provide an adequate equalising response, then all frequencies must be treated equally. Thus the logical weighting function is a flat characteristic to 5 MHz.

3.4 The Model Channel

The ideal model channel is a perfect low pass filter with a constant amplitude characteristic to 5 MHz and zero beyond. As such a filter cannot be realised, the model characteristic chosen must satisfy the following criteria -

1. It must have an acceptable subjective response because it forms the basis for the equalisation of the transmission channel.
2. The required circuit must be economically realisable.

A model channel filter characteristic has already been proposed by Potter [21]. His choice was made on the basis that -

1. The filter should have a K factor of less than 0.5%.
2. The response of the filter should have a cutoff ring which has the same frequency as that of the ideal filter response (5 MHz).

The required amplitude characteristic for this response is one which is skew symmetrical about 5 MHz. As the maximum channel width that should be aimed at is 5.5 MHz [24] the flank of the proposed amplitude characteristic

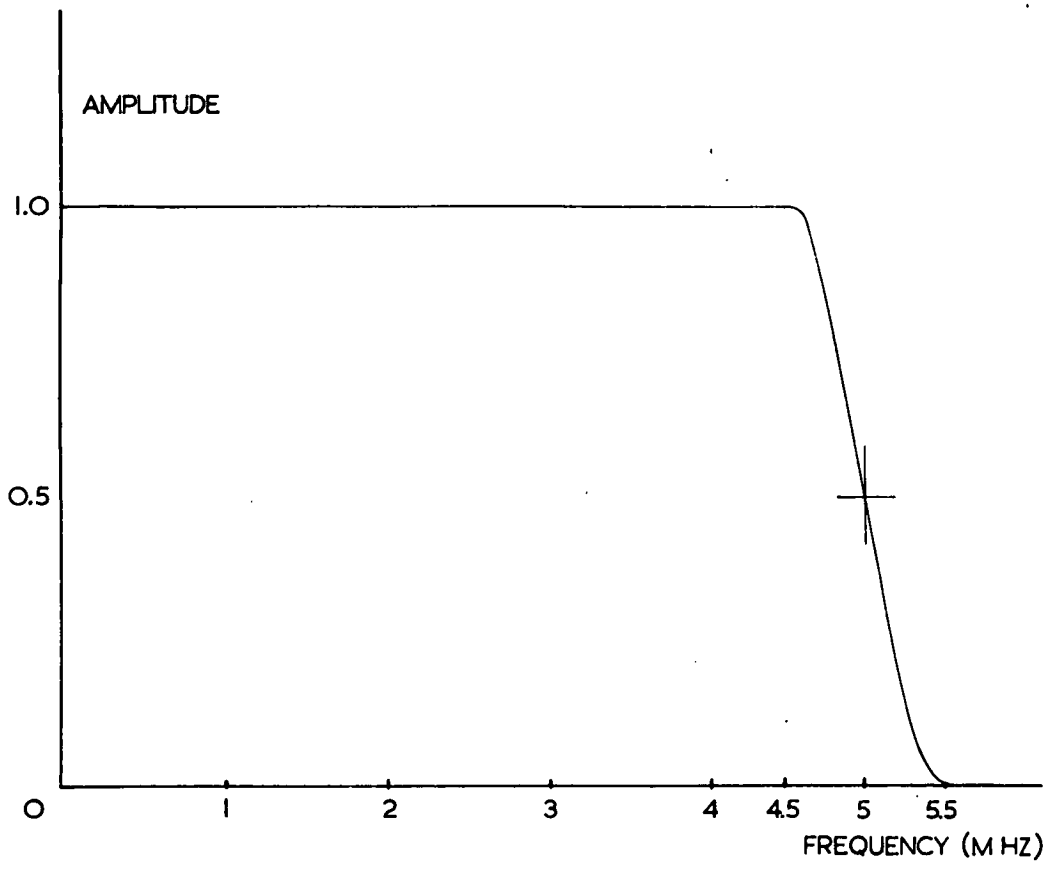

FIG. 3.2 MODEL CHANNEL FILTER AMPLITUDE CHARACTERISTIC

extends from 4.5 MHz to 5.5 MHz with the 6 db point at 5 MHz. The actual flank shape chosen was a cosine function (fig. 3.2). To achieve a suitable approximation to this characteristic a ninth order network with five all pass phase equalisers was required. From a circuit complexity point of view it is therefore undesirable to increase the cutoff rate.

The K factors of this model channel are less than 0.5% with the exception of K_4. This factor is related to the cutoff ring of the response and the high value (1.3%) is obtained because of the method used to calculate it. Potter maintains that the model should be satisfactory as the cutoff ring is guaranteed by the amplitude characteristic.

A modification of this filter is discussed in section 5.4.

3.5 The Adjustable Equaliser

The basic adjustable equaliser is a variable transfer function generator consisting of a linear combination of linearly independent functions $F_1(s)$, $F_2(s)$, ... $F_N(s)$. Consideration has been given to both orthogonal functions, in particular the set of Laguerre functions, and the delay line. The major factor in the choice of the equaliser transfer functions is the accuracy of the equalisation that can be achieved.

The orthogonal functions have the advantage of simpler circuitry. However, it is probable that the same degree of equalisation can be achieved with less taps if more complex transfer functions were selected. The advantage of the simpler circuits may therefore be lost because of the extra number of taps required. The delay line uses relatively complex transfer functions and has the advantage that it is already commonly used as a television equaliser.

A full investigation into the optimum adjustable equaliser for the television system is beyond the scope of this thesis. A comparison between results obtained from an experimental adaptive equaliser using both a delay line and a set of Laguerre functions is given in chapter 4.

3.6 The Automatic Control System

Of the various control systems presented in section 2.4.2 the two major considerations in the choice of the control system to be employed are the method of tap control and the choice of the function $\mathcal{F}$. Both a continuous and a discrete method of tap adjustment have been discussed. The two functions considered for $\mathcal{F}$ have been $\mathcal{F}(e) = e$ and $\mathcal{F}(e) = \text{sgn}(e)$.

If the discrete method of tap adjustment is employed the accuracy of the equalisation is dependent on the number of attenuator steps chosen. As the tap values will only be adjusted every 20 or 40 milliseconds (the field and frame rates) the larger the number of steps chosen then the slower will be the rate of convergence.

Ideally the accuracy of the control system is limited by noise in the received signal. Thus, there is a minimum step size below which improvements in accuracy will be offset by errors introduced by the control system. Arnon chose 255 steps for both the positive and negative gains of each tap. This gave him a step to noise ratio of 6 db, which may be considered as operating in a noise free environment. The convergence time he achieved with this number was approximately 5 seconds.

The use of the continuous method of tap control appears attractive because for a similar accuracy of equalisation to the discrete system the rate of convergence may be faster. During picture transmission the tap settings of the continuous system must be maintained by hold circuits. The accuracy of the equalisation is therefore dependent on the relative magnitude of the a.c. components to the d.c. component of the outputs of the correlators. If necessary the effects of the a.c. components may be reduced by introducing low pass filters in the correlation circuits. The resultant system would then be similar to Lucky and Rudin's with the stepping process replaced by an integrator. The introduction of these low pass filters, however, would affect the stability margin of the system.

The major problem associated with the continuous method is the realisation of continuously variable gain circuits (analogue multipliers) for the tap settings. The important requirement for these analogue multipliers is

that they reproduce the video waveform correctly. To prevent non-linear distortion of the video signal, multipliers used for this purpose must be linear for the video input. The variable gain input, however, may be of very low tolerance as any gain discrepancies will be corrected by the feedback loop.

The choice of an infinite clipper for the function $\mathcal{F}$ has the advantage of simplifying the circuit realisation of the control system. However the overall effect of such a modification to the system needs to be investigated before being employed. For example, the infinite clipper will introduce increased variation of the correlation outputs about their mean values. This has the effect of reducing the accuracy of the equalisation. It must be evaluated together with the different convergence rate and the simpler circuitry achieved before a decision is made on the use of such a scheme.

3.6.1 The Rate of Convergence of the Equaliser

The rate of convergence of the discrete method is determined by the length of the period between tap adjustments. If the attenuators are adjusted only once during each vertical blanking interval then the rate of convergence of this type of television equaliser is fixed.

The maximum rate at which an equaliser may be adjusted is determined by the time required for the correlators to settle to their steady state values after each adjustment. This settling time is dependent on the time constant of the correlation averaging circuits, which would be chosen to be equivalent to several periods of pseudo random noise. It appears, therefore, that only one adjustment would be made during each blanking interval. This could be increased during initial convergence if required, but the settling time obtained by Arnon indicates that this would not be necessary.

The continuous control method does not lend itself to an accurate and detailed analysis. Consequently an accurate analysis of the rate of convergence has not yet been established. An approximate result for this method has been

obtained by Sondhi. It is based on the assumptions that equation (2.34)

$$\frac{dR^T R}{dt} = -2KR^T X \mathcal{F}(R^T X)$$

can be averaged over the X ensemble and the vector R assumed independent of X on the right hand side. This assumption is justified if K is small and hence R slowly varying.

When X is a zero mean Gaussian signal, Sondhi obtained the following results:-

$$\frac{d}{dt} \langle\langle R^T R \rangle\rangle = -2K\sigma^2 \langle\langle R^T \Phi R \rangle\rangle \qquad \text{for } \mathcal{F}(e) = e \qquad 3.3$$

and

$$\frac{d}{dt} \langle\langle R^T R \rangle\rangle = -2K\sigma \sqrt{\frac{2}{\pi} \langle\langle R^T \Phi R \rangle\rangle} \qquad \mathcal{F}(e) = \text{sgn}(e) \qquad 3.4$$

where σ is the standard deviation of $x_n(t)$ and Φ is the N X N correlation matrix of the $x_n(t)$. The brackets $\langle\langle\ \rangle\rangle$ denote ensemble averaging. From these two equations he obtained the upper and lower bounds of the convergence rates as:-

$$\lambda_{min} R^T R \leq R^T \Phi R \leq \lambda_{max} R^T R \qquad 3.5$$

where λ_{min} and λ_{max} are the minimum and maximum eigen values of Φ.

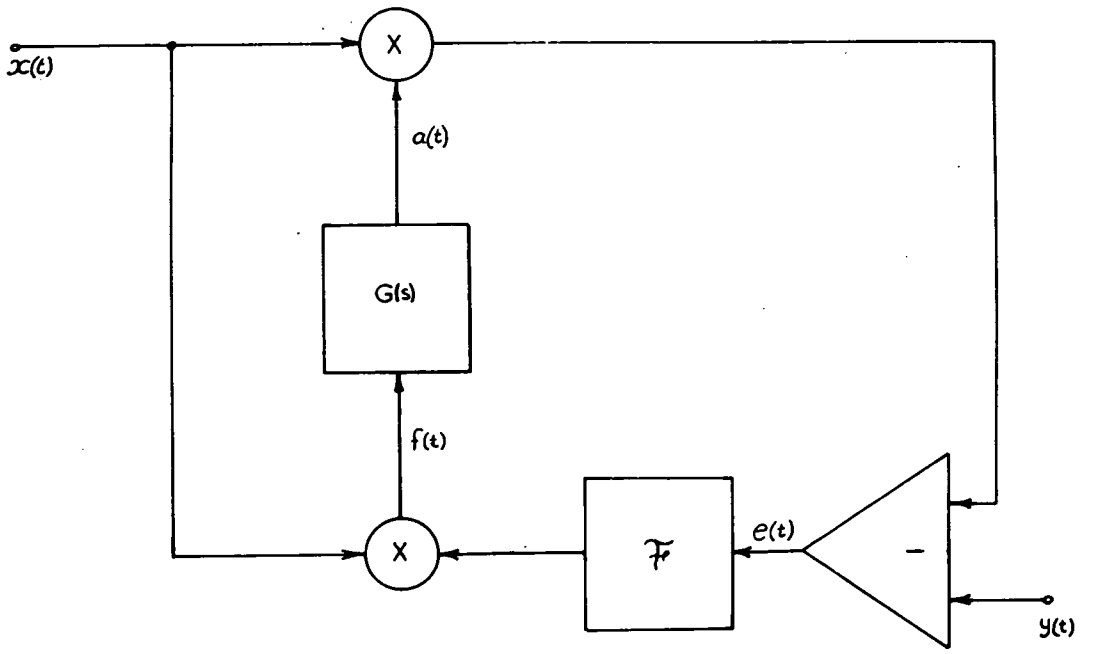

FIG. 3.3 BLOCK SCHEMATIC OF SIMPLE MODEL

Thus for $\mathcal{F}(e) = e$

$$\sqrt{R^T R}_{|t=o} \exp(-K\sigma^2\lambda_{max}t) \leqslant \sqrt{R^T R} \leqslant \sqrt{R^T R}_{|t=o} \exp(-K\sigma^2\lambda_{min}t) \quad 3.6$$

and for $\mathcal{F}(e) = \text{sgn}(e)$

$$\sqrt{R^T R}_{|t=o} - \sqrt{\frac{2}{\pi}}K\sigma\lambda_{max}^{\frac{1}{2}}\, t \leqslant \sqrt{R^T R} \leqslant \sqrt{R^T R}_{|t=o} - \sqrt{\frac{2}{\pi}}K\sigma\lambda_{min}^{\frac{1}{2}}\, t \quad 3.7$$

These bounds are close to each other if Φ is nearly diagonal, which is the case when $x_n(t)$ is broadband.

3.7 Investigation of a Simplified Model

To enable a more detailed examination of the convergence to be attempted, a much simplified model was chosen for investigation. This also allowed the effects of an extra time constant in the correlation circuits and also the effects of using non Gaussian test signals to be investigated. The simple model is a single loop system as shown in fig. 3.3, where G(s) is the transfer function of the correlation averaging circuit.

This model was chosen for the following reasons -

1. It is a simple model of the complete system.
2. It applies to each tap of an orthogonal multitap system with $\mathcal{F}(e) = e$. If $\mathcal{F}$ is a non-linear function such a model does not apply to each tap. However, it was expected that an improved insight into the convergence characteristics could be obtained.
3. It provided a means of investigating any instabilities likely to be found in the practical system.

Consider first the case where the transfer function, G(s), is an integrator (i.e. $G(s) = \frac{K}{s}$) and $\mathcal{F}(e) = e$.

An exact analysis of the convergence does not provide a convenient solution when a signal such as pseudo random noise is used. The equation of the tap response -

$$\frac{da(t)}{dt} + Kx^2(t)a(t) = Kx^2(t)\ \left(\frac{y(t)}{x(t)}\right) \qquad 3.8$$

has the solution [25] (for zero initial conditions)

$$a(t) = \int_0^t \frac{y(\tau)}{x(\tau)}\ Kx^2(\tau) e^{-\int_\tau^t Kx^2(u)du}\, d\tau \qquad 3.9$$

which cannot be given in terms of ordinary functions.

Equation 3.8 can be solved by either assuming a series solution then calculating the terms algebraically or by expressing it as a difference equation -

$$a(t_{n+1}) = K[x(t_n)y(t_n) - x^2(t_n)\ a(t_n)]\ \Delta t + a(t_n) \qquad 3.10$$

These solutions, however, are not practical with a signal such as pseudo random noise.

To simplify the analysis, an approximation of the response must be made. As an integrator is used for the correlation, it is assumed that the a.c. components of the output of the correlator may be ignored compared with the magnitude of the d.c. component. This approximation is valid provided the loop gain is relatively low.

The d.c. output of the correlation multiplier is given by -

$$f_{dc}(t) = \phi_{xy} - a(t)\ \phi_{xx} \qquad 3.11$$

where $f_{dc}(t)$ is the d.c. value of f(t), ϕ_{xy} is the cross-correlation of x(t) and y(t) with time shift $\tau = o$, and ϕ_{xx} is the autocorrelation of x(t) with time shift $\tau = o$.

For $G(s) = \frac{K}{s}$ then

$$\frac{da(t)}{d(t)} = K[\ \phi_{xy} - a(t)\ \phi_{xx}] \qquad 3.12$$

The step response is therefore -

$$a(t) = \frac{\phi_{xy}}{\phi_{xx}} [\ u(t) - \exp(-K\phi_{xx}t)] \qquad 3.13$$

where $u(t) = 1$ for $t > o$.

Applying the equation obtained by Sondhi (equation 3.6) to this simple model it can easily be demonstrated that it is identical to equation 3.13.

The same procedure may also be used to calculate the response of the system with an extra time constant in the correlation circuit.

For

$$G(s) = \frac{K}{s(s + \beta)} \quad \text{then:-}$$

$$\frac{d^2a(t)}{dt^2} + \beta \frac{da(t)}{dt} + K\phi_{xx}a(t) = K\phi_{xy} \qquad 3.14$$

The step response for this system is identical to that of a type 1 second order system with the natural resonant frequency equal to $\sqrt{K\phi_{xx}}$ and the damping factor given by

$$\frac{\beta}{2\sqrt{K\phi_{xx}}}$$

If the function $\mathcal{F}$ is altered to an infinite clipper with an output of ± V volts, then the value of $f_{dc}(t)$ will be altered. The added complexity resulting from the introduction of the infinite clipper prevents a relatively simple analysis of the convergence as achieved without the infinite clipper.

For the following analysis it will be assumed that the signal y(t) is given by -

$$y(t) = cx(t) + c_1 x_1(t) \qquad 3.15$$

and that the two components of y(t) are uncorrelated.

It must also be assumed that the signals x(t) and $x_1(t)$ are stationary zero mean Gaussian signals and that y(t) and x(t) possess a normal joint distribution function. Under these conditions the d.c. output of the correlation multiplier is given by the true cross-correlation of x(t) and e(t) multiplied by Booton's constant [26, 27].

Thus only the d.c. value resulting from the auto-correlation of the x(t) component of the error signal and the input signal need be considered.

Without the infinite clipper

$$f_{dc}(t) = c\phi_{xx} - a(t)\phi_{xx} \qquad 3.16$$

With the infinite clipper

$$f_{dc}(t) = c_B c\phi_{xx} - c_B a(t)\phi_{xx} \qquad 3.17$$

The constant c_B is Booton's equivalent gain of the infinite clipper and is given by -

$$c_B = \frac{1}{\sigma_e \sqrt{2\pi}} \int_{-\infty}^{\infty} \bar{e}\, \bar{\mathcal{F}}(\bar{e}) \exp\left(\frac{-\bar{e}^2}{2}\right) d\bar{e} \qquad 3.18$$

where $\bar{\mathcal{F}}(\bar{e})$ is the normalised form of the function $\mathcal{F}(e)$, and σ_e^2 is the variance of the input signal to the infinite clipper. For an infinite clipper with an output of ± V volts the value of c_B is given by -

$$c_B = \frac{V}{\sigma_e} \sqrt{\frac{2}{\pi}} \qquad 3.19$$

For this particular case, if the variances of $x(t)$ and $x_1(t)$ are σ_x^2 and $\sigma_{x_1}^2$ respectively, then the variance of the error signal is given by -

$$\sigma_e^2 = (c-a(t))^2 \sigma_x^2 + c_1^2 \sigma_{x_1}^2 \qquad 3.20$$

Therefore -

$$f_{dc}(t) = \frac{\sqrt{\frac{2}{\pi}}\, V\phi_{xx}\,(c-a(t))}{\sqrt{(c-a(t))^2 \sigma_x^2 + c_1^2 \sigma_{x_1}^2}} \qquad 3.21$$

As $\sigma^2_x = \phi_{xx}$ then -

$$f_{dc}(t) = \frac{\pm \sqrt{\frac{2}{\pi}}\, V\, \sigma_x}{\sqrt{1 + \frac{c_1^2 \sigma_{x_1}^2}{(c-a(t))^2 \sigma^2_x}}} \qquad 3.22$$

The sign of the d.c. value is dependent on whether c is greater or less than $a(t)$. For $c > a(t)$ the d.c. value is positive.

The tap response is therefore dependent on $c_1^2 \sigma_{x_1}^2$.

Case (i) for

$$c_1^2 \sigma_{x_1}^2 \ll (c-a(t))^2 \sigma_x^2$$

then

$$f_{dc}(t) \simeq \pm \sqrt{\frac{2}{\pi}}\, V\sigma_x \qquad 3.23$$

Case (ii) for

$$(c-a(t))^2\sigma_x^2 \ll c_1^2\sigma_{x_1}^2$$

then

$$f_{dc}(t) \simeq \pm\sqrt{\frac{2}{\pi}}\ \frac{V\sigma_x^2}{c_1\sigma_{x_1}}\ (c-a(t)) \qquad 3.24$$

If $G(s) = \frac{K}{s}$ then the tap response for case (i) is given by -

$$a(t) = \pm\ KV\sigma_x\sqrt{\frac{2}{\pi}}\ t \qquad 3.25$$

For case (ii) the tap response is exponential with a time constant of

$$KV\sqrt{\frac{2}{\pi}}\ \frac{\sigma_x^2}{c_1\sigma_{x_1}}$$

For the multitap system the value of σ_e decreases with time as all taps converge to their appropriate values. Thus the reason for the linear tap response with the infinite clipper, as distinct from the exponential response of the linear system, is the effective increasing gain of the infinite clipper during convergence (equations 3.19 and 3.20).

For most practical cases there will be a residual error which cannot be equalised. As the system converges, the variance of the residual error eventually becomes large compared with the variance of the equalisable part of the error signal. The tap response will then change from case (i) to case (ii). Thus, in the practical case, the response will be linear for the first part, then gradually become exponential. The cross-over point between the two characteristics is determined by the relative magnitude of the residual error.

The equation obtained by Sondhi (3.7) and applied to an ideal single loop system, for which

$$y(t) = cx(t)$$

and

$$\lambda_{min} = \lambda_{max} = 1,$$

is identical to the result obtained for the model system (equation 3.25).

For $G(s) = \frac{K}{s(s+\beta)}$ the tap response for case (i) is given, in the frequency domain, by -

$$a(s) = \pm KV\sigma_x \sqrt{\frac{2}{\pi}} \quad \frac{1}{s^2} \quad \frac{1}{s+\beta} \quad \text{for } c \gtrless a(t) \qquad 3.26 \begin{matrix}(i)\\(ii)\end{matrix}$$

If c is a positive value the initial response, in the time domain, is given by

$$a(t) = KV\sigma_x \sqrt{\frac{2}{\pi}} \left[-\frac{1}{\beta^2} u(t) + \frac{1}{\beta^2} \exp(-\beta t) + \frac{1}{\beta} t\right] \qquad 3.27$$

As there is now a second time constant in the system some overshoot of a(t) about c will result. Let $t = t_1$, when $a(t) = c$. At $t_1 + \Delta t$, the response of the system is given by equation 3.26(ii) with the initial conditions of c and $\dot{a}(t_1)$. The time response is then given by -

$$a(t+t_1) = -KV\sigma_x \sqrt{\frac{2}{\pi}} \left[-\frac{1}{\beta^2}u(t) + \frac{1}{\beta^2}\exp(-\beta t) + \frac{1}{\beta}t\right] + \dot{a}(t_1)\left[\frac{1}{\beta}u(t) - \frac{1}{\beta}\exp(-\beta t)\right]$$

$$+ cu(t) \qquad 3.28$$

This also results in a second overshoot of the value c by a(t) with the characteristic changing again to equation 3.26(i). The new initial conditions are $\dot{a}(t_2)$ and c. This technique must be continued until the desired accuracy of the converged value is obtained. For, c, a negative value, equations 3.27 and 3.28 must be preceded by a negative sign.

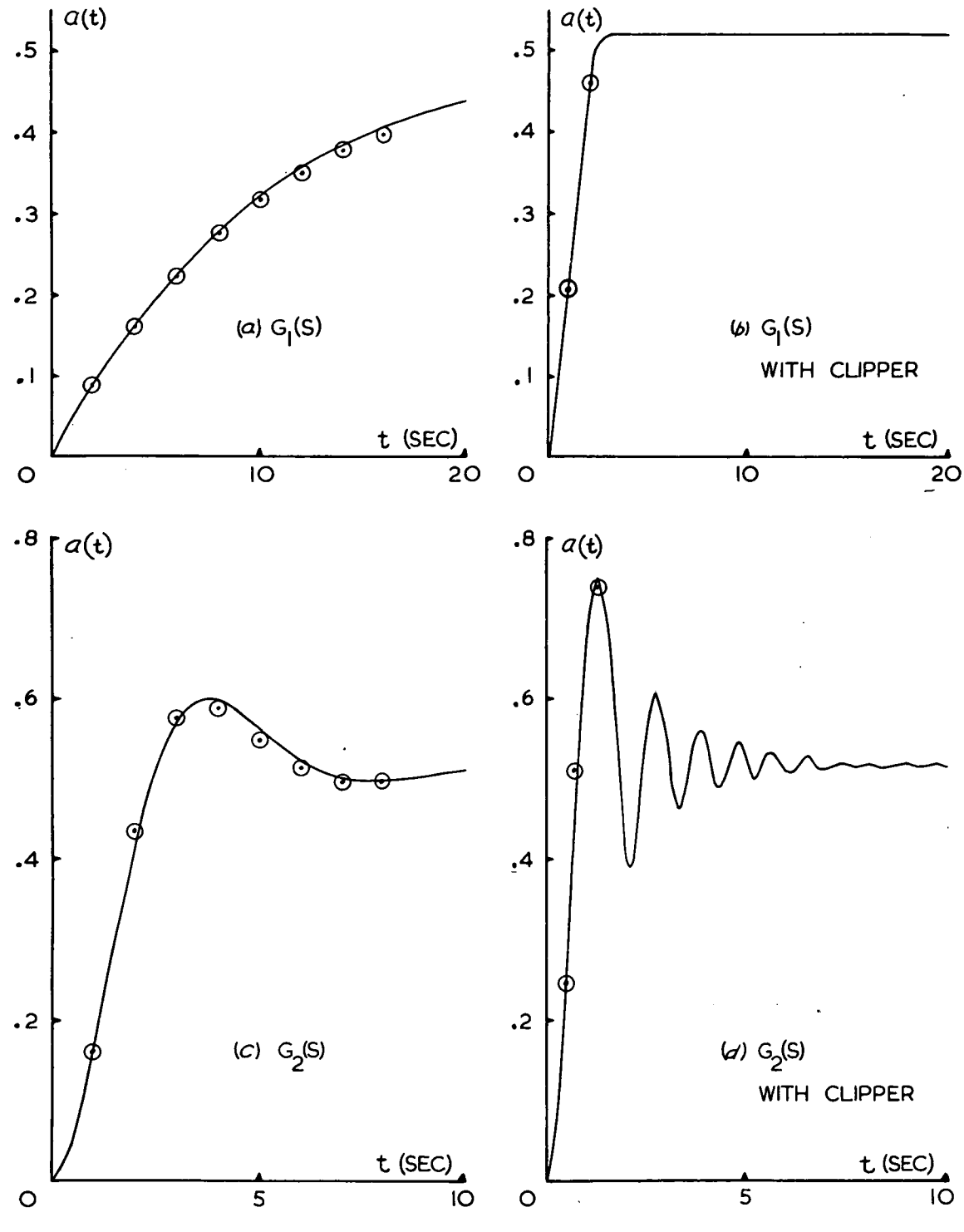

FIG. 3.4 TIME RESPONSE OF MODEL SYSTEM

For case (ii) the result is again similar to that obtained for the linear system. The response is the same as that of a type 1 second order system with the natural resonant frequency given by -

$$\omega_n = (KV\sqrt{\frac{2}{\pi}}\ \frac{\sigma_x^2}{c_1\sigma_{x_1}})^{\frac{1}{2}}$$

and the damping factor equal to $\frac{\beta}{2\omega_n}$.

For the practical case the actual tap response will again be a combination of both characteristics.

3.7.1 Practical Investigation

To verify the theoretical results obtained for the model system a practical simulation was set up on an analogue computer. The loop gain of the system was purposely kept low to enable an X-Y plotter to plot the tap response.

Two different correlation circuits were used, both with and without the infinite clipper. These were -

$$G_1(s) = \frac{1}{100s}$$

and

$$G_2(s) = \frac{1}{10s(s+1)}$$

The test signal used was pseudo random noise with N = 10, a clock frequency of 100 KHz and a filter cutoff of 5 KHz. The same signal, except for a difference in amplitude, was used for both the received and reference signal. Thus, the value of $c_1\sigma_{x_1}$ for both systems when using the infinite clipper was equal to zero.

The results are shown in fig. 3.4(a), (b), (c) and (d) together with the theoretical response, calculated using the equations obtained in section 3.7.

The major difference between the theoretical and practical results obtained was caused by the accuracy of the various parameters used in the practical simulation.

3.7.2 Stability of the System

During the practical investigation it was found that the system could be made unstable. This was achieved, with particular transfer functions for G(s), by sufficiently increasing the loop gain and input signal amplitude. Any such instabilities could not be tolerated within a practical system.

The stability of the control system shown in fig. 2.4 is assured with $\mathcal{F}(e) = e$. This is demonstrated with the analysis derived by Narendra and McBride [28]. They consider the time domain differential equations of the tap gains -

$$\frac{da_j(t)}{dt} = Kx_j(t)e(t)$$

$$= -Kx_j \sum_n a_n(t)x_n(t) + Kx_j(t)y(t) \qquad 3.29$$

or in vector notation

$$\dot{A} = -KXX^TA + Ky(t)X \qquad 3.30$$

Considering only the homogeneous part of 3.30

$$\dot{A} = -KXX^TA \qquad 3.31$$

they show this to be at least neutrally stable for all positive K by choosing the Liapunov function,

$$V_L = \sum_n a_n^2(t)$$

$$= A^TA > 0 \text{ for all } A \neq 0 \qquad 3.32$$

Then

$$\frac{dV_L}{dt} = 2A^T\dot{A} = -2KA^TXX^TA$$

$$= -2K(X^TA)^2 \leqslant 0 \qquad 3.33$$

Therefore, providing that y(t) is bounded, a bounded input will produce a bounded output regardless of the value of K.

The describing function concept [37] is employed to extend the analysis to include the infinite clipper. It can easily be shown that the fundamental component of the output is not phase shifted relative to a sinusoidal input to the infinite clipper. Thus, within the limitations of the describing functions, the infinite clipper may be considered as a variable gain element with the gain dependent on the input signal amplitude. Under this condition the system is still stable as the infinite clipper may be considered as part of the loop gain K.

No instabilities were detected within the experimental system using just integrators in the correlation circuits.

With the introduction of an extra time constant the system could be made unstable. When using pseudo random noise as the test signal the frequency of the unstable oscillation obtained was a multiple of half the fundamental frequency of the pseudo random noise (i.e. $\frac{n\omega_p}{2}$ where ω_p is the fundamental frequency of pseudo random noise). The most common instabilities were at the fundamental frequency itself and the half subharmonic of this frequency.

The conditions under which the model system is unstable may be obtained by analysing the feedback loop within the system using a method similar to the describing function technique. The effects of the reference signal and the d.c. component of a(t) are ignored. For pseudo random noise, the input signal is of the form -

$$x(t) = b_1\cos(\omega_p t + \theta_1) + b_2\cos(2\omega_p t + \theta_2) + \ldots \qquad 3.34$$

If a(t) has the form (neglecting the d.c. component) -

$$a(t) = a\sin\omega t$$

then the output of the multiplier is (neglecting the d.c. component)-

$$f_{ac}(t) = -a\sin\omega t\,(b_1\cos(\omega_p t + \theta_1) + b_2\cos(2\omega_p t + \theta_2) + \ldots)^2 \qquad 3.36$$

$$= -a\sin\omega t(B_o + B_1\cos(\omega_p t + \psi_1) + B_2\cos(2\omega_p t + \psi_2) + \ldots) \qquad 3.37$$

For $\omega = \frac{n\omega_p}{2}$ where n = 1, 2 ... the output of the multiplier has two components at the frequency ω. These are -

1. $-aB_o \sin \omega t$

2. $\frac{aB_1}{2} \sin (\omega t + \psi_1)$ for $\omega = \frac{\omega_p}{2}$

   $\frac{aB_2}{2} \sin (\omega t + \psi_2)$ for $\omega = \omega_p$

   and so on.

As

$$[B_o + B_1 \cos(\omega_p t + \psi_1) + \ldots] = (b_1 \cos(\omega_p t + \theta_1) + \ldots)^2$$

then

$$B_o \geq B_1, B_2 \ldots$$

Consider the case for n equal to 1, then the output of the multiplier at the frequency ω is given by -

$$f'_{ac}(t) = -a[B_o \sin \omega t - \frac{B_1}{2} \sin (\omega t + \psi_1)]$$

$$= -aB' \sin(\omega t + \psi) \qquad 3.38$$

where

$$B' = \sqrt{B_o^2 + \frac{B_1^2}{4} - B_o B_1 \cos \psi_1} \qquad 3.39$$

and

$$\psi = \arccos \left[\frac{B_o - \frac{B_1}{2} \cos \psi_1}{B'} \right] \qquad 3.40$$

$$= \arcsin \left[\frac{-\frac{B_1}{2} \sin \psi_1}{B'} \right] \qquad 3.41$$

Because the output of G(s) is $a\sin(\omega t)$ the onset of instability, for a phase shift, γ, and a gain, G, introduced by G(s) at the frequency ω, is given by:-

1. $aB'G = a$

That is

$$G = \frac{1}{\sqrt{B_o^2 + \frac{B_1^2}{4} - B_o B_1 \cos \psi_1}} \qquad 3.42$$

2. $$\gamma = 180^\circ - \psi \qquad 3.43$$

These equations still apply for n = 2, 3 ... with the constants ψ_n and B_n substituted for ψ_1 and B_1.

As $B_o \geq B_1, B_2 \ldots$ it can be seen from equations 3.40 and 3.41 that ψ lies within $\pm 90^\circ$ regardless of the value of ψ_1. Thus for $\gamma = 90^\circ$ the system is always stable.

This analysis illustrates the form of the instabilities which may occur when pseudo random noise is used. Due to the difficulty of obtaining the practical values of B_o, B_1 ... however, these results were not checked with the practical simulation.

3.8 Computer Simulation

For preliminary investigations into a multitap system two lines of investigation were started. These were -

1. A digital computer simulation (using an Elliott 503 digital computer).
2. A practical simulation.

The first computer simulation attempted was an equalising system using a three tap delay line with one pre-echo and one post-echo. The control system employed consisted of continuous feedback loops with both an integrator and an extra time constant in each correlation circuit. The purpose of this simulation was a study of the stability, accuracy and rate of convergence of the multitap system. The relatively small system was employed to enable a

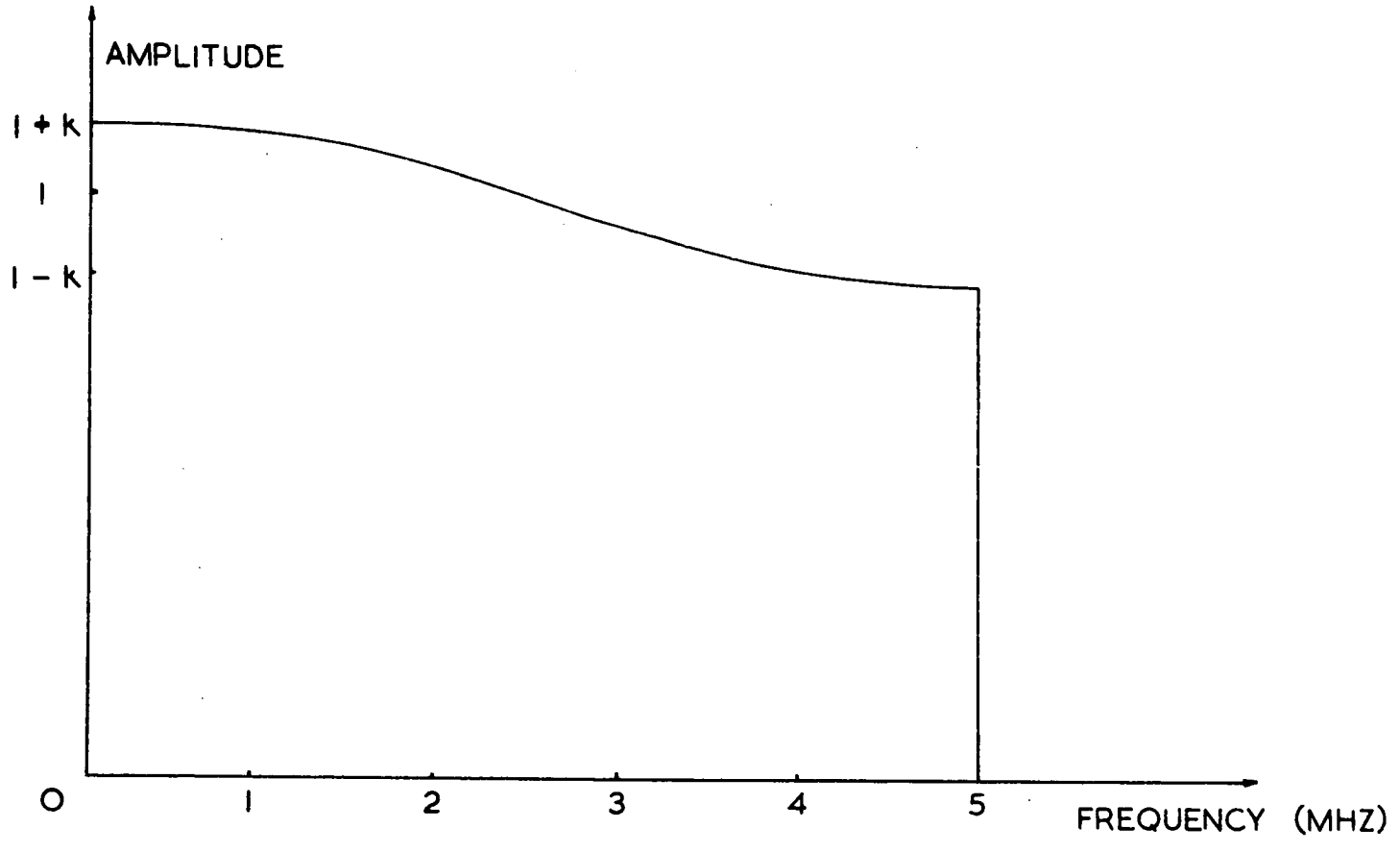

FIG.3.5 COMPUTER SIMULATION DISTORTION AMPLITUDE CHARACTERISTIC

simple computer programme to be written on which the investigation could be based. It was hoped that the number of taps and overall complexity of the system could then be gradually increased to allow a comprehensive investigation to be carried out.

The distortion characteristic chosen for this simulation is shown in fig. 3.5. The amplitude characteristic was $1 + k\cos(\omega T)$ to 5 MHz and zero beyond and the phase characteristic was linear with zero time delay. This characteristic was chosen because -

1. It can be produced by a delay line having one pre-echo and one post-echo with the main tap having the value unity and the two echo taps having the value +k (equations (1.2) and (1.3)).

   If the model channel used in the simulation is a perfect 5 MHz cutoff filter the three tap delay line is then capable of providing the required equalising characteristic. The resultant tap values after settling should be -k, 1, -k. The use of this characteristic provided a quick means of evaluating the accuracy of the equalisation.

2. It is a characteristic for which the impulse response may be calculated very easily. This response was required to obtain the distorted signal time series values using digital convolution.

For the initial simulation two computer programmes were written.

The first programme was used for the generation of the required test signal. The equivalent test signal used was one period of pseudo random noise generated by a ten stage shift register with a clock frequency of 100 MHz, the output of which was then filtered by a perfect 5 MHz low pass filter. The time series obtained from this programme was used as data for the next programme.

The second programme calculated the time series values of the distorted waveform and delayed the ideal signal time series by an amount equivalent to T to provide the one pre-echo. These two time series were the basis for the calculations required to obtain the time response of the tap settings.

To further simplify this initial programme, only the two echo taps were adjusted. During the calculations the main tap was given the value of unity and was not included in the convergence process.

A number of encouraging results were obtained from this computer simulation. The accuracy of the settled tap values obtained was within approximately 3%. An accuracy of this order was expected as the equations upon which these results were based are only approximations. Detailed information of the time responses was not obtained, however, as it was evident that a study of the convergence over a longer period was necessary. This was not practical as the computer running time would have become excessive. The long running time was due to the convolution process required for the extra time constant in the feedback loops.

Although this initial programme could have been improved to reduce the running time it was not attempted. It was evident that difficulty would still be encountered with the more complex programmes required to simulate the practical system. The removal of the extra time constants would have simplified the programme to a large extent. However, this was not attempted because -

1. The convolution processes required to obtain the time series of the required waveforms was still relatively long.
2. The removal of the extra time constants prevented a study of any instability within the multiloop system.
3. To improve the programme sufficiently a different computing algorithm such as the fast fourier transform was required. However, there was insufficient time available to develop such a programme.

Because of the limited time available for this investigation, work on the computer simulation was stopped and the extra time devoted to the development of the practical simulation. It was considered that the practical simulation would not only provide information on the performance of the proposed equaliser, but would also indicate possible practical problems which may be encountered within a television system. This would not be so with a computer simulation.

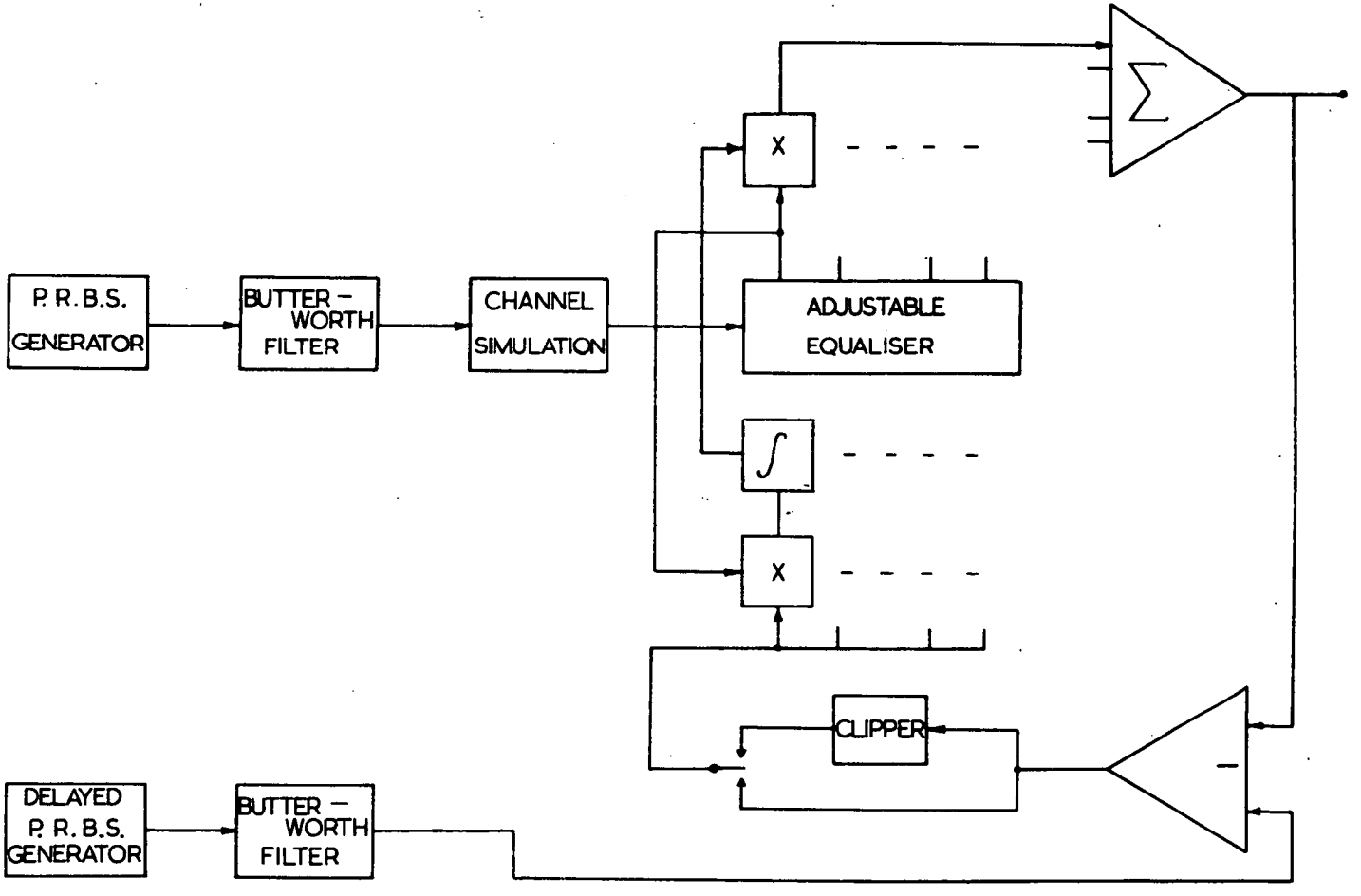

FIG. 4.1 BLOCK DIAGRAM OF EXPERIMENTAL EQUALISER

CHAPTER 4

TEST RESULTS OF THE EXPERIMENTAL EQUALISER

4.1 General

To allow a comprehensive investigation into the possibility of using the control methods introduced in section 2.4.2 an experimental system was built. The main aim of this investigation was to assess the performance of such a system. This included such factors as accuracy of the equalisation, settling time, the stability of the system and the dependence of these factors on the various parameters of the system.

As the investigation was only concerned with the performance of the basic automatic equaliser, a simplified system was used. The detailed problems of adapting an automatic equaliser to operate within a television network were not considered. These problems include -

1. Gating the test signal into the vertical blanking interval of the video signal.
2. Timing the reference waveform at the receiver, and
3. Operating the system at 5 MHz.

The block diagram of the complete experimental equaliser studied is shown in fig. 4.1. To simplify the circuitry required the experimental system was frequency scaled relative to the real system by a factor of one thousand. This reduced the bandwidth to 5 KHz.

Two analogue computers were employed in the circuit realisation. This minimised the circuit complexity and maximised the use of available equipment. The Butterworth filters indicated in fig. 4.1 were fourth order Butterworth filters with a bandwidth of 5 KHz. The transfer function chosen for the channel simulation was

$$\frac{1}{\left(\frac{s}{\omega_o}\right)^2 + 2\xi\frac{s}{\omega_o} + 1} \quad \text{where } \omega_o = 2.44_{10}4 \text{ and } \xi = 0.275$$

The detailed design and performance of circuits used for the experimental equaliser is presented in appendix B.

As a study of the general equalising characteristics of the system was the aim of this practical investigation a constant gain circuit was used as the model channel. Thus, for perfect equalisation the equaliser had to simulate the inverse transfer function of the distortion produced by the channel simulation network.

Initially a three tap system using a two section delay line was built and tested. This system contained only the basic automatic equaliser, one Butterworth filter and the pseudo random noise generator. The input to the delay line only differed from the reference signal by a constant gain factor c. The accuracy of the equaliser was easily tested using this system as the tap settings should have converged to the values $a_1 = c$; $a_2 = 0$ and $a_3 = 0$.

After the three tap equaliser had been tested and was working satisfactorily, the system was enlarged to ten taps. The performance of this system was studied using both a delay line and Laguerre functions for the adjustable equaliser.

The results obtained from the experimental equaliser are presented in this chapter.

4.2 The Three Tap Equaliser

4.2.1 Static Performance

When this preliminary system was completed it was found that the accuracy of the equalisation obtained without the infinite clipper was very poor. Convergence could only be assured for large signal amplitudes at the input of the delay line and the error signal was still relatively large after the tap settings had settled to their final values. For low amplitude input signals the tap settings would not converge at all, the output integrators would merely drift off until saturation of their amplifiers occurred.

The cause of this poor convergence characteristic was traced to the d.c. offset of the correlation multipliers. For the single loop system, discussed in chapter 3, the relationship between the tap setting and the d.c.

output of the correlation multiplier, with no d.c. offset, is given by equation 3.11 -

$$f_{dc}(t) = \phi_{xy} - a(t)\phi_{xx}$$

If the correlation multiplier has a d.c. offset then the final value of a(t) is determined by the cross-correlation required to cancel this d.c. offset. The error of the tap setting after settling is therefore directly proportional to the d.c. offset of the correlation multipliers and inversely proportional to the value of ϕ_{xx}.

The static performance of the system could have been improved with better zeroing of the correlation multipliers. With the trimmer potentiometers used in the multiplier circuits this was not practically possible. The time required to adjust all multipliers to a sufficient accuracy (< 10mV) was excessive. It must be remembered that although the d.c. offset was sufficient to reduce the accuracy of the equalisation the offset value was within the tolerance of the multipliers (3% of the maximum output, i.e. 0.3 volts).

From the above equation it can be seen that increasing the values of both ϕ_{xx} and ϕ_{xy} will reduce the effect of any d.c. offset on the accuracy of the equalisation. This may be achieved by amplifying the error signal. For one particular case amplifying the error by a factor of ten reduced the error signal from 0.6 to 0.2 volts peak to peak. By increasing this gain factor the accuracy of the equalisation could have been improved even further. The increased gain, however, produced overloading of the difference amplifier before the system had converged.

The solution to this particular problem, therefore, is the use of the infinite clipper in the error circuit.

With the introduction of the infinite clipper the error signal was reduced to within one to two per cent of the value of the input signal to the delay line. Thus, the resulting accuracy obtained was better than the tolerance of the analogue multipliers.

Positive verification of the improved accuracy achieved with the use of the infinite clipper was obtained by considering only the main tap and disconnecting the two delayed taps. An identical static accuracy was obtained from both the linear and non-linear systems by carefully adjusting the zero of the correlation multiplier very accurately for the linear case. Even deliberately applying a relatively large amount of d.c. into the integrator failed to prevent convergence when using the infinite clipper.

4.2.2 Dynamic Performance

A brief investigation of the dynamic performance of this system was also carried out. The convergence characteristics were recorded using an ultra-violet recorder, with each tap setting connected to one channel of the recorder.

The results obtained from this system were similar to those obtained from the simple system described in chapter 3. The convergence rate was proportional to the square of the amplitude of the input signal to the delay line for the linear system and directly proportional to this amplitude for the non-linear system. The tap responses of the linear and non-linear systems were exponential and linear respectively. With extra time constants in the correlation circuits the characteristic overshoots and resulting oscillations of the tap settings about their final values were obtained.

These characteristics were the same for all three taps. For identical correlation circuits the convergence characteristics of all three taps were almost identical. With the linear system, even altering the initial value of any of the taps had no significant effect on the response of the remaining taps. This indicated that it was an orthogonal system. From the autocorrelation function of the output signal of the Butterworth filter, shown in fig. 4.11, it can be seen that this was almost the case.

To demonstrate the effect of this property the variation of the two delayed taps about their mean values caused by the oscillation of the main tap was recorded. This was achieved by adding a large time constant to the correlator of the main tap. With the convergence of the tap values from 0, -0.5, -0.5 to 0.5, 0, 0 the main tap oscillated about its final value with a

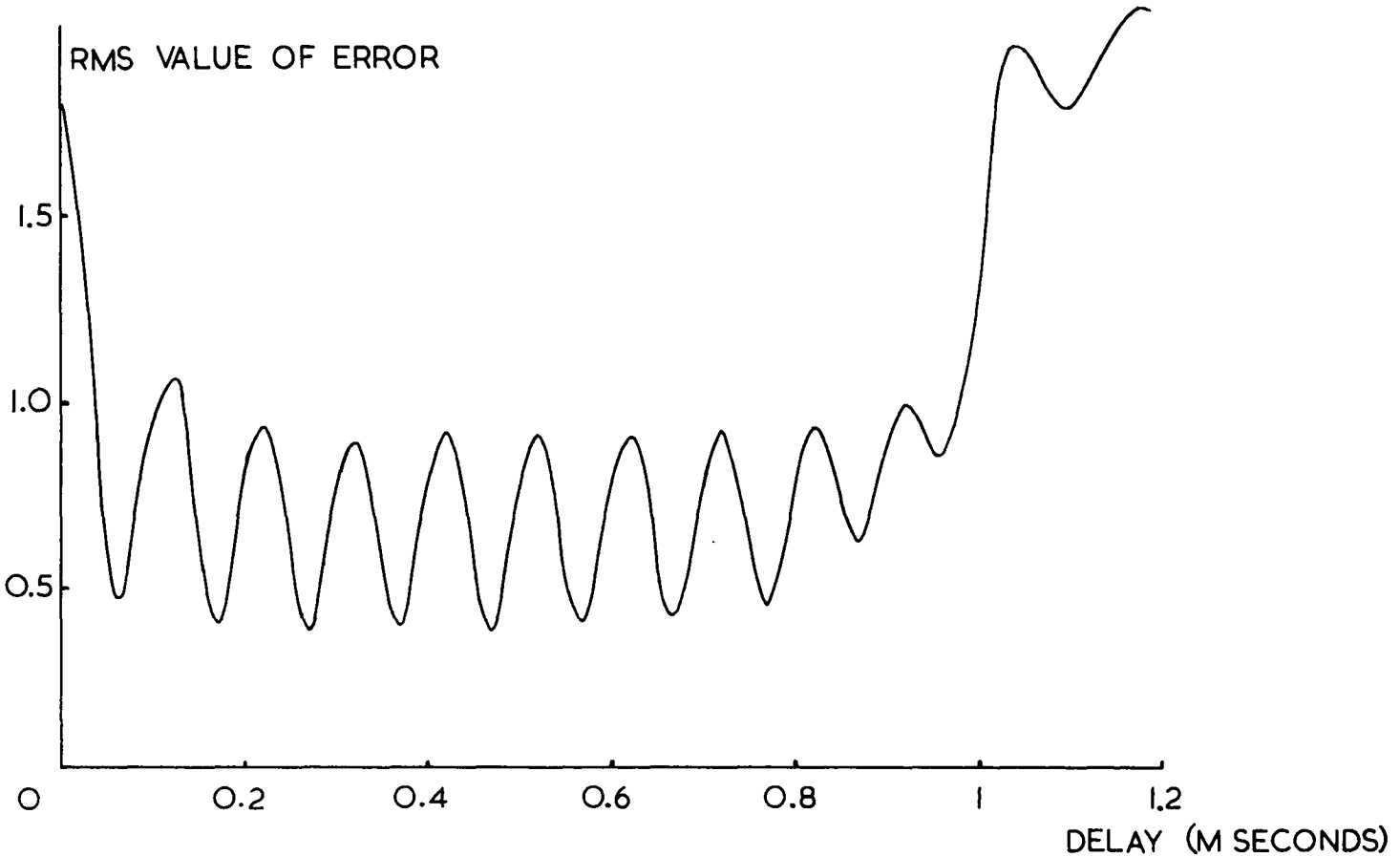

FIG. 4.2 EFFECT OF REFERENCE SIGNAL DELAY ON ACCURACY OF EQUALISATION (DELAY LINE)

relatively large amplitude long after the other taps had converged. No appreciable variation of the second tap could be observed after it had converged to zero. The third tap, however, oscillated with a constant phase relationship relative to the main tap with an amplitude of approximately 2% of that of the main tap. This result was expected because the value of the autocorrelation function of the input signal to the delay line (fig. 4.11) at the delay T is less than the value at 2T.

4.3 Static Accuracy of the Completed Experimental Equaliser

The results of the static accuracy obtained by the experimental equaliser were measured under ideal noise conditions ($\frac{S}{N} = \infty$). The effects of noise on the received signal are discussed in section 4.6. The test signal used was pseudo random noise with a clock frequency of 100 KHz and the value of N equal to ten.

Unless otherwise mentioned, the infinite clipper was used during convergence to ensure the correct performance figures were measured.

4.3.1 The Delay Line Equaliser

To provide accurate equalisation the timing of the reference signal relative to the received signal is very important. To illustrate this fact the delay between the "transmitted" and reference signals of the experimental equaliser was varied and the resultant effects on the accuracy of the equalisation investigated.

The r.m.s. value of the error voltage was measured after the system had settled for a particular value of the delay. All other parameters were kept constant and the process repeated for different delay values. The graph of the results is shown in fig. 4.2.

This graph illustrates the two major factors that affected the accuracy of the equalisation. The first is the time delay of the "transmitted" signal produced by the distortion. The positioning of the taps relative to the input signal is therefore very important. For the practical television system this is determined by the timing of the reference waveform relative to the received signal.

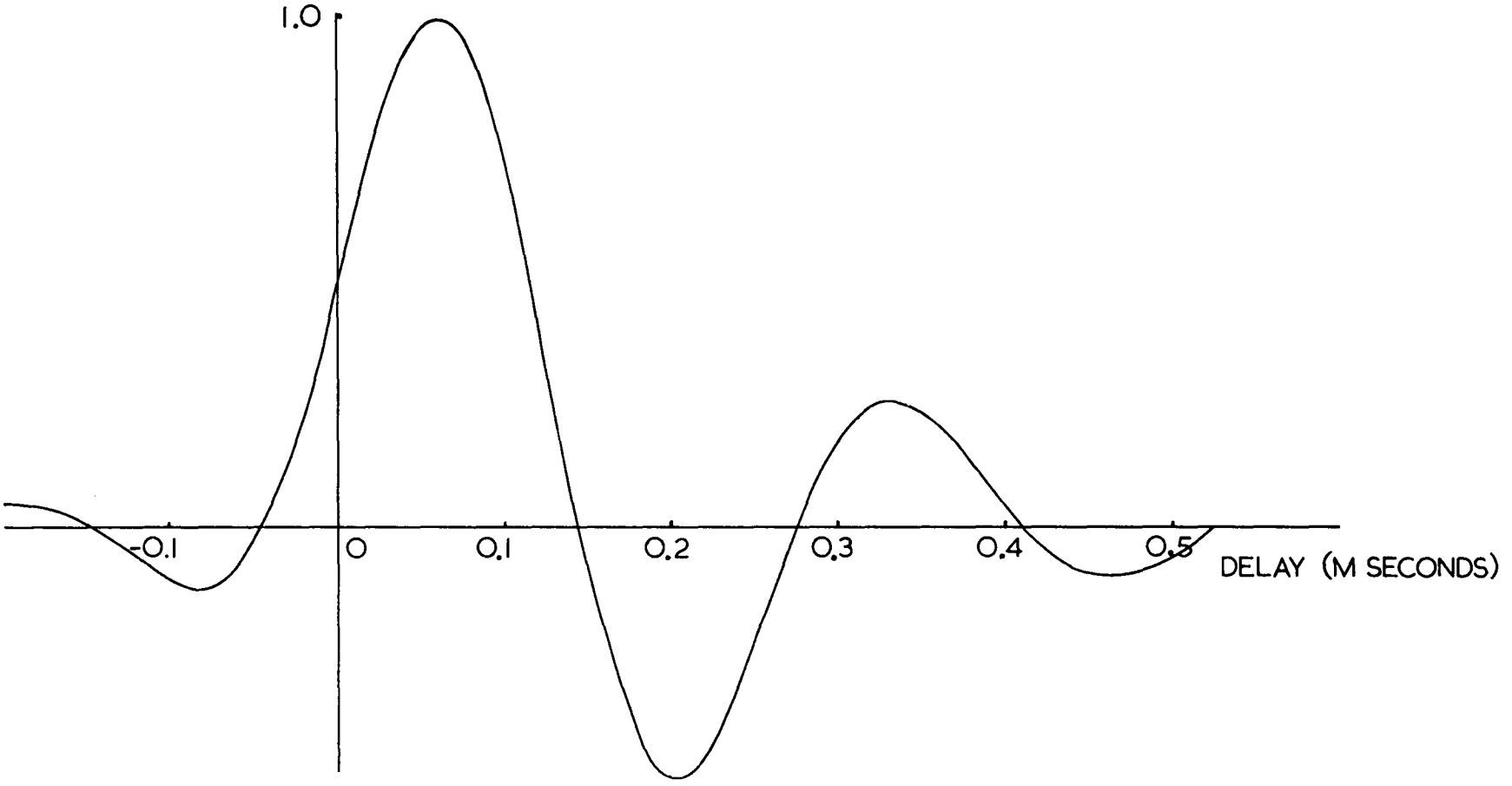

FIG. 4.3 CROSSCORRELATION FUNCTION OF INPUT – OUTPUT SIGNALS OF CHANNEL SIMULATION FILTER

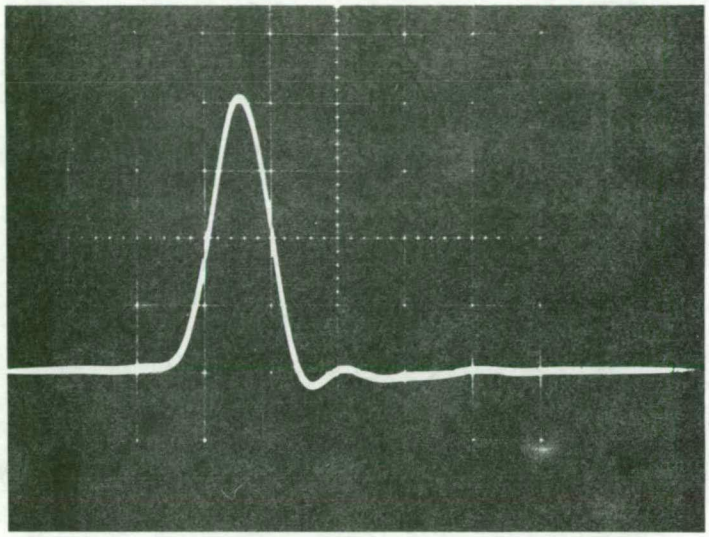

FIG. 4.4 EQUALISED 2T PULSE RESPONSE (DELAY LINE)

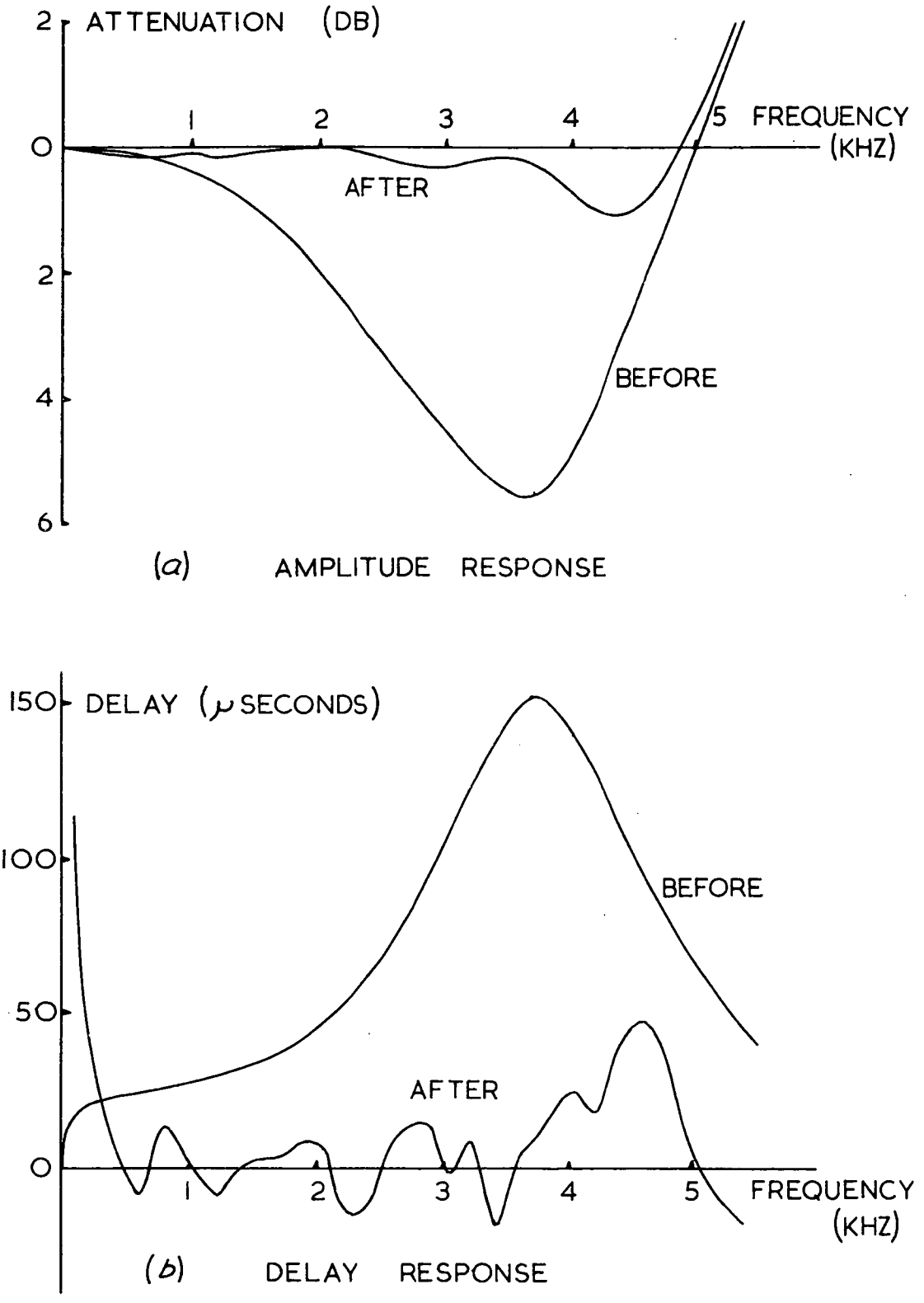

FIG. 4.5 FREQUENCY RESPONSE BEFORE AND AFTER EQUALISATION USING DELAY LINE

The second factor is the relative number of pre-echoes and post-echoes of the received signal generated by the delay line. Increasing the delay of the reference signal by 100 microseconds was equivalent to moving the main tap one section down the delay line, thereby producing one extra pre-echo and one less post-echo.

From fig. 4.2 it can be seen that a minimum value of the error occurred at the time delay values of (100k + 70) microseconds, where k = 0, 1 ..., 10. Thus, the expected value of delay introduced by the channel simulation filter is 70 microseconds. This was proved correct by measuring the cross-correlation function of the input signal to the channel simulation filter with the output of the filter (fig. 4.3). The maximum value of this function is at a delay value of 70 microseconds.

Fig. 4.2 also indicates that for the system having from one to four pre-echo taps the minimum value of the error obtained was approximately constant. The absolute minimum value measured was for the delay of 470 microseconds. The accuracy of the equalisation achieved for the reference signal delayed by 470 microseconds is illustrated by the pulse response and frequency characteristics of the equalised simulation channel (figs. 4.4 and 4.5).

The 2T pulse response was measured by holding the tap settings and replacing the pseudo random noise input signal with the sine squared pulse. Thus, the equalised pulse must be compared with the response of the Butterworth filter (fig. B.5 in appendix B) to establish the accuracy of the equalisation.

The equalised pulse has a K_{2T} rating of approximately 2.1 compared with the unequalised pulse 7.0 (fig. B.7) and the reference pulse 1.15 (fig. B.5). This indicates quite a marked improvement in the performance of the simulated channel.

To measure the delay versus frequency response of the equalised channel a low frequency generator was connected to the input of the channel simulation filter. A phase meter was used to detect the phase shifts, ϕ_1 and ϕ_2, between the input to the channel simulation filter and the output of the summation amplifier, at the frequencies ω_1 and ω_2. The time delay,

τ , was then calculated from the relation:-

$$\tau = -\frac{d\phi}{d\omega}$$

$$\simeq -\frac{\phi_2 - \phi_1}{\omega_2 - \omega_1} \qquad 4.1$$

Because of the logarithmic frequency scale on the signal generator the accuracy of the higher frequency results was very limited. The time delay graphs of the equalised responses are therefore not accurate plots. The unequalised response, however, was calculated theoretically.

These curves also indicate the marked improvement in the transmission characteristic after equalisation.

To complete the static measurements, the effect of varying the length of the pseudo random binary sequence (by varying the value of N) on the static accuracy of the equalisation was investigated. To carry out this investigation the r.m.s. amplitude of the reference signal and the output of the channel simulation filter were maintained at constant values. The r.m.s. amplitude of the error was then measured after the system had settled for each value of N. The delay between the reference and "transmitted" signals was kept at 470 microseconds. To obtain this delay with the signal generator used the maximum value of N was limited to ten.

With the output of the simulation filter and the reference signal set at 0.7 volts and 0.5 volts respectively, the error voltage varied insignificantly from 0.1 volts for N taking the values ten, nine and seven. A slight increase was noticed for N equal to seven but the change was not sufficient to be measured with the voltmeter used.

For N equal to six or five the system would not converge when using the infinite clipper. However, without the infinite clipper and with the correlation multipliers adjusted for minimum d.c. offset, correct equalisation could still be maintained for both these values of N. Switching the infinite clipper back into the circuit after the taps had settled to their final values again produced divergence from the equalised condition until all the integrators reached saturation.

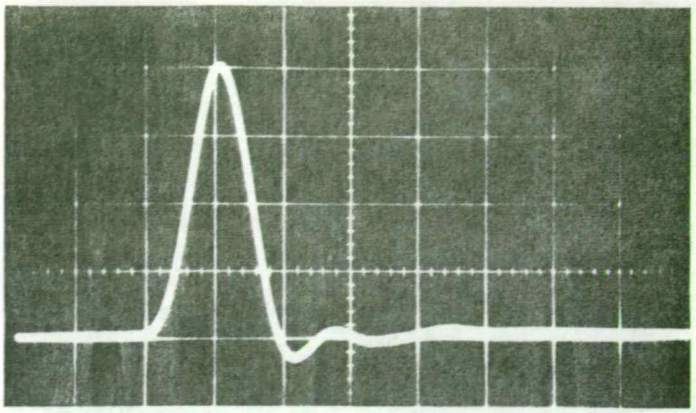

0.2 MS/DIV

(a) $\alpha = \frac{2}{3}B$

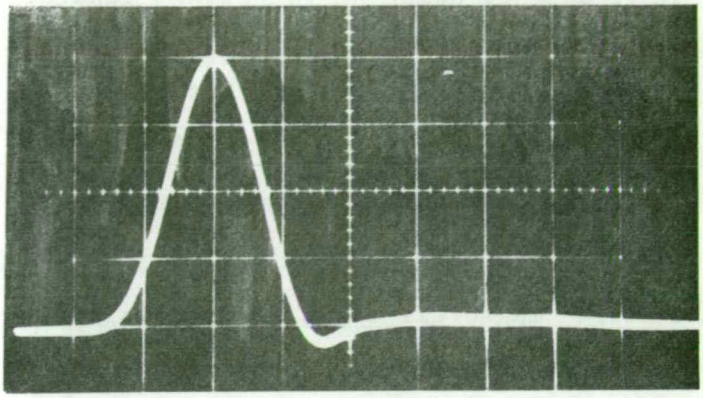

0.2 MS/DIV

(b) $\alpha = B$

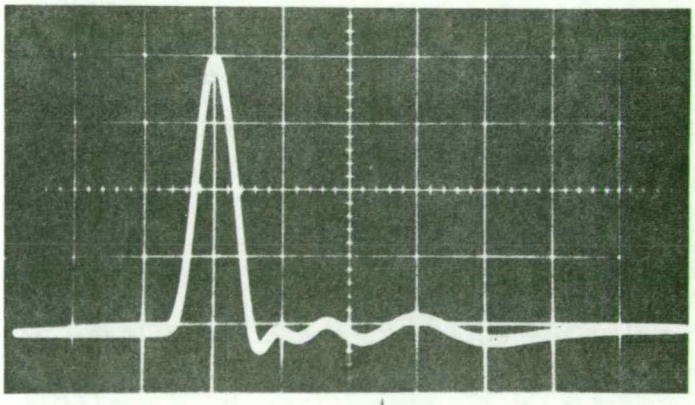

0.2 MS/DIV

(c) $\alpha = \frac{1}{2}B$

FIG. 4.6 EQUALISED 2T PULSE RESPONSES WITHOUT CHANNEL SIMULATION FILTER (LAGUERRE FUNCTIONS)

It must be noted that, for these two cases, the period of the pseudo random noise was shorter than the dispersion produced by the channel simulation filter. Lucky and Rudin have indicated that if the period of the pseudo random noise is shorter than the length of the dispersion of the channel the cross-correlators will react to properties of the test signal rather than properties of the channel. This provides a good example of the need for a relatively high value of N to obtain convergence for all distortions likely to be found in practical situations.

4.3.2 The Laguerre Functions

A major difference between the Laguerre functions and the delay line is that the delay line may simulate a perfect transmission channel with just the main tap. Because of the low pass filter at the input of the Laguerre variable function generator, a number of Laguerre functions must be used. For this reason the accuracy of the equalisation obtained using the Laguerre functions was first measured without the channel simulation filter being used in the system. The delay between the two test signals was set at zero. The value of α chosen for the Laguerre functions was $20.95_{10}{}^{3}$ radians per second. This value was based on the value used by Sondhi, that is two thirds the bandwidth of the system.

The resulting 2T pulse response is shown in fig. 4.6(a). From this response which has a K_{2T} factor of 2.2, it is obvious that more than ten taps were required. This was also evident from the value of the tenth tap, which was at 6% of the value of the first tap.

The effects of varying the value of α relative to the cutoff frequency of the system were also investigated. Instead of varying the transfer functions of the Laguerre networks however, it was far simpler to change the cutoff frequency of the Butterworth filter patched on the analogue computer by altering the feedback condensers in the inverse ratio to the frequency change. Because no delay was required between the reference and "transmitted" signals the output of this filter was used for both these signals. To compensate for the alteration in the bandwidth of the system the half amplitude duration of the 2T pulses were also adjusted to maintain the correct frequency relationship.

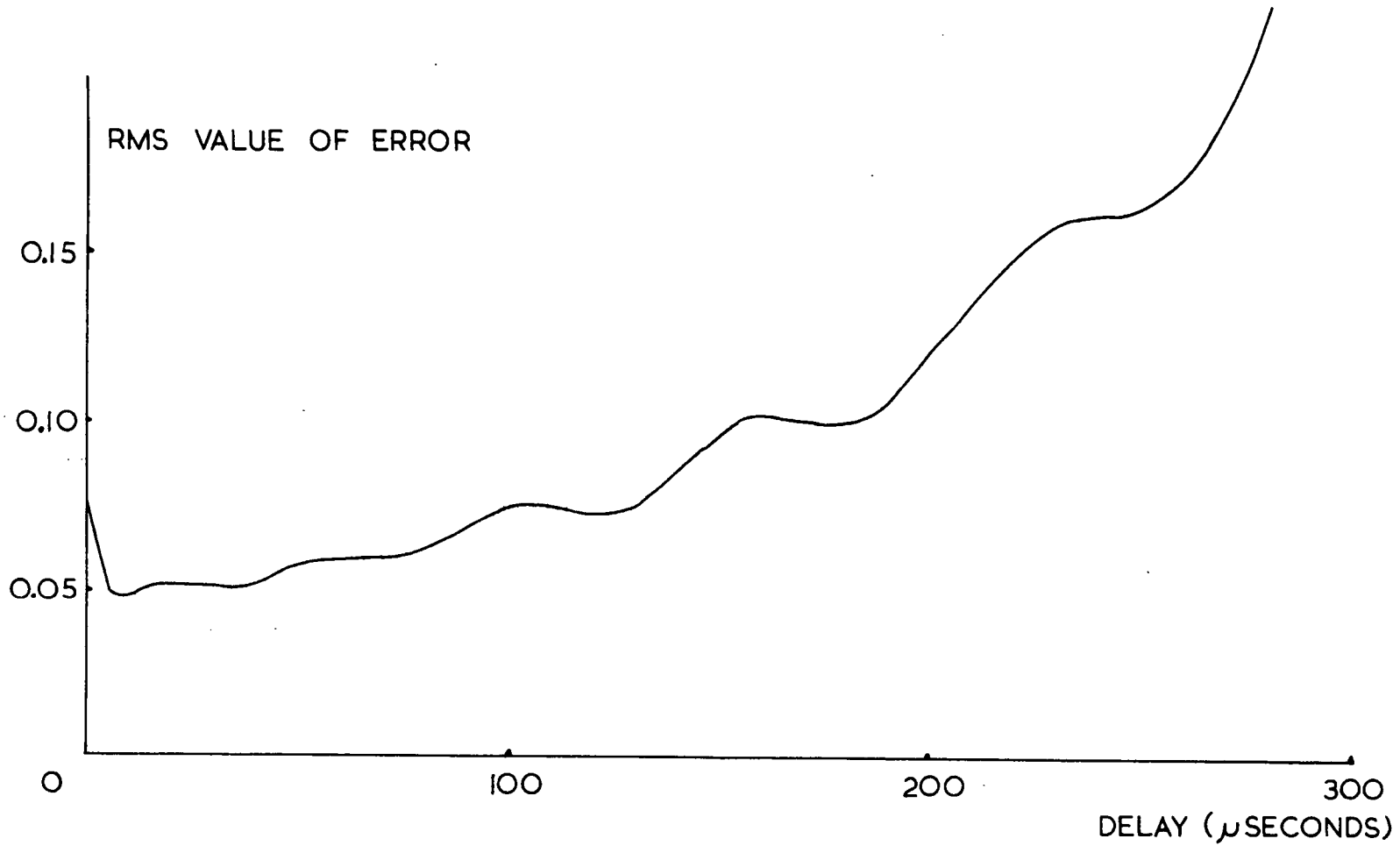

FIG. 4.7 EFFECT OF REFERENCE SIGNAL DELAY ON ACCURACY OF EQUALISATION (LAGUERRE FUNCTIONS – NO DISTORTION)

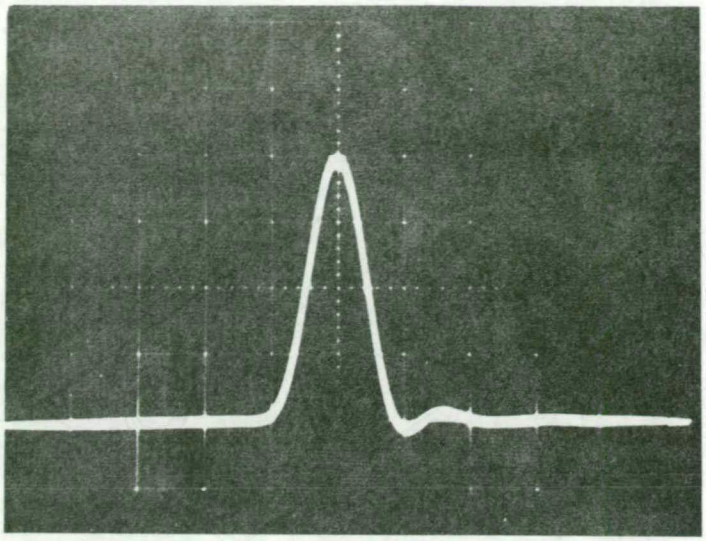

FIG.4.8 EQUALISED 2T PULSE RESPONSE WITHOUT CHANNEL SIMULATION FILTER - 10 MICROSECOND DELAY (LAGUERRE FUNCTIONS)

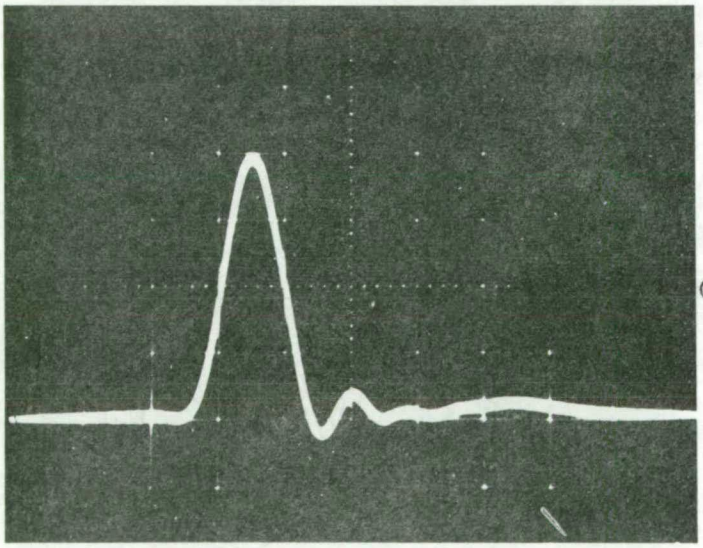

FIG. 4.9 EQUALISED 2T PULSE RESPONSE WITH CHANNEL SIMULATION FILTER (LAGUERRE FUNCTIONS)

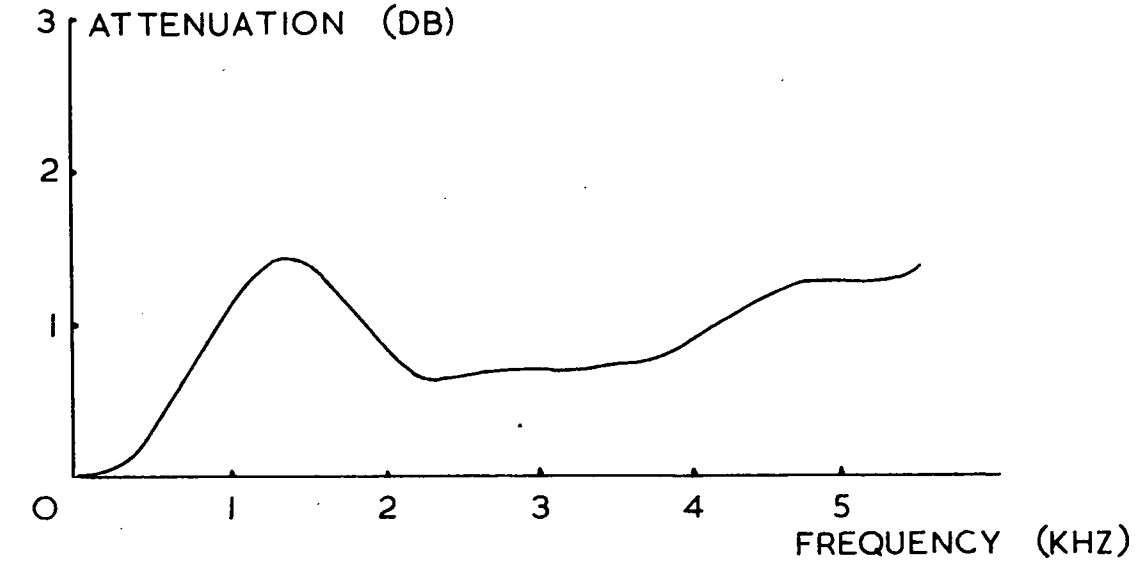

(a) AMPLITUDE RESPONSE

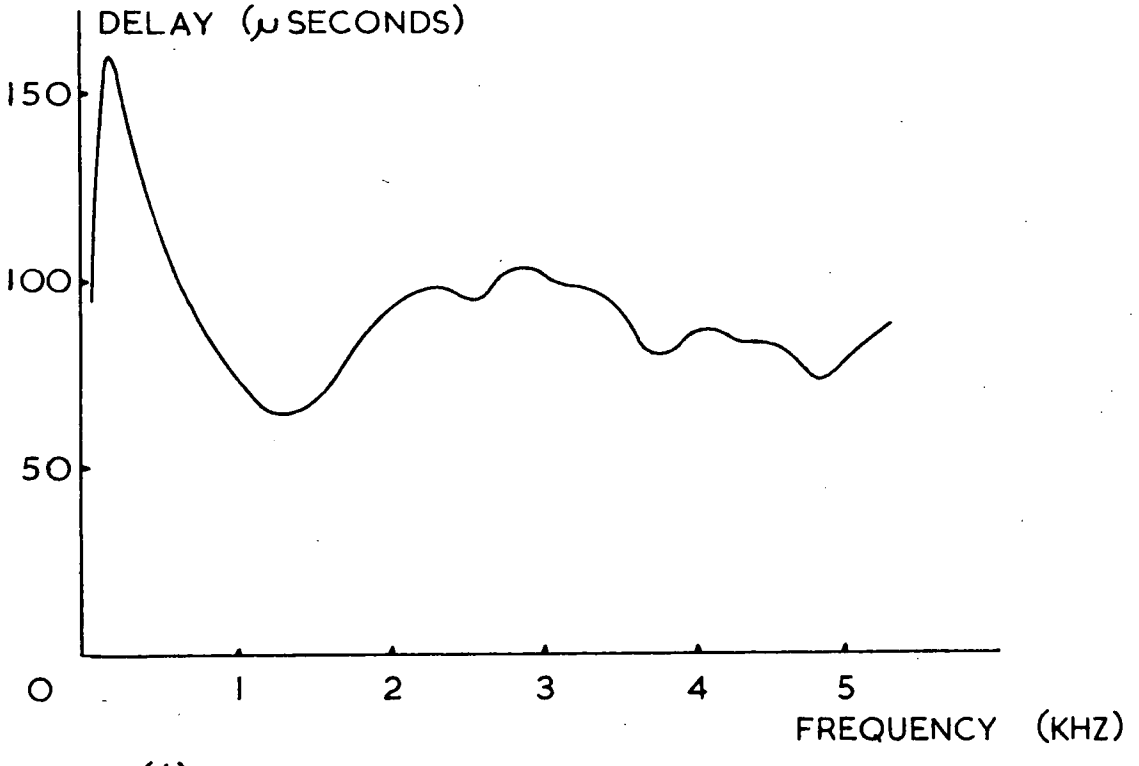

(b) DELAY RESPONSE

FIG. 4.10 FREQUENCY RESPONSE AFTER EQUALISATION USING LAGUERRE FUNCTIONS

The equalised response with the value of α equal to the bandwidth of the system is shown in fig. 4.6(b) and with α equal to half the bandwidth in fig. 4.6(c).

To investigate the effect of varying the delay between the reference and "transmitted" signals when using the Laguerre function generator ($\alpha = \frac{2}{3}$ B) the same procedure was adopted as previously used for the delay line. The results, without the channel simulation filter, are shown in fig. 4.7.

The best equalisation was achieved with a delay of 10 microseconds. The improved equalisation, compared with the result using no delay (fig. 4.6(a)) can be seen from the pulse response shown in fig. 4.8 (K_{2T} factor 1.16).

With the introduction of the channel simulation filter the best equalisation was achieved with a delay of 90 microseconds. The equalised pulse and frequency responses are shown in fig. 4.9 and 4.10. The K_{2T} rating of this pulse response is approximately 4.7. This poor K_{2T} factor, the result of the distortion occurring more than 8T from the pulse, could have been reduced by a larger equaliser. The frequency responses also indicate that the quality of the equalisation was poorer than that obtained with the delay line equaliser.

4.4 Dynamic Performance of the Experimental Equaliser

To measure the dynamic performance of the completed experimental equaliser a U.V. recorder was used to record the mean square value of the error during the convergence process. The circuit used to obtain the mean square error was the same as that used for the cross-correlation measurements (appendix B, fig. B.25). The time constant of the low pass filter was chosen to minimise the a.c. component of the signal on the recorded output but with a sufficiently high cutoff frequency so as not to distort the convergence transient.

4.4.1 The Delay Line Equaliser

An extensive investigation of the dynamic performance of this equaliser was carried out. This included measuring the system's performance both with the channel simulation filter connected and without any distortion in the "transmission" channel.

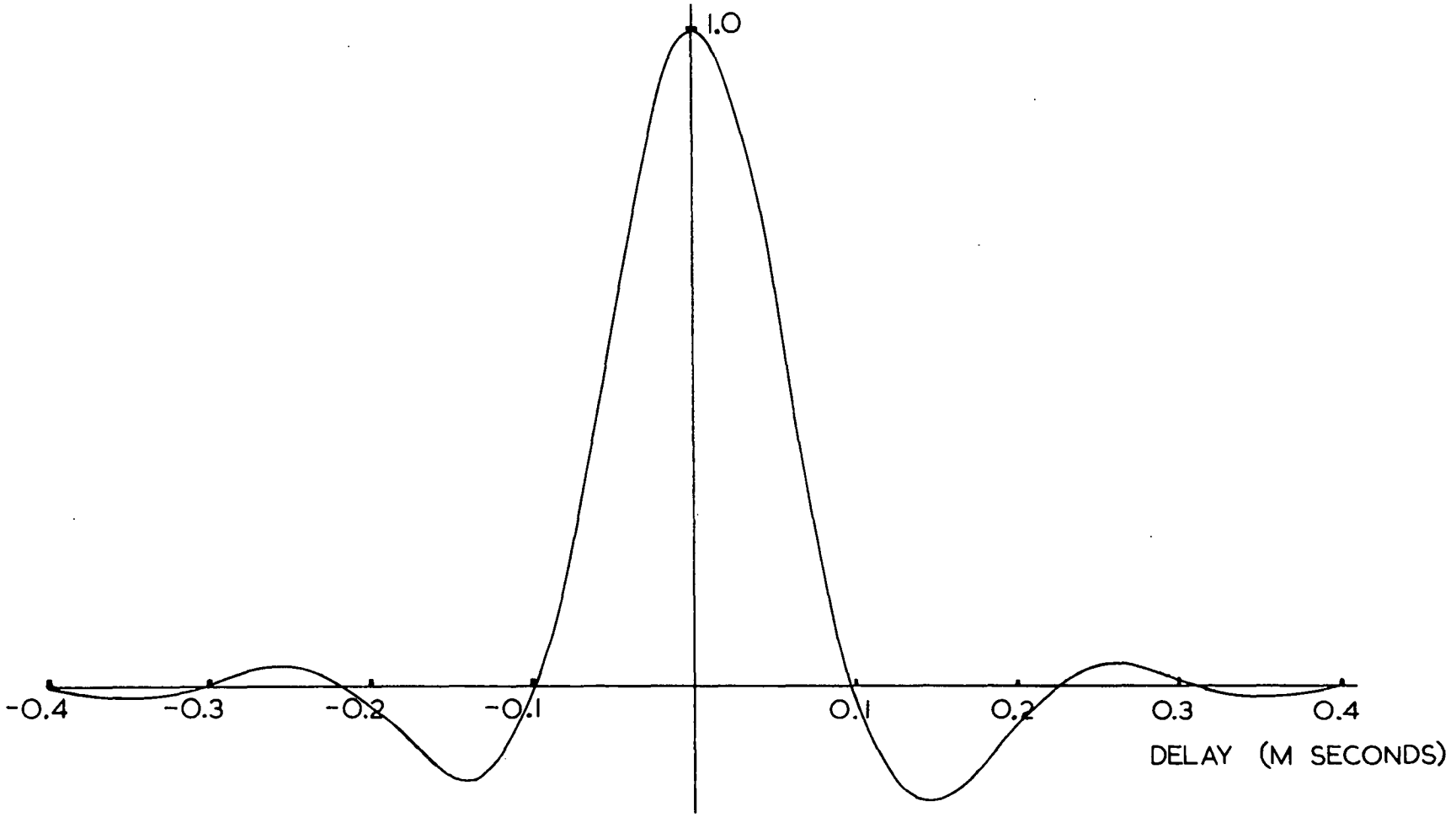

FIG. 4.11 AUTOCORRELATION FUNCTION OF OUTPUT SIGNAL OF BUTTERWORTH FILTER

From the U.V. records obtained, using integrators only in the correlation circuits, the following observations were made -

1. With the infinite clipper in the error circuit the settling time was -
   (a) Inversely proportional to the r.m.s. value of the input voltage to the delay line.
   (b) Directly proportional to the value of $\sqrt{R^T R}\big|_{t=0}$
   (c) Inversely proportional to the gain of the feedback loops.
2. Without the infinite clipper the settling time was -
   (a) Inversely proportional to the mean square value of the input voltage to the delay line.
   (b) Independent of the value of $\sqrt{R^T R}\big|_{t=0}$
   (c) Inversely proportional to the gain of the feedback loops.

These results substantiate the linear transient response obtained with the infinite clipper and the exponential transient response obtained without the infinite clipper, as shown theoretically in chapter 3.

Some of the settling times measured, together with the system parameters used, are shown in the following table. Because of the exponential characteristics measured, the results indicated were the times taken for the mean square value of the error to settle to within 5% of its initial value.

	no distortion in "transmission" channel	with channel simulation filter
Amplitude of input signal to the delay line (v.r.m.s.)	1.5	1.5
Amplitude of reference signal (v.r.m.s.)	1.0	1.0
Delay of reference signal (microseconds)	300	470
Correlation averaging circuit transfer functions (G(s))	$\frac{10}{s}$	$\frac{10}{s}$
Output of clipper (volts)	±8	±8
Settling time with clipper (95%) (seconds)	0.48*	0.73
Settling time without clipper (95%) (seconds)	6.0	7.3

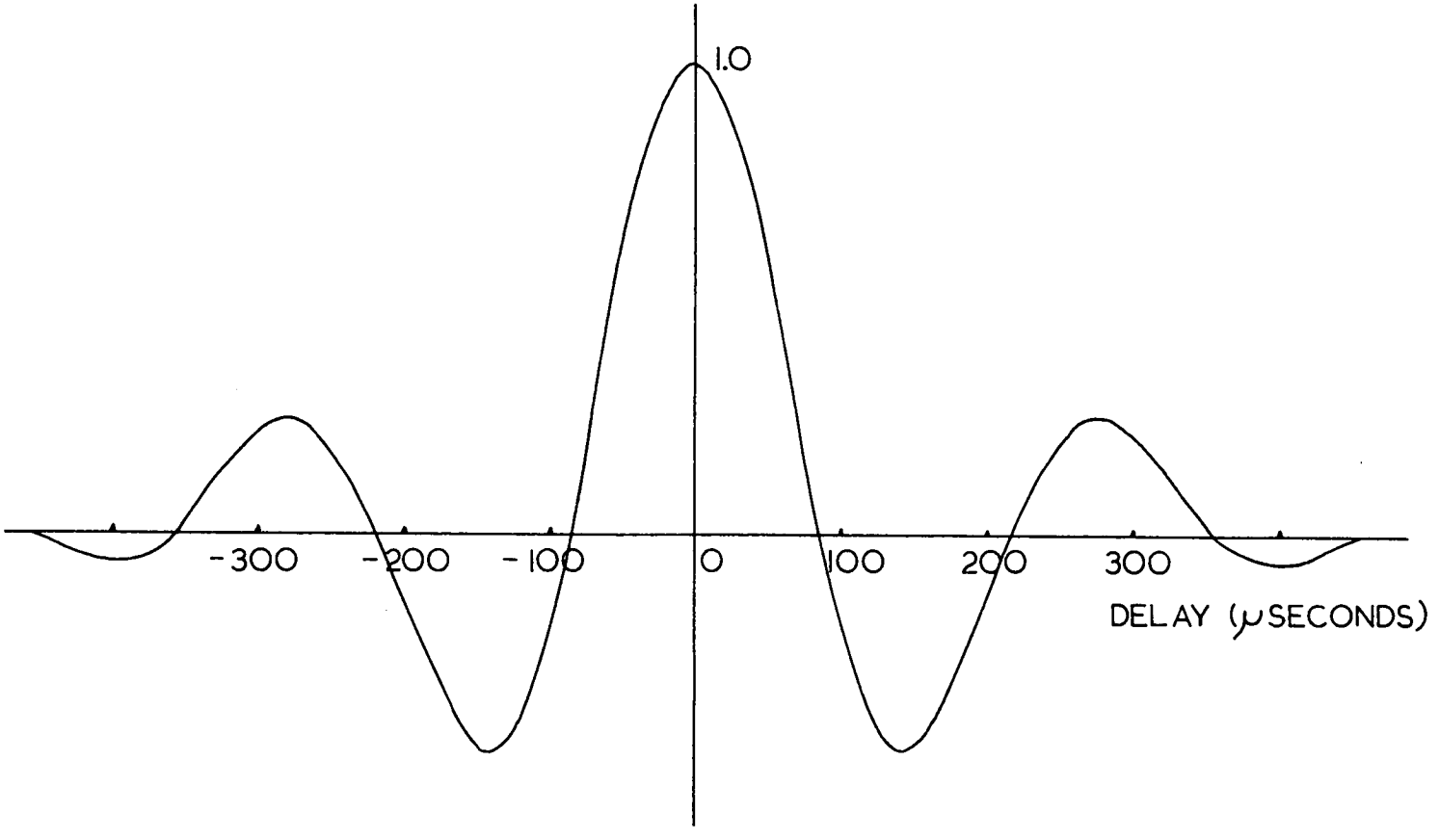

FIG. 4.12 AUTOCORRELATION FUNCTION OF OUTPUT SIGNAL OF CHANNEL SIMULATION FILTER

With the exception of the result marked with an asterisk the nature of the recorded traces limited the accuracy of the measured results to approximately 5%. The limited accuracy was the result of a.c. components on the recorded signal and the very flat slopes recorded during the latter stages of convergence. In the case of the marked result the rate of convergence was sufficiently fast to enable an accurate estimate of the settling time to be made.

The dependence of the settling times on the orthogonal property is readily demonstrated with these results.

From the experiments performed with the three tap equaliser it was noticed that the tap responses were typical of an orthogonal system. To extablish this fact the auto-correlation function of the output of the Butterworth filter was measured, and the results shown in fig. 4.11. From this graph it can be seen that using the delay line equaliser, with each delay section providing a delay of 100 microseconds, the resulting system is very nearly orthogonal.

The autocorrelation function of the output of the channel simulation filter is shown in fig. 4.12. This figure illustrates the loss of the orthogonal property with the introduction of this distortion.

The effect on the settling times can be seen from the results obtained without the infinite clipper. For this case the settling times are independent of the value of $\sqrt{R^T R}\big|_{t=0}$. While the amplitude of the input signal to the delay line was constant there was an increase in the settling time by a factor of approximately 1.25 with the introduction of the channel simulation filter.

The settling times obtained, without the channel simulation, were compared with theoretical results, calculated using equations 3.6

$$\sqrt{R^T R}\big|_{t=0} \exp(-K\sigma^2\lambda_{max}t) \leq \sqrt{R^T R} \leq \sqrt{R^T R}\big|_{t=0} \exp(-K\sigma^2\lambda_{min}t)$$

and 3.7

$$\sqrt{R^T R}\big|_{t=0} - \sqrt{\frac{2}{\pi}} K\sigma\lambda_{max}^{\frac{1}{2}} \quad t \leq \sqrt{R^T R} \leq \sqrt{R^T R}\big|_{t=0} - \sqrt{\frac{2}{\pi}} K\sigma\lambda_{min}^{\frac{1}{2}} \quad t$$

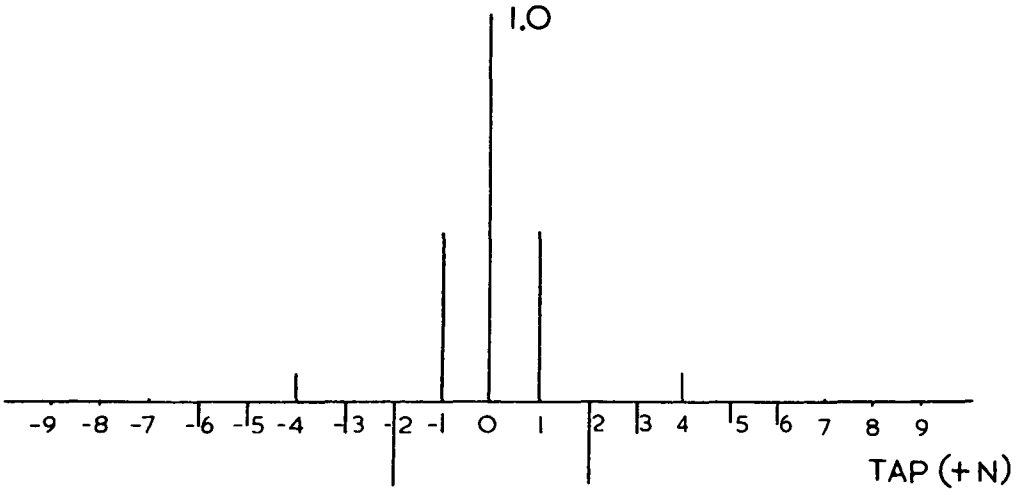

(a) NO DISTORTION

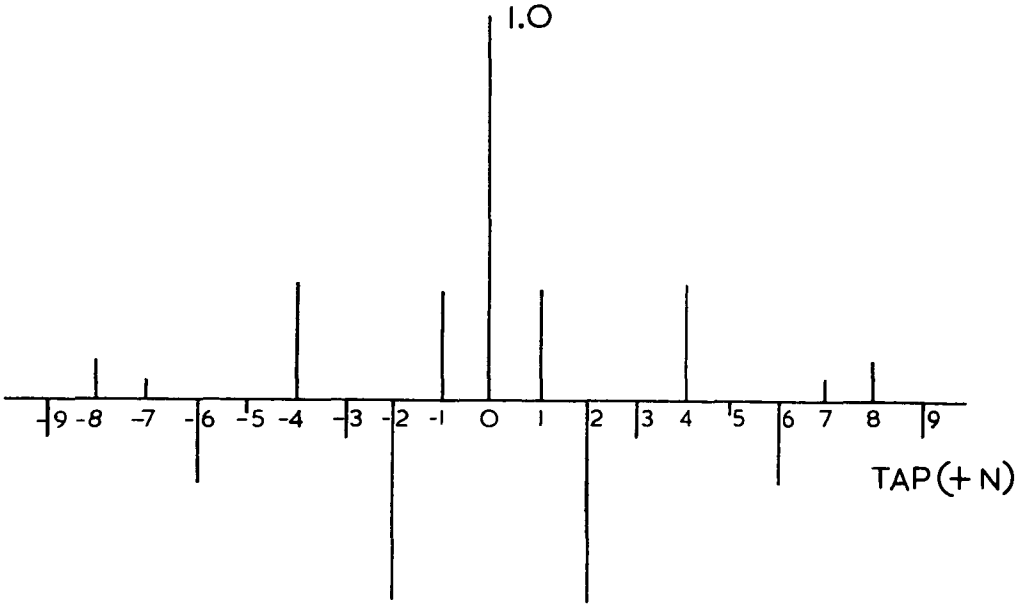

(b) WITH CHANNEL SIMULATION FILTER

FIG. 4.13 CROSSCORRELATION VALUES OF OUTPUT SIGNALS OF LAGUERRE FUNCTIONS WITH OUTPUT SIGNAL OF N^{TH} LAGUERRE FUNCTION

with $\lambda_{min} = \lambda_{max} = 1$. The two sets of results agreed to within the accuracy that the system's parameters could be measured.

From the above equations it can be seen that the two responses are essentially linear or exponential depending on whether or not the infinite clipper is employed. Due to the inequalities, however, the rate of convergence of the linear response or the time constant of the exponential response, may change as the equaliser settles. When using the channel simulation filter it was observed that the rate of convergence of the linear response decreased with convergence and the time constant of the exponential response increased with convergence. When using the infinite clipper, it must also be remembered that during the latter stages of convergence the effect of the residual error is to decrease the rate of convergence (equations 3.23 and 3.24).

If a second time constant was placed in any of the correlation circuits then unstable oscillations at multiples of half the pseudo random noise repetition frequency could be introduced by sufficiently increasing the loop gain of the circuit. This instability could be introduced both with and without the channel simulation filter in the circuit.

With the infinite clipper it was noticed that the unstable condition occurred only after a significant settling period. This was obviously due to the increasing gain provided by the infinite clipper as the error diminished and the instability being produced after the critical loop gain value was reached.

4.4.2 The Laguerre Function Equaliser

The investigation of the dynamic performance of this equaliser followed similar lines to the investigation of the delay line equaliser.

The U.V. recordings taken indicated that the linear and exponential characteristics also applied to this system. The settling time, measured for $\alpha = \frac{2}{3}B$, together with the system parameters used are shown in the following table.

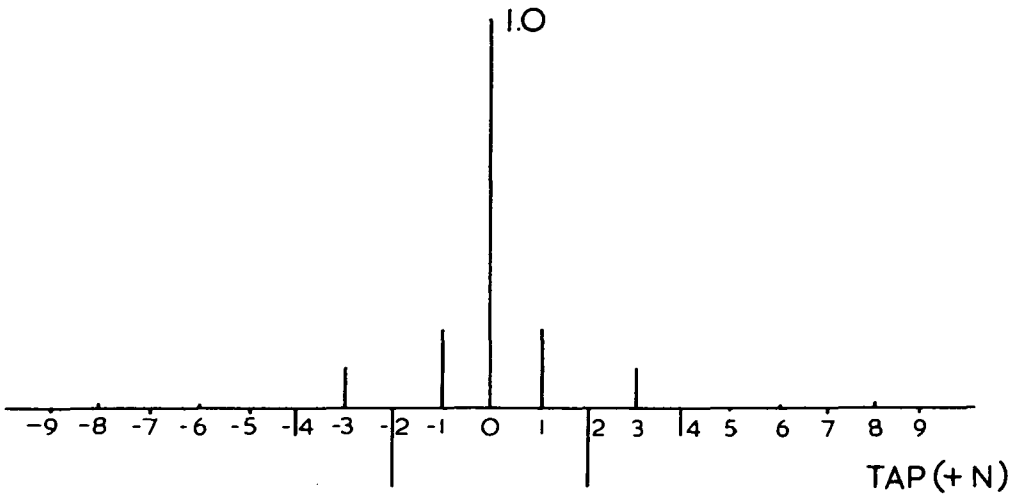

(a) $\alpha = \frac{1}{2}B$

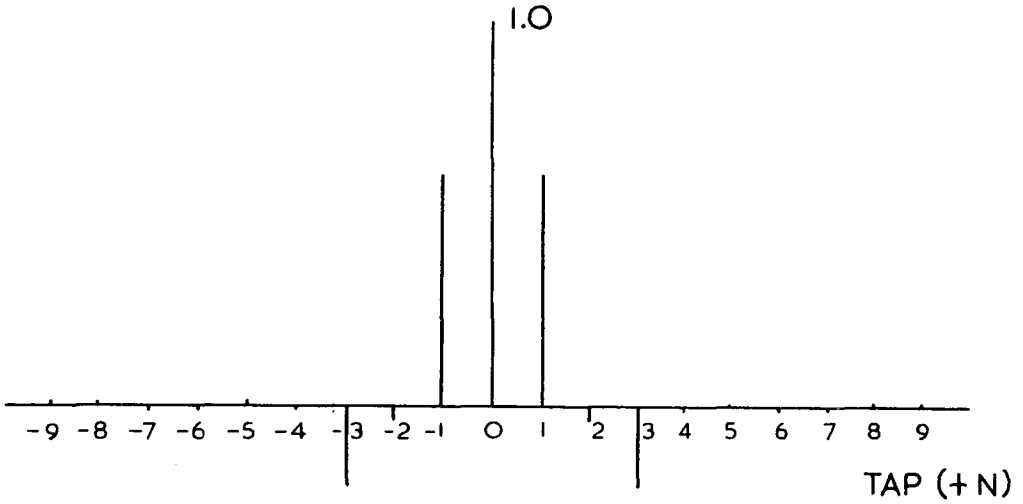

(b) $\alpha = B$

FIG. 4.14 CROSSCORRELATION VALUES OF OUTPUT SIGNALS OF LAGUERRE FUNCTIONS WITH OUTPUT SIGNAL OF N^{TH} LAGUERRE FUNCTION

	no distortion in "transmission" channel	with channel simulation filter
Amplitude of input signal to Laguerre functions (v.r.m.s.)	1.91	1.89
Amplitude of output signal of Laguerre functions (v.r.m.s.)	1.5	1.5
Amplitude of reference signal (v.r.m.s.)	1.0	1.0
Delay of reference signal (microseconds)	10	90
Correlation averaging circuit transfer functions (G(s))	$\frac{10}{s}$	$\frac{10}{s}$
Output of clipper (volts)	± 8	± 8
Settling time with clipper (95%) (seconds)	1.73	1.38
Settling time without clipper (95%) (seconds)	18.6	22.98

Comparing these results with those obtained for the delay line it can be seen that the settling times were much greater with the Laguerre functions. The reason for this is readily demonstrated by the cross-correlations of the output signals, shown in fig. 4.13. This figure illustrates the loss of the orthogonal property when not using a wideband signal with these functions.

The cross-correlation values of the output signals of the Laguerre functions, without the channel simulation filter in the circuit were also measured for each of the other two values of α used previously (fig. 4.14).

Further investigation of the dynamic performance of the Laguerre function equaliser produced similar results to those obtained for the delay line equaliser. These included -

1. When using the infinite clipper the rate of convergence decreased with convergence.
2. Without the clipper the time constant of the transient response increased with convergence.

3. Adding a second time constant to the correlation circuits produced similar instabilities to those recorded with the delay line equaliser.

4.5 The Effect of Noise on the Static Accuracy of the Equaliser

To complete the investigation of the performance of the experimental equaliser the effect of noise on the static accuracy of the system was analysed. From equation 2.20 -

$$\phi_{\eta j} = \Big(\sum_{n=-N}^{N} a_n x_n(t) - y(t) \Big)(x_j(t)) + \sum_{n=-N}^{N} a_n \eta_n(t) \eta_j(t)$$

it can be seen that the impairment by noise on the static accuracy of the equaliser is dependent on three factors -

1. The amplitude of the noise.
2. The cross-correlation values of the noise components of the tap output signals.
3. The values of a_n.

The impairment is therefore dependent on both the characteristics of the noise and those of the transmission channel.

The effect of the amplitude of the noise on the static performance of the equaliser was measured by allowing the system to settle with noise added to the "transmitted" signal. The tap settings were then held and the noise removed from the "transmitted" signal. The effect on the accuracy of the equalisation was then measured by observing the r.m.s. value of the error signal. As the error of an ideal noiseless system is proportional to the amplitude of the reference waveform, the measured error voltages were normalised by dividing the results by the r.m.s. value of the reference signal.

Experiments were performed with the noise introduced both before and after the system had settled.

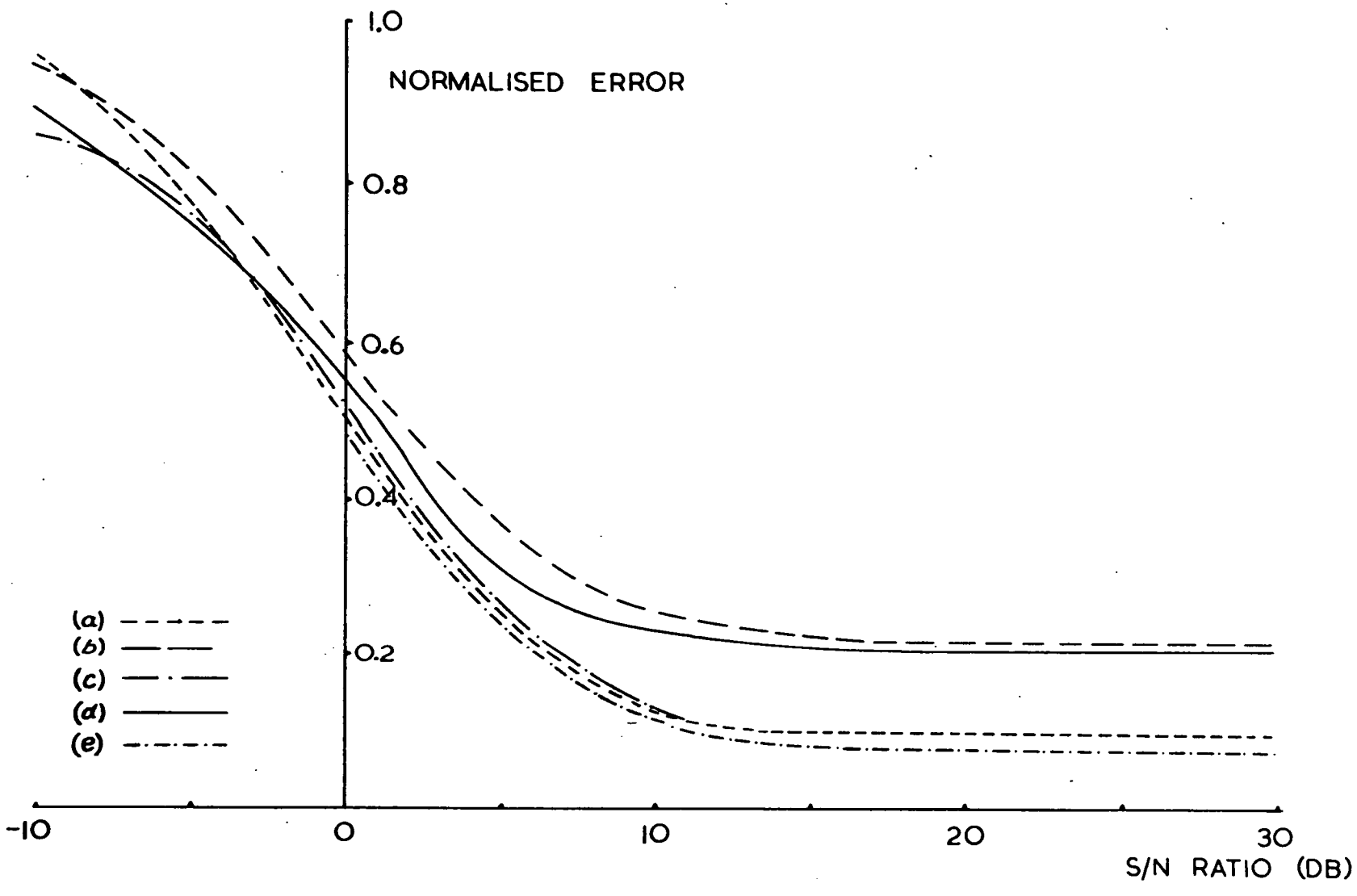

FIG. 4.15 EFFECT OF NOISE ON ACCURACY OF EQUALISATION

Initial results using the delay line were measured without the channel simulation filter in the circuit. For a noise bandwidth of 5 KHz the resulting error amplitude was measured for a number of input signal to noise ratios. The graphs of the results of this test both with and without the infinite clipper are shown in fig. 4.15 (graphs (a) and (b)).

Because the received noise spectrum is often wider than that of the transmitted signal the frequency cutoff of the noise filter was increased to 7.5 KHz. The results obtained using this filter together with the infinite clipper are shown in fig. 4.15 (graph (c)).

Similar results, obtained when using the channel simulation filter, are also shown in this figure (graph (d)). This set of results only varied within 2% when the noise was introduced into either the Butterworth filter, the channel simulation filter or directly into the delay line.

The final graph (e), in fig. 4.15, was the result of measurements taken using the Laguerre functions with the infinite clipper and without the channel simulation filter.

As mentioned previously these experiments were conducted with the noise introduced both before and after the equalisers had settled. From the values measured it was found that in all cases the results were the same, within the accuracy of the equipment used.

The impulsive noise performance objective (S/N ratio) for the Australian television network is 25db. This represents the most severe noise figure to be expected within the network. Thus, the graphs shown in fig. 4.15 indicate that the noise within the transmission channel would have little effect on the equalisation under this condition. Even if this impulsive noise could produce any noticeable distortion, it would be removed during the equalisation period within the following vertical blanking interval. Noise is therefore not expected to be a problem with this form of equalisation.

To illustrate the effect of a large noise component on the resultant equalisation, several pulse responses were photographed after the system had converged with a S/N ratio of zero db. These are shown in fig. 4.16.

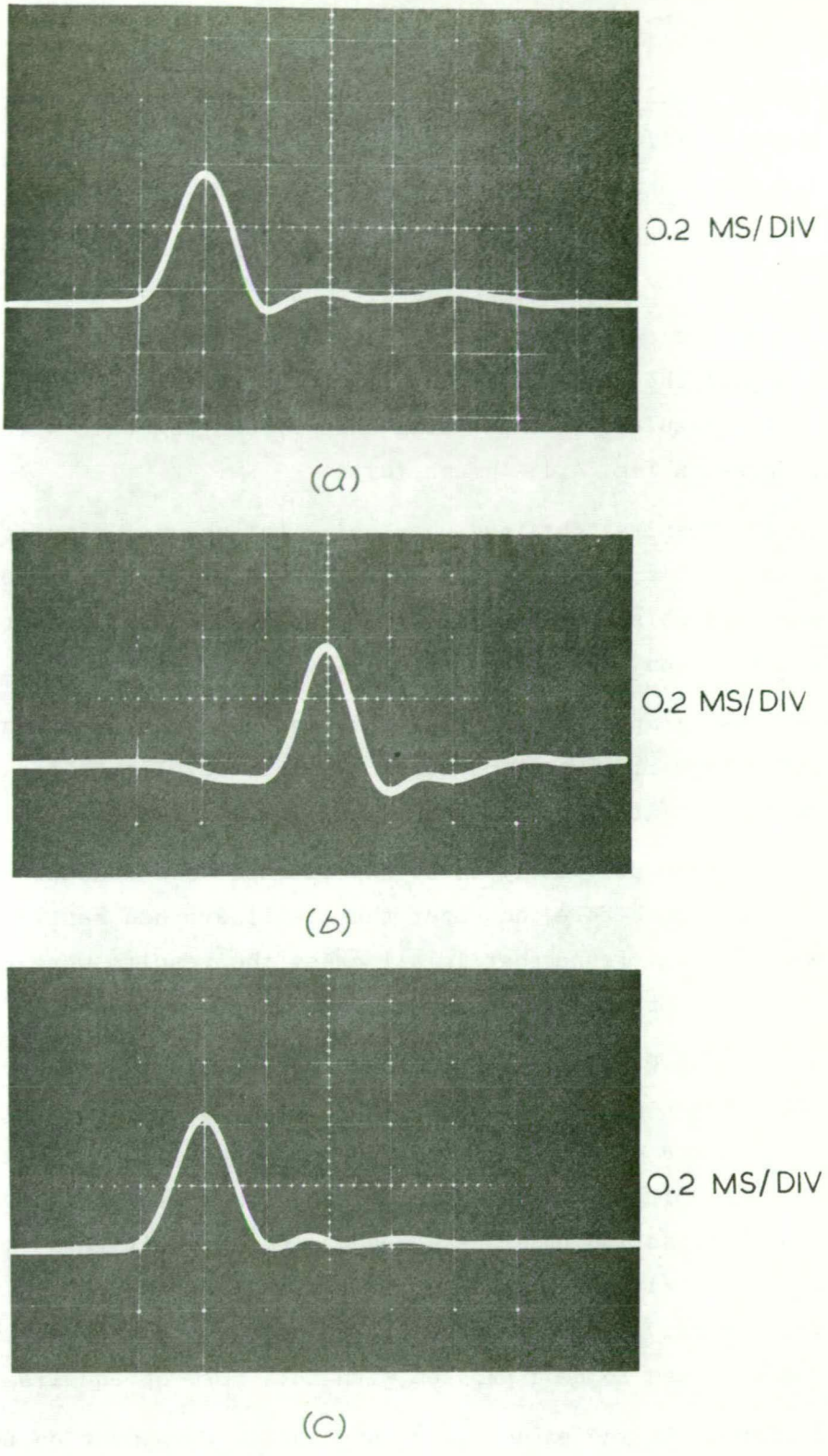

FIG. 4.16 EQUALISED 2T PULSE RESPONSES AFTER CONVERGENCE WITH NOISE (S/N = 0 DB)

Fig. 4.16(a) was the result using the delay line without the channel simulation filter and fig. 4.16(b) the result with the introduction of this filter. The result using the Laguerre functions without the channel simulation filter is shown in fig. 4.16(c). In all three cases the equalised pulse height after settling without noise added to the "transmitted" signal would have been four divisions.

CHAPTER 5

FURTHER CONSIDERATIONS OF THE ADAPTIVE TELEVISION EQUALISER

5.1 General

The definite potential of the proposed method of equalisation has been demonstrated by the results obtained from the experimental system. The performance achieved by the experimental equaliser, however, would have to be improved upon to meet the specifications required of a practical equaliser. Although the 2T pulse response of the equalised channel, using the experimental delay line equaliser was well within television specifications, it can be seen from the amplitude and phase responses that the equalised characteristics were not of sufficiently high standard. With the Laguerre functions the standard of equalisation was even lower.

An important objective in the design of the experimental system was the simplicity of the circuits used. This minimised both the construction time and the cost of the electronic components. One means of improving the static performance of the experimental equaliser therefore, would have been the use of more sophisticated circuitry to improve the overall circuit performance.

Neglecting any imperfect performance of circuits within the equaliser, the accuracy of the equalisation is dependent on the following factors -

1. The number of taps within the adjustable equaliser.
2. The resolution of the tap settings.
3. The accuracy of the timing between the received and reference waveforms.

If more than ten taps had been employed better equalisation would have been achieved by both the delay line and the Laguerre functions. This is clearly illustrated by the equalised pulse response obtained in both cases (figs. 4.4 and 4.9).

For the delay line this fact is also emphasised by the equalised amplitude characteristic (fig. 4.5). From this figure it can be seen that to a first approximation the equalised amplitude characteristic can be represented by the equation

$$|H(j\omega)| = k_o + k_n \cos n\omega T$$

where n = 5, k_o and k_n are constants. To represent the characteristic more accurately then values of n greater than five must also be considered. With reference to equations 1.2 and 1.3 it is readily demonstrated that a larger number of taps are required to further improve the equalisation.

Using a continuous method of tap control, as in the experimental equaliser, an infinite tap resolution can be obtained. However, the accuracy of the tap settings is dependent on the presence of a.c. components on the output signals of the cross-correlators. This fact is discussed in section 5.6.2 and is shown to be a negligible problem.

The timing of the reference waveform relative to the received waveform is very important if optimum use is to be made of the adjustable equaliser. This has already been demonstrated by figs. 4.2 and 4.7, with the experimental system.

The minimum delay adjustment provided by the signal generator used was ten microseconds. Examining closely the results, illustrated by the graph in fig. 4.2, it can be seen that this delay variation was not fine enough to produce the best equalisation possible. An acceptable minimum delay adjustment would have been one microsecond. This corresponds to a timing accuracy of one nanosecond for the practical system. Arnon has also shown, for his particular system, that a tolerance of the order of one nanosecond is required to produce an acceptable equalised delay characteristic. The accuracy of the equalisation provided by the experimental system could have been improved therefore, had the minimum delay adjustment between the two pseudo random noise signals been much finer.

Considering the limitations of the experimental equaliser, the static accuracy results indicate that a satisfactory performance could be expected from a television equaliser based on the same principles.

The settling time of the practical television equaliser using a continuous method of tap control may be calculated by assuming the practical equaliser to be a frequency scaled version of the experimental system. Under this condition the settling times of the practical equaliser are one thousandth the settling times measured for the experimental system.

The settling times obtained with the experimental delay line equaliser for 95% convergence were of the order of 0.7 seconds with the infinite clipper and seven seconds without it. Thus, the equivalent settling times for a frequency scaled practical television equaliser are 700 microseconds and seven milliseconds respectively.

Because the television equaliser can only be adjusted during the vertical blanking interval the overall time taken for the practical equaliser to settle will be much longer. The time interval between horizontal synchronising pulses is 59 microseconds. The insertion of the test signal for one complete horizontal line per frame will give an overall settling time of approximately 0.475 seconds when using the infinite clipper. Without the infinite clipper the settling time required is approximately 4.75 seconds.

These figures would be halved if the equaliser were allowed to converge during one line per field.

The actual rate of convergence of the television equaliser will depend on the circuit parameters used. These must be chosen to suit the specific requirements of the television channel. The above results give an indication of the convergence times that may be expected when using the continuous tap control method. The effects of varying any of the circuit parameters may be calculated using the theoretical results discussed in chapter 3.

The settling time results indicate that the rate of convergence of the continuous equaliser would be satisfactory. These times compare favourably with the settling time of five seconds expected of the discrete tap control method, with a tap resolution of approximately ± 255 steps and the taps

adjusted once per frame, as obtained by Arnon.

The performance of the experimental equaliser has indicated that such an equaliser is expected to provide the quality of equalisation and the dynamic performance required of a television equaliser. It has also indicated the relative performance which may be expected between the delay line and Laguerre function equalisers, the performance of the system in the presence of noise, and the performance of the continuous system with extra filtering provided in the correlation circuits.

With this knowledge in mind the design of the equaliser best suited to the requirements of the television channel can be considered. This is discussed in the remaining sections of this chapter.

5.2 The Test Signal

The length of the binary sequence generator is considered in this section. In choosing the value of N there are several factors which must be considered -

1. The length of the time slot during which the test signal may be transmitted.
2. The minimum length of the binary sequence generator required for adequate equalisation.
3. The desirability of a complete number of pseudo random noise periods to be transmitted.

The time available for the transmission of the test signal within one horizontal line is 59 microseconds. Using a pseudo random noise generator with a clock frequency of 100 MHz and N equal to 9, 10, 11 and 12, the periods of the generated signals are 5.11, 10.23, 20.47 and 40.95 microseconds respectively.

The number of complete periods, of these particular signals, which may be inserted within one horizontal line are 11, 5, 2 and 1, with the resulting transmission times of 56.21, 50.15, 40.94 and 40.95 microseconds.

There are several advantages in choosing a relatively small value of N, the most obvious of which is the simpler noise generator required. The shorter signal period produced allows the cross-correlation values of the discrete system to be averaged over a number of periods of the test signal.

For smaller values of N more efficient use can be made of the time available within the horizontal line because the signal may be transmitted for a longer period of time. A significant amount of time must be available within the horizontal line, however, during which the test signal is not transmitted. This must be provided to prevent the horizontal synchronising pulses from affecting the equalisation and to allow any signal transients time to decay.

The advantage of using a larger value of N is the improved distribution and spectral properties of the test signal.

The value of ten is a suitable compromise between these factors. Using this value there are approximately nine microseconds within the duration of the horizontal line in which the test signal is not transmitted.

5.3 Synchronising the Test Signals

The need for accurately synchronising the reference and received waveforms has already been adequately demonstrated in chapter 4. Practically, this will involve controlling, very accurately, both the frequency of the two pseudo random noise generator clocks and the relative phases of the two waveforms. The timing accuracy must also be independent of any distortion within the channel.

Crystal oscillators must be used to maintain the frequency of the generator clocks within the required accuracy.

Two methods of synchronising the waveform generators have been described in the literature, one by Lucky and Rudin [14] and the other by Arnon [17].

The method described by Lucky and Rudin was designed specifically for the mean square error equaliser and may be used regardless of what type of adjustable equaliser is employed.

This technique is based on the fact that the autocorrelation function of pseudo random noise has the shape as indicated in fig. 3.1. (A smoother function is generated at the equaliser because of the filtering action of the $W(\omega)$ weighting function).

An estimate of the arrival time T_a of the received signal $x(t)$ is required, from which the reference signal $y(t)$ can be correctly synchronised. The maximum likelihood estimate of T_a under the assumption that the test signal is Gaussian, white and additive, is found by adjusting T_a so that -

$$q(T_a) = \int_0^{t_1} y(t + T_a)\, x(t)\, dt \qquad 5.1$$

is a maximum.

Because of the noise component in $x(t)$ there will be some ambiguity in deciding where the maximum of $q(T_a)$ is, but this ambiguity can be reduced by increasing the length of the observation time t_1. For a distorted signal $x_d(t)$, only an approximation to the maximum likelihood estimate of T_a is obtained. Again -

$$q(T_a) = \int_0^{t_1} y(t + T_a)\, x_d(t)\, dt \qquad 5.2$$

is maximised.

This has already been demonstrated by the results indicated in chapter 4. Near optimum performance was obtained from the delay line equaliser (fig. 4.2) for a reference signal delay, relative to the main tap, equal to the delay for the maximum of the cross-correlation between the received and reference signals (fig. 4.3).

To find the maximum of $q(T_a)$, assuming it to be convex function, the partial derivative of equation 5.2 with respect to T_a is set to zero.

$$\frac{\partial q(T_a)}{\partial T_a} = 0 = \int_0^{t_1} \dot{y}(t + T_a)\, x_d(t)\, dt \qquad 5.3$$

where $\dot{y}(t)$ is the time derivative of $y(t)$. The correct reference signal timing

can be obtained by using another cross-correlator to correlate the signals $y(t + T_a)$ and $x_d(t)$ and adjusting the phase of the generator clock according to the sign of the output of the correlator.

Such an approach cannot be used directly however, as $q(T_a)$ will not be a convex function. This is readily demonstrated by the graph in fig. 4.3.

Lucky and Rudin overcame this problem by using two successive modes to search for the absolute maximum. The first mode was designed to roughly line up the reference signal with the received signal as it appeared at the main tap. This coarse alignment was achieved by performing the cross-correlation indicated by equation 5.2 and adjusting the phase of the reference timing signal until the output of the cross-correlator reached a predetermined threshold. The function $q(T_a)$ could then be assumed to be convex over a small region about this position. The second mode was then the application of the technique indicated by equation 5.3.

As the television system is a synchronised system sufficient timing information could be extracted from the received signal to obviate the necessity of using the coarse adjustment mode for the television equaliser.

The problem with using the technique indicated by equation 5.3 for the television equaliser is that the test signal is only transmitted for a very short period of time. Under this condition there will be insufficient time for the timing of the reference signal to be adjusted correctly before the commencement of the equalisation process.

This problem may be overcome by transmitting a test sequence within the horizontal line preceding the line in which the equalisation process is performed. Once the two generator clocks have been synchronised the phase of the reference generator clock would be locked ready for transmission of the actual test signal. Thus, synchronisation of the two signal generators is achieved before the equalisation process commences. If required, the phase of the reference generator clock may also be controlled during the equalising period.

The method used by Arnon for synchronising the two waveforms involves transmitting a timing reference over the channel and synchronising both waveforms relative to this timing reference. This method was designed for use with Arnon's absolute error equaliser and is not as suitable for the proposed method of equalisation as the technique described by Lucky and Rudin.

Using this method the timing reference would be provided by a 5 MHz crystal oscillator at the transmitter which is locked to a 100 MHz clock. A short burst would be cut from the 5 MHz oscillator and added to the horizontal line preceding the line in which the test signal is transmitted. This burst provides a timing reference, relative to the 100 MHz oscillator at the transmitter, which can be extracted at the receiver.

At the receiver, the zero crossings of the 5 MHz burst would be detected and used to phase lock the local 100 MHz oscillator. The last cycle of the 5 MHz burst would then be detected and used as the timing reference from which the reference signal generator would by synchronised. After a predetermined number of cycles of the 100 MHz oscillators following this reference both oscillators would be connected to their binary sequence generators. Viewed from the receiver, both signals would commence at the same time.

A disadvantage of this system is that the timing reference may be delayed by a distortion within the transmission channel. As this reference is a single frequency the delay may not be representative of the delay imposed on the test signal by the distortion. For this reason this method is not expected to be suitable for the proposed method of equalisation.

5.4 Accurate Equalisation over the Complete Television Spectrum

The standard Australian television channel consists of an ideal low pass characteristic with a cut-off of 5 MHz. Since it is not possible to produce an ideal filter characteristic it is normal for television channels to be produced with a cut-off frequency higher than 5 MHz so that the overall cut-off of the television system plus broadcast transmitter produces an acceptable characteristic up to 5 MHz. To maintain such a characteristic after equalisation, Potter [21] suggests the use of the model channel in both

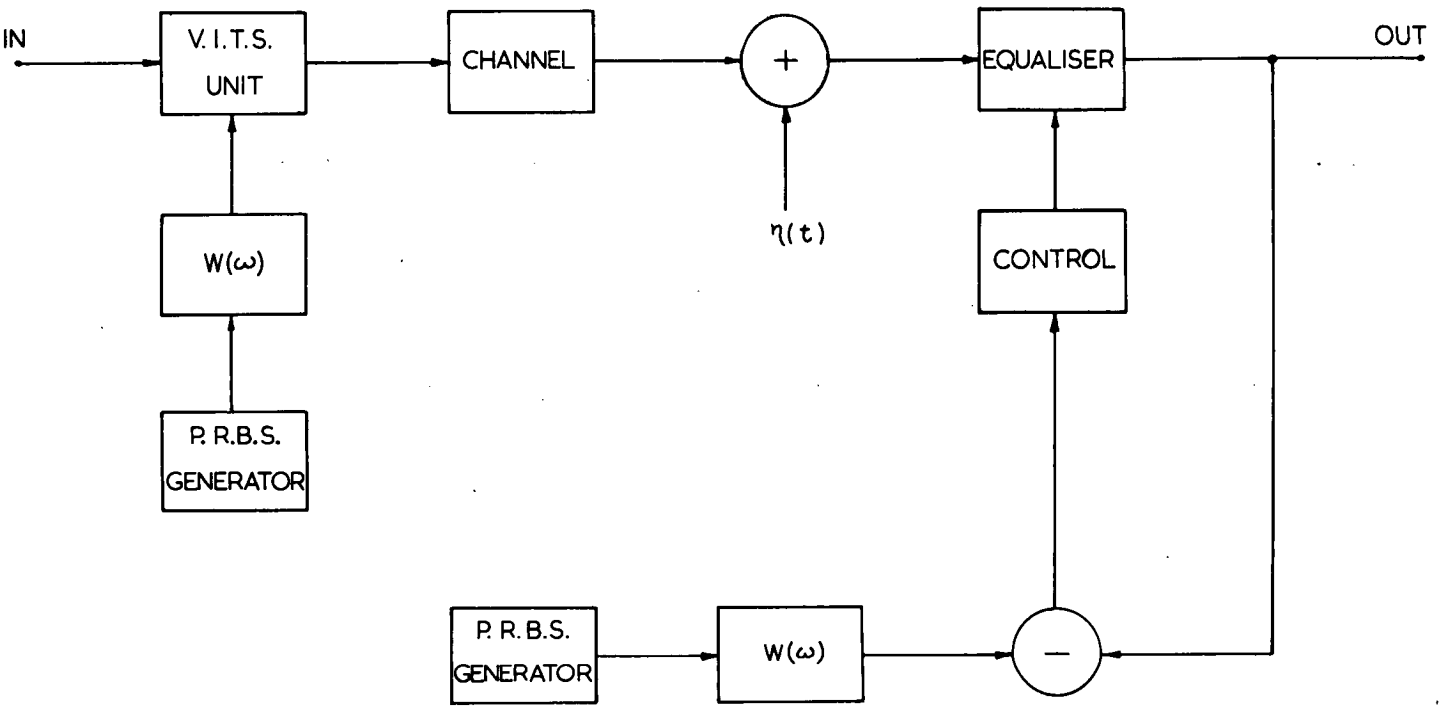

FIG. 5.1 ADAPTIVE EQUALISER FOR A T.V. CHANNEL

signal paths leading to the equaliser control network. The model channel proposed by Potter is the filter characteristic discussed previously in section 3.4.

In the equalising system envisaged by Potter the extra model channel is placed between the adjustable equaliser, after the output of the direct signal path, and the difference circuit used to obtain the error between the equalised and reference waveforms. Placing the model channel outside the direct signal path ensures that the benefit accruing from a channel cut-off frequency greater than 5 MHz is maintained.

If this extra model channel filter is to be included when using correlation techniques, then it must be placed at some other point within the system. This will be necessary to prevent it being placed within the controlling feedback loop of the automatic equaliser. The system shown in fig. 5.1 may be used to remove the filter from the direct signal path and from within the control network.

Referring to Lucky and Rudin's original system (fig. 2.3) the two model channel filters then effectively become the spectral weighting functions of the mean square error equalising system. The actual model channel is then a perfect characteristic with flat amplitude and linear phase responses within the frequency band of interest. The resulting equalising system is similar to the experimental system discussed in chapter 4.

To ensure accurate equalisation over the full television spectrum for his particular equaliser, Arnon chose the equalisation bandwidth to be 10% higher than the bandwidth of the television channel. This was to reduce the effect of timing errors which tended to produce large delay errors at the top of the passband. The extra 10% equalised bandwidth provided a guard band which absorbed these errors.

This technique could be used with the proposed method of equalisation. However, provided the timing accuracy of the reference waveform can be maintained within acceptable limits the system shown in fig. 5.1 should prove of sufficient worth without the need for equalising over a larger bandwidth.

Consideration must now be given to the choice of the spectral weighting functions.

The reason for the inclusion of the spectral weighting functions within the equalising system is to provide a means of assigning a relative weight to the equalisation error at each frequency. From equation 2.11

$$D_{MS} = \int_{-\infty}^{\infty} |H(\omega) - G(\omega)|^2 \, |W(\omega)|^2 \, d\omega$$

it can be seen that the effective weighting is provided by the non-negative function $|W(\omega)|^2$. The phase characteristic of the weighting filters is therefore not important. As phase equalisers are not required to produce an acceptable pulse response from these filters a sharper cut-off characteristic could be employed than is suggested by Potter [21], without an increase in the complexity of the filters.

As the equaliser is only required to correct residual distortions within a channel, an attempt to minimise the settling time can be made by choosing a filter characteristic which produces an orthogonal system for an undistorted channel. As discussed in chapter 2, it is not possible to produce an orthogonal system regardless of the equalisation required, as the channel distortion may affect the auto-correlation function of the received signal.

For the delay line equaliser a filter producing the required auto-correlation function can be realised by modifying the model channel characteristic proposed by Potter. The modifications are necessary to produce a power spectrum characteristic identical to the amplitude characteristic suggested by Potter (fig. 3.2). It is shown in appendix C that the output auto-correlation function of such a filter will, under the conditions described above, produce an orthogonal system. However, it must be remembered that as pseudo random noise is to be used as the test signal the calculated auto-correlation function will be modified slightly.

This proposal is made in an attempt to improve the dynamic as well as the static performance of the equaliser.

5.5 D.C. Restoration

To ensure correct operation of the correlation circuits the d.c. level of the received waveform must be accurately restored.

A clamping unit similar to that used by Arnon could be employed for restoration of the d.c. component. This unit forced the back porch of the horizontal synchronising pulse to ground potential and maintained it there within a fraction of a millivolt. The unit was also used to suppress any d.c. transients generated by the equaliser.

5.6 Considerations in Choosing the Optimum Adaptive Equaliser

5.6.1 The Adjustable Equaliser

The results obtained from the experimental equaliser (figs. 4.4, 4.5, 4.9 and 4.10) indicate that the delay line provides improved equalisation over the Laguerre functions for a similar number of taps. The dynamic performance results obtained (sections 4.4.1 and 4.4.2) also indicate the improved performance obtained using a delay line.

The delay line also has the added advantage that when used in conjunction with the spectral weighting function described in section 5.4 the overall equalising system can be made to approximate an orthogonal system.

Considering these points it appears that the delay line equaliser is the adjustable equaliser better suited to the requirements of the television system. This statement, however, is based purely on the results obtained from the limited number of measurements taken from the experimental equaliser. A more thorough investigation must be carried out before a final decision is made.

5.6.2 The Cross-correlators

Consideration has so far been given to two types of cross-correlators. The first is an approximation to an exact correlator and uses an analogue multiplier and the second, a Stieltjes correlator, uses an infinite clipper and switched modulator.

For the continuous tap control method the use of the Stieltjes correlator has a number of advantages -

1. Because the infinite clipper acts as a high gain amplifier with limiting to prevent saturation, the settling time of the equaliser is decreased.

2. The high gain within the error circuit provided by the infinite clipper minimises the effects of d.c. offsets in the correlation circuits. An increase in the accuracy of the equalisation is the direct result.

3. It allows switched modulators to be used instead of analogue multipliers. These are technically simpler devices and can be realised with an accurate and stable transfer characteristic. The performance required of analogue multipliers would include wide bandwidth operation from d.c. to at least 5 MHz on both inputs, good accuracy, and negligible d.c. drift.

The use of the Stieltjes correlators therefore appears the more practical solution for the continuous equaliser.

For the discrete tap control method advantages 2 and 3 still apply. A reservation in using this scheme is raised, however, due to the high loop gain produced by the infinite clipper when the system has almost settled. It is expected that the equaliser tap settings would only be adjusted if the measured cross-correlations were above a pre-determined threshold. This would prevent continual oscillation of the taps between adjacent settings once the equaliser had settled. The high loop gain produced by the infinite clipper under certain circumstances (e.g. low residual error), would prevent such a scheme from operating correctly.

For the continuous tap control system it was initially thought that it may be necessary to use extra filtering in the correlation averaging circuits to suppress oscillations on the mean tap settings. With the experimental system however, using the infinite clipper, channel simulation filter, delay line and the circuit parameters as indicated in section 4.5.1 the variation of the tap voltages about their mean values was within ± 5 millivolts.

Thus, the accuracy of the tap settings due to the a.c. components on the output of the integrators was within 0.05% of the maximum tap voltage.

The loop gain of the system or the received signal amplitude, or both, could have been considerably increased before oscillations on the tap settings would become a problem. To achieve a similar tap resolution to Arnon an increase by a factor of 8.9 in the magnitude of the oscillations could have been tolerated. Increasing the above parameters would further reduce the settling times indicated in section 5.1.

Thus, extra filtering is not required to suppress oscillations on the tap settings. As such a scheme jeopardises the stability of the system, especially when using the infinite clipper, and also increases the settling time, its use is not recommended.

Although they should not be necessary, different correlation methods could be employed in an attempt to further simplify the correlation circuitry required. One such technique is that proposed by Bogner [38].

Employing this technique the infinite clipper in the error circuit would still be used and an extra infinite clipper, connected in the second input circuit to the multiplier, would be added to each cross-correlator. The advantage of using these extra infinite clippers is that the multiplication functions may then be performed with digital exclusive or circuits. The disadvantage of using this technique, however, is that a signal with a rectangular probability distribution over the voltage range of the tap outputs (e.g. triangular waveform) must be added to the inputs of these extra infinite clippers to maintain the correct cross-correlation values.

5.6.3 The Method of Tap Control

Both the discrete and continuous methods of tap control have been discussed in this thesis. The choice between these two methods is a decision between the simpler discrete method and the improved static and dynamic performance, as indicated by the experimental equaliser, obtained using the continuous method.

The operation of the discrete method requires the averaging of the output of each correlation multiplier or switched modulator, the sampling of the polarity of the cross-correlation values at the completion of transmission of the test signal and the adjustment of the digitally controlled attenuators one step in the direction determined by the measured polarities.

The continuous method on the other hand requires some form of hold circuit to maintain the tap values during the transmission of the video signal. This hold must be released during the equalising period. As the hold circuits are only required to maintain the tap values for a period of either 20 or 40 milliseconds between tap adjustments, depending on whether the values are adjusted once every field or frame, these circuits will not pose a major technical problem.

The major difference in the complexity of the two systems therefore, is the realisation of the different variable gain circuits for the tap settings. With due consideration of the recent technical advances made with electronic analogue multipliers, it appears that the improved static and dynamic performance obtained using the continuous method favours the choice of this control scheme.

CONCLUSIONS

The use of correlation techniques for the implementation of an adaptive television equaliser has been extensively investigated. From this investigation it appears that the proposed techniques are suitable for use within a practical television equaliser.

An improvement in the K_{2T} rating of a simulated distorted transmission channel from 7.0 to 2.1 was obtained using the experimental delay line equaliser. The experimental equaliser was a simplified model of a television equaliser and its performance was limited by the simplicity of the circuits used and the number of delay functions provided. Considering these limitations, better results are expected of a practical television equaliser.

As a result of the practical and theoretical investigations presented, an adaptive equaliser most suited to the requirements of the television system is proposed. This proposal includes the use of a continuous method of tap control and a Stieltjes correlation technique [26].

Using these techniques with a delay line equaliser the results obtained from the experimental system indicate that a settling time in the order of 0.5 seconds may be expected of the practical television equaliser. Variation of the settling time due to changes in circuit parameters may be calculated using the theoretical results presented in chapter 3. Good agreement was found between the theoretical results presented in chapter 3 and the measured dynamic performance of the experimental equaliser.

Further aspects of this work include investigations into the adjustable equaliser to be employed and the realisation of a practical television equaliser.

Consideration in this thesis has been given to both the delay line and Laguerre functions for use as an adjustable equaliser. Preliminary results obtained from the experimental equaliser indicated that a better performance could be expected from the delay line equaliser. A complete investigation into the adjustable equaliser most suited to the television system is beyond the scope of this thesis.

This investigation has been concerned with the basic principles required to provide an adaptive television equalising facility. The technical problems of providing this facility have not been considered in detail. Careful circuit design will be required to provide the fine degree of equalisation required over the complete video spectrum.

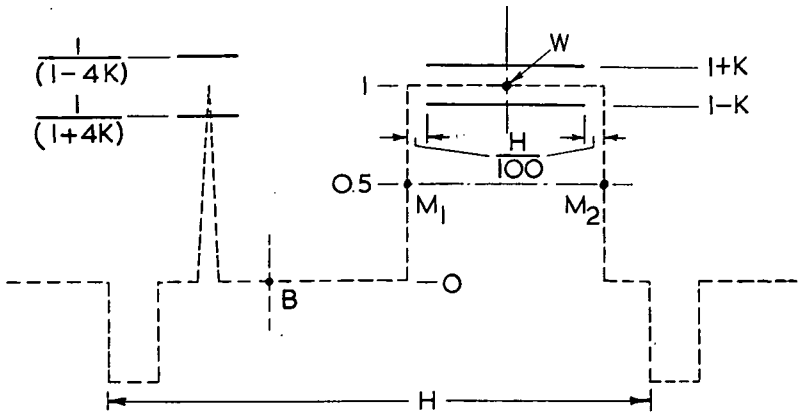

(a) RESPONSE TO 2T PULSE AND BAR TEST SIGNAL

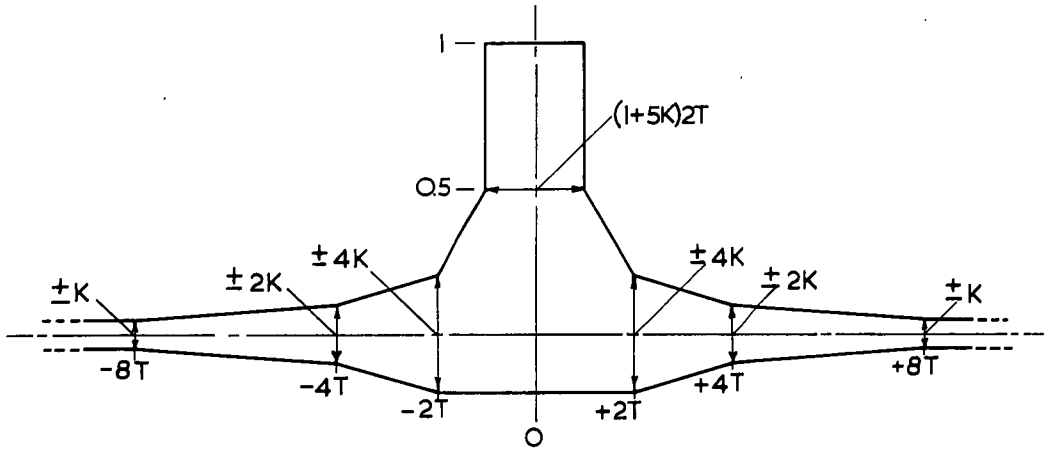

(b) RESPONSE TO 2T PULSE AND BAR TEST SIGNAL

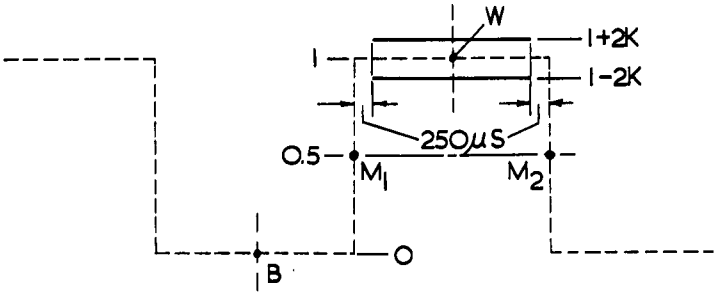

(c) RESPONSE TO 50HZ SQUARE WAVE TEST SIGNAL

FIG.A.1 WAVEFORM RESPONSE LIMITS

APPENDIX A

ESTIMATING CHANNEL PERFORMANCE USING TEST WAVEFORMS

Using pulse and bar waveforms there are two methods for obtaining the K rating of a channel:

a. The Routine Test Method: This method involves the comparison of the output pulse and bar waveforms with standard K factor graticules (similar to those shown in fig. A.1) mounted on the front of the c.r.o. screen. The actual graticules used are engraved for a specific value of K, the pulse having a K rating equal to or less than this value if it lies within the mark. Four different values of K are measured.

1. Using a 2T (or T) pulse, with the correct time sweep, the first value, $K_{2T}(K_T)$, is measured with the mask shown in fig. A.1(b). The T pulse is only used for wideband equipment, such as amplifiers and internal vision cables. Subjective tests have indicated that errors in the waveform close to the pulse are not as significant as similar errors positioned further away from the pulse. This is allowed for in the design of the mask.

2. The K factor, K_{ref}, applies to reflections delayed greater than 8T after the 2T pulse.

3. K_{bar} is measured using the bar response and the mask shown in fig. A.1(a). To obtain more information about the rise time and overshoot of this response an expanded time sweep, together with different graticule markings, is often used.

4. K_{pb} is a measure of the ratio of the 2T pulse and bar heights. This factor (from the mask shown in fig. A.1(a)) is related to the high frequency response of the system.

The overall K factor is obtained by taking the largest of the four individual factors.

A further K factor is measured using a 50 Hz square wave and the mask shown in fig. A.1(c). This factor is recorded separately as distortions at this frequency are usually removed by a black level clamp at the transmitter.

b. The Acceptance Test Method [29]: This method requires a photograph of the T pulse response, from which a time series at intervals of $\frac{T}{2}$ is obtained. Using time series manipulation techniques K factors similar to those obtained by the routine test method are then calculated mathematically. This method is more exact but is very time consuming.

No impairment of the picture quality occurs for a K factor of less than 3%. Beyond 5% the impairment becomes intolerable. The performance objective for a "national reference video connection" as defined by the C.C.I.R. (International Radio Consultative Committee) is 5%.

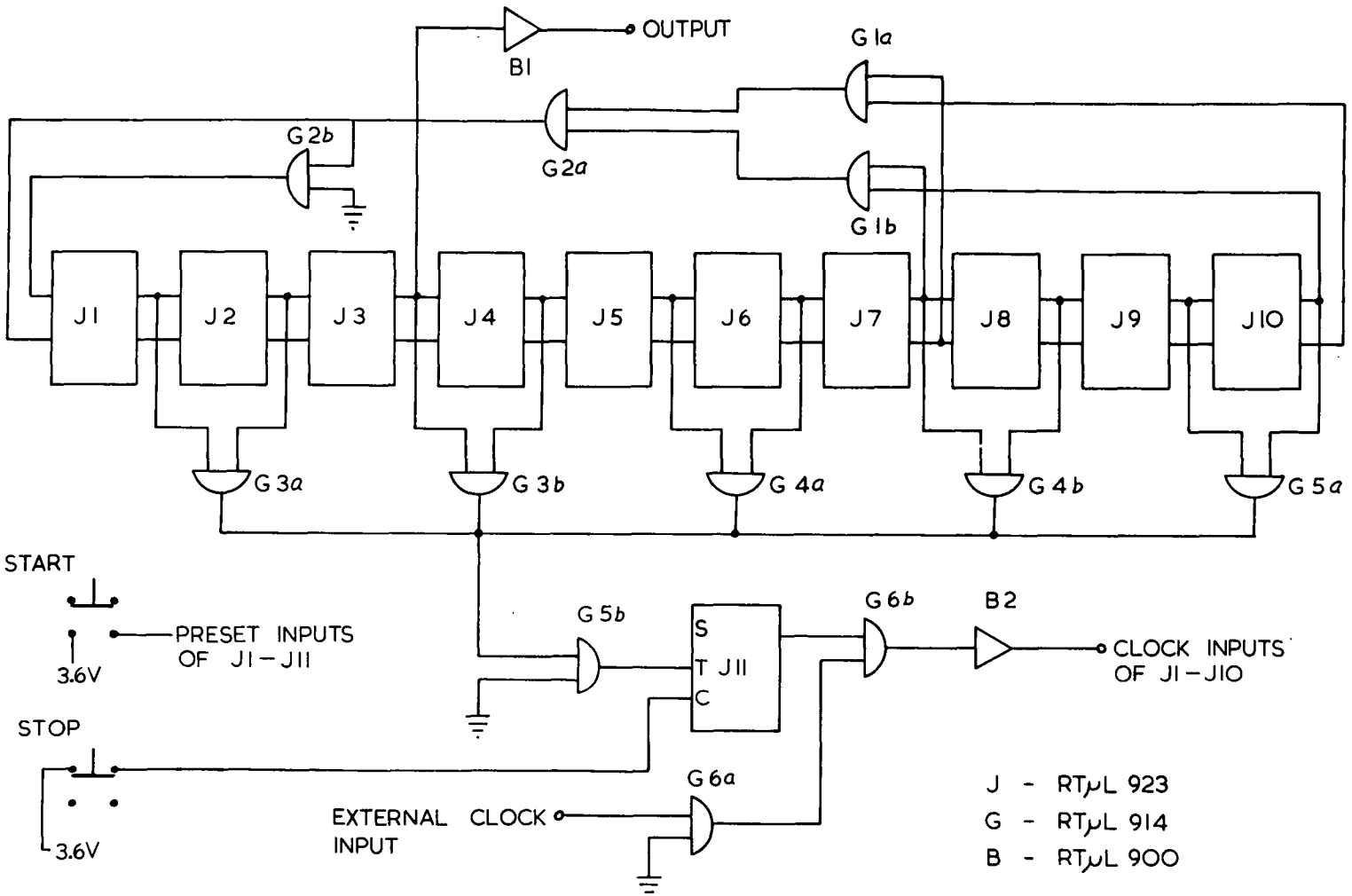

FIG. B.1 PSEUDO RANDOM NOISE GENERATOR

APPENDIX B

HARDWARE REALISATION OF THE EXPERIMENTAL EQUALISER

The design of the circuits required for the experimental system is presented in this appendix.

B.1 The Test Signal Generators

Two signal generators were used with the experimental equaliser -

1. a pseudo random noise generator which provided the test signal necessary for the operation of the equaliser, and
2. a sine squared pulse generator for testing the accuracy of the equalisation.

B.1.1 The Pseudo Random Noise Generator

The two important design considerations for the pseudo random noise generator were the clock frequency and the length of the shift register to be used. A clock frequency of 100 KHz was chosen on the basis of twenty times the cut-off frequency of the experimental system. The ultimate length of the shift register was a compromise between the improved signal obtained from a larger shift register and the cost of the extra number of components. The value chosen was ten.

The basic pseudo random noise generator is shown in fig. B.1. To reduce the number of active components required and to provide a variable frequency facility if needed an external oscillator was used as the clock.

The generator control circuit, also shown in fig. B.1, fulfilled two purposes -

1. It provided the generator with a manual stop and start.
2. It prevented the generator starting in the condition with the output of all the flip flops at "0".
3. It ensured that the generator stopped after a complete sequence.

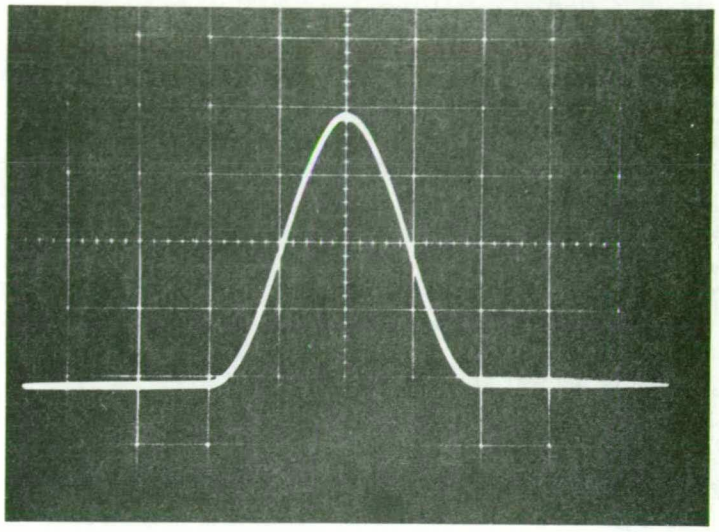

0.1 MS/DIV

FIG. B.2 2T PULSE

To minimise any d.c. drift of the correlators, the generator was a.c. coupled to the rest of the system. Thus, no attempt was made to provide a symmetrical output voltage swing for the generator.

During the latter stages of this investigation, a Solartron pseudo random noise generator became available. This generator had the advantages of providing both a variable clock frequency, in a number of discrete steps, and a variable shift register length. For $N \leq 10$ (where N is the number of flip flops in the shift register) it also had the added advantage of providing two outputs, one a delayed version of the other. The delay between the two signals was adjustable in multiples of the clock period from zero to one thousand.

With the use of the Solartron generator, additions to the circuit shown in fig. B.1, to provide delayed signals and a variable sequence length, were not required.

B.1.2 The Sine Squared Pulse Generator

To generate sine squared pulses a low frequency waveform generator was used (Feedback Test Waveform Generator TWG500). When triggered externally, this unit had the facility of providing a single period of a sine wave at a number of different phases relative to the triggering waveform.

The sine squared pulse was produced by using a single period, from 0 to 2π, of an inverted cosine waveform. The generator was clocked, using another signal generator, at a frequency of 100 Hz for all measurements.

A c.r.o. trace of the pulse produced by the generator is shown in fig. B.2.

B.2 The Signal Weighting Function

For the signal weighting function a filter with a flat amplitude characteristic up to 5 KHz and a sharp cut-off was required. The filter chosen was a fourth order Butterworth filter with a bandwidth of 5 KHz. A higher order filter, although having a better cut-off response, was not used because of the increased circuit complexity required. The transfer

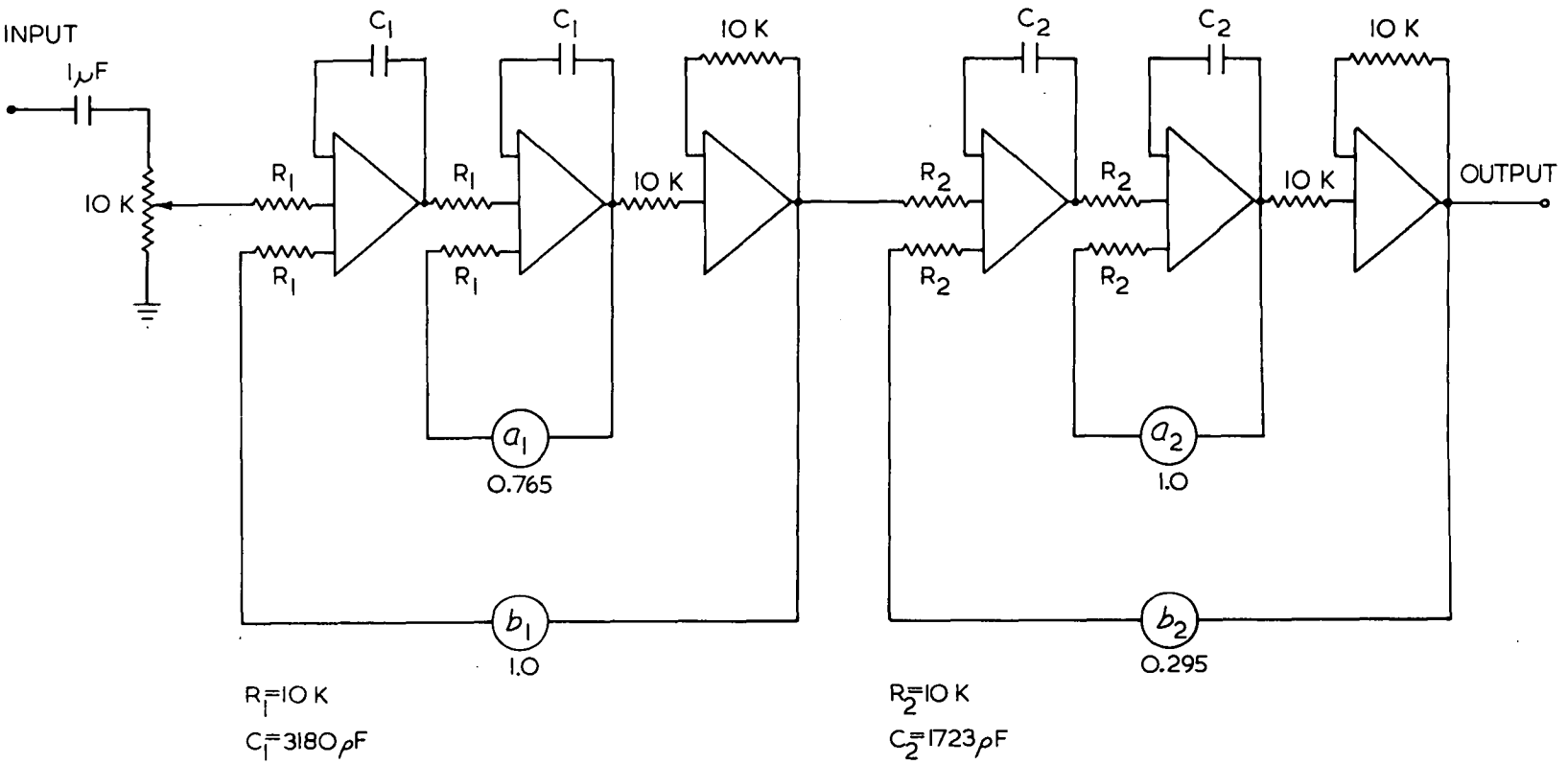

FIG.B.3 SIGNAL WEIGHTING FILTER

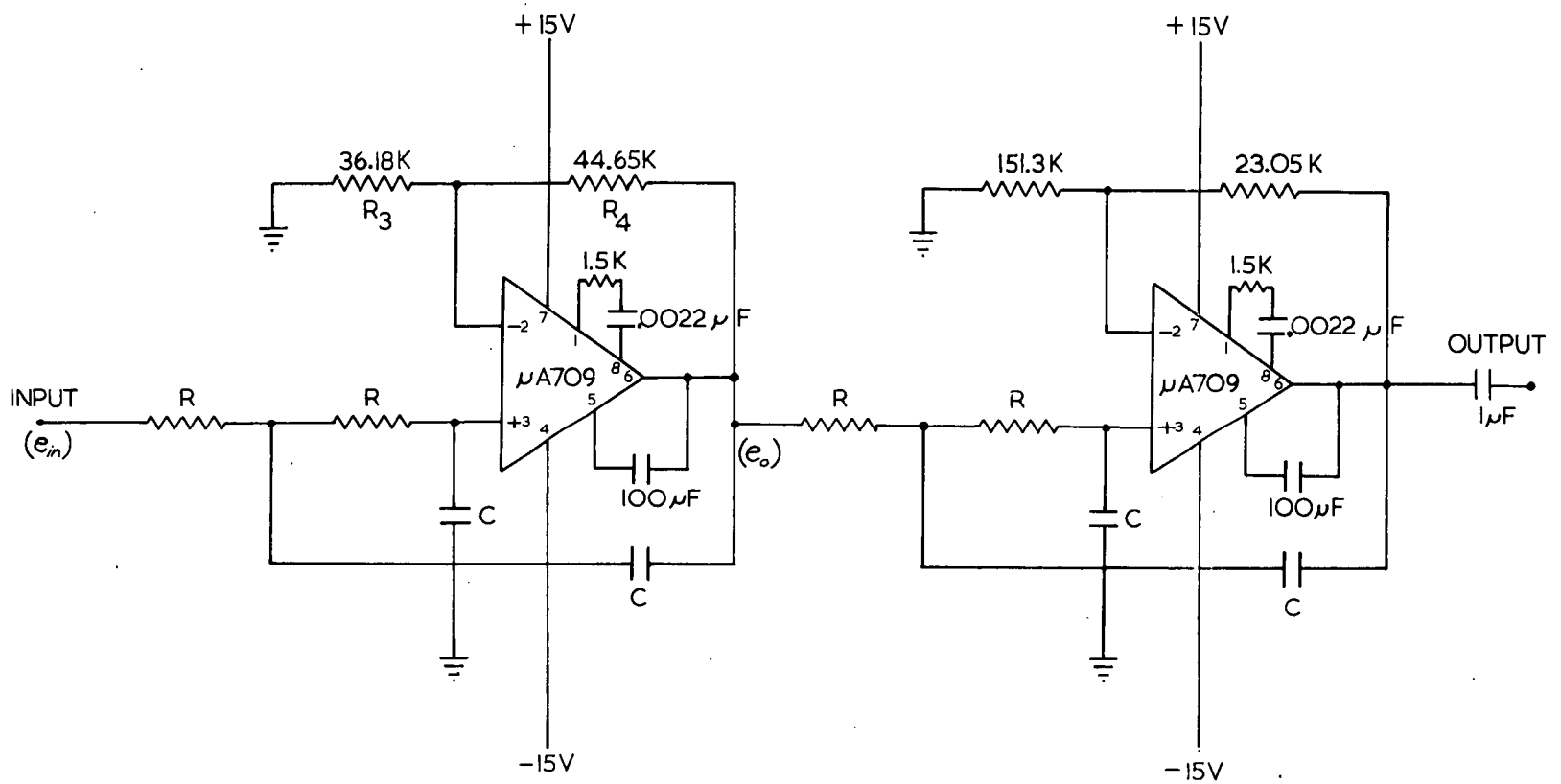

FIG. B.4 SIGNAL WEIGHTING FILTER

function of the filter used was -

$$\frac{1}{\left(\frac{s^2}{\omega_o^2} + 0.7636\,\frac{s}{\omega_o} + 1\right)\left(\frac{s^2}{\omega_o^2} + 1.8477\,\frac{s}{\omega_o} + 1\right)} \quad \text{where } \omega_o = 3.14_{10}4 \text{ rad/sec.}$$

During the initial experiments, when only the one pseudo random noise source was available, only one filter was required. For convenience, it was patched on the analogue computer using two standard second order filter circuits [30] connected in series. The circuit of the complete filter is shown in fig. B.3. The transfer function of the second order filter is -

$$\frac{1}{\left(\frac{s^2}{\omega_o^2} + a\,\frac{s}{\omega_o} + b\right)}$$

where $\omega_o = \frac{1}{RC}$, a is the potentiometer setting within the inner feedback loop and b is the potentiometer setting within the outer feedback loop.

To realise the transfer function -

$$\frac{1}{\left(\frac{s^2}{\omega_o^2} + 1.8477\,\frac{s}{\omega_o} + 1\right)}$$

using this circuit the expression must be altered, with ω_o replaced by ω'_o, where $\omega'_o = 1.8477\omega_o$.

Neglecting the constant gain factor, the final result is -

$$\frac{1}{\left(\frac{s^2}{\omega'^2_o} + \frac{s}{\omega'_o} + 0.295\right)} \quad \text{where } \omega'_o = 5.8_{10}4 \text{ rad/sec.}$$

A second identical filter was also required for the delayed signal. Two μA709 operational amplifiers were used to provide the two second order functions. The complete circuit is shown in fig. B.4.

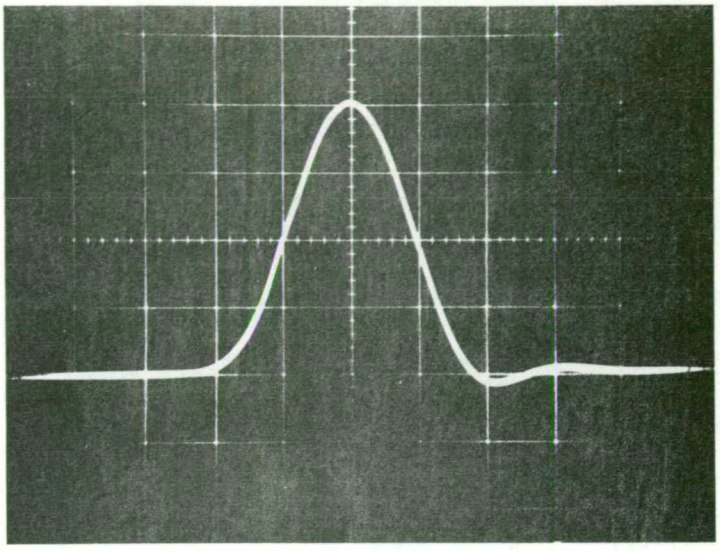

FIG. B.5 2T PULSE RESPONSE OF BUTTERWORTH FILTERS

With the negative feedback of the operational amplifiers arranged as indicated in fig. B.4, the positive gain of the amplifiers is given by -

$$K = 1 + \frac{R_4}{R_3} \qquad \text{B.1}$$

If the output of the amplifier is e_o then the voltage at the positive input of the amplifier is $\frac{e_o}{K}$. From a nodal analysis of the positive input circuit it can be shown that the input voltage is given by -

$$\frac{e_o(s)}{K} = \frac{e_{in}(s) + RCse_o(s)}{R^2C^2s^2 + 3RCs + 1} \qquad \text{B.2}$$

The transfer function of the complete circuit is therefore -

$$\frac{e_o(s)}{e_{in}(s)} = \frac{K}{R^2C^2s^2 + (3-K)RCs + 1} \qquad \text{B.3}$$

The resistance and capacitance values indicated were chosen to provide the two transfer functions required and also the correct bias conditions for the amplifiers.

The 2T pulse response of the 5 KHz fourth order Butterworth filters is shown in fig. B.5. The K_{2T} rating of this response, determined using the technique discussed in appendix A, is approximately 1.15. This K_{2T} response would be acceptable within a television network.

The low K_{2T} rating is the result of the frequency spectrum of the 2T pulse. The Butterworth filter has a flat amplitude characteristic and an approximate linear phase characteristic over the lower section of the passband where the majority of the energy of the 2T pulse is contained.

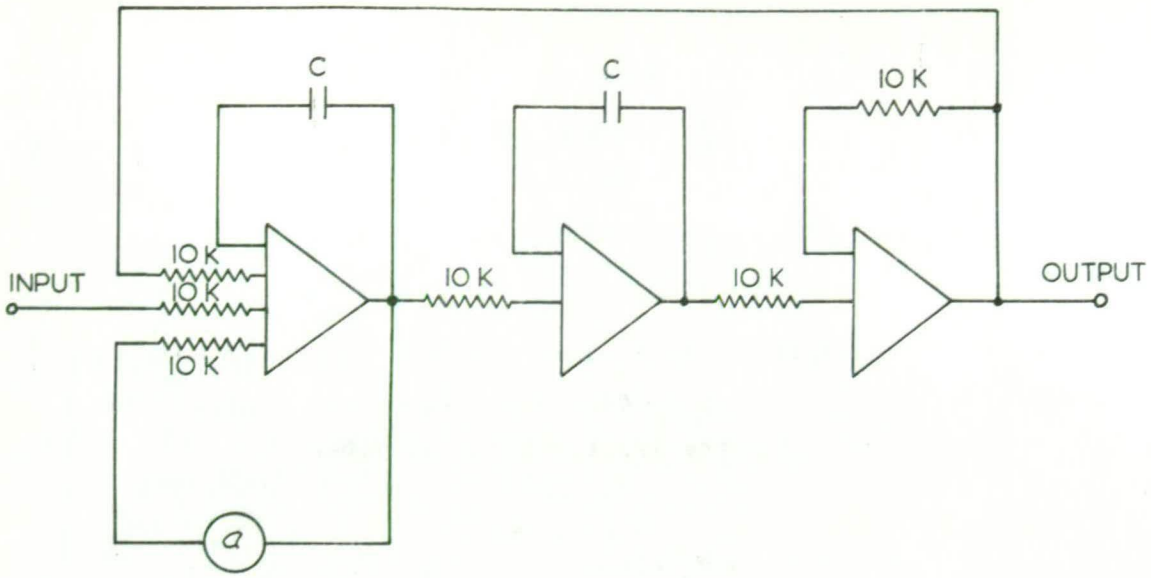

FOR $\omega_o = 24.4\ 10^3$ $\quad \xi = 0.275$ THEN $\quad C = 0.0041\mu F$ $\quad a = 0.55$

FIG. B.6 CHANNEL SIMULATION FILTER

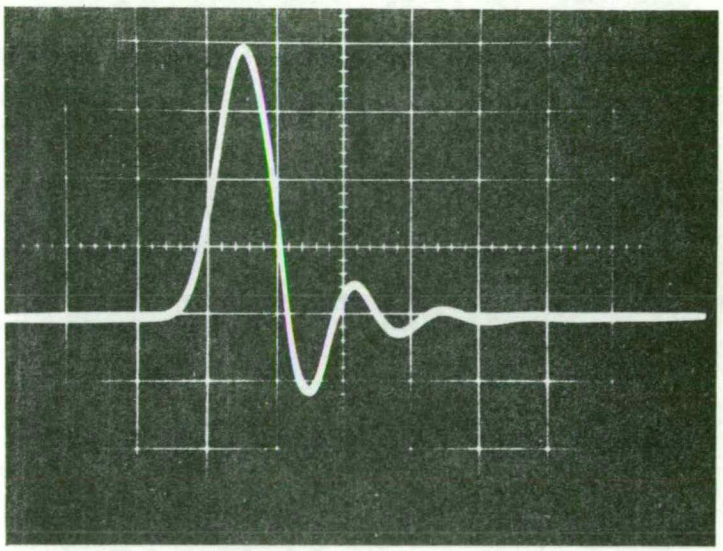

FIG. B.7 2T PULSE RESPONSE OF CHANNEL SIMULATION FILTER CASCADED WITH BUTTERWORTH FILTER

B.3 The Transmission Channel Simulation

To simulate a distorted channel a second order filter was used. The transfer function chosen was -

$$\frac{1}{\left(\frac{s^2}{\omega_o^2} + 2\xi\frac{s}{\omega_o} + 1\right)}$$

with $\omega_o = 2.44_{10}4$ rad/sec.

and $\xi = 0.275$

The values of ω_o and ξ were chosen to produce a pulse response with a large amplitude ringing characteristic which is maintained for a relatively long period of time. Such a pulse response would be most undesirable within a television system. The effectiveness of the equaliser with a severe distortion within the system could then be measured. The resultant circuit, shown in fig. B.6, was patched on the analogue computer.

The waveform response of the channel simulation filter cascaded with the Butterworth filter is shown in fig. B.7. From this photograph the K_{2T} rating of the response was estimated to be approximately 7.0. This distortion would be quite intolerable in a practical television system (appendix A).

B.4 The Automatic Equaliser

B.4.1 The Delay Line

Initially it was intended to build the experimental system to operate at one hundredth of the frequency of the television system. To provide equalisation over the complete passband of 50 KHz, the delay required for each section of the delay line was ten microseconds.

Because this is a relatively short delay it was decided that the delay approximation outlined by Mason and Zimmerman [31] would be used.

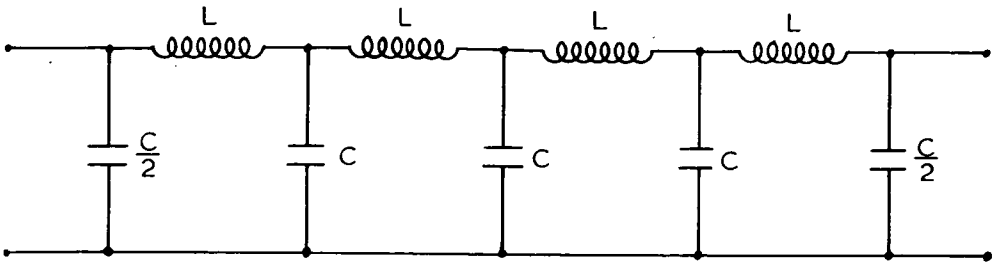

(a) PASSIVE DELAY CIRCUIT ($n=4$)

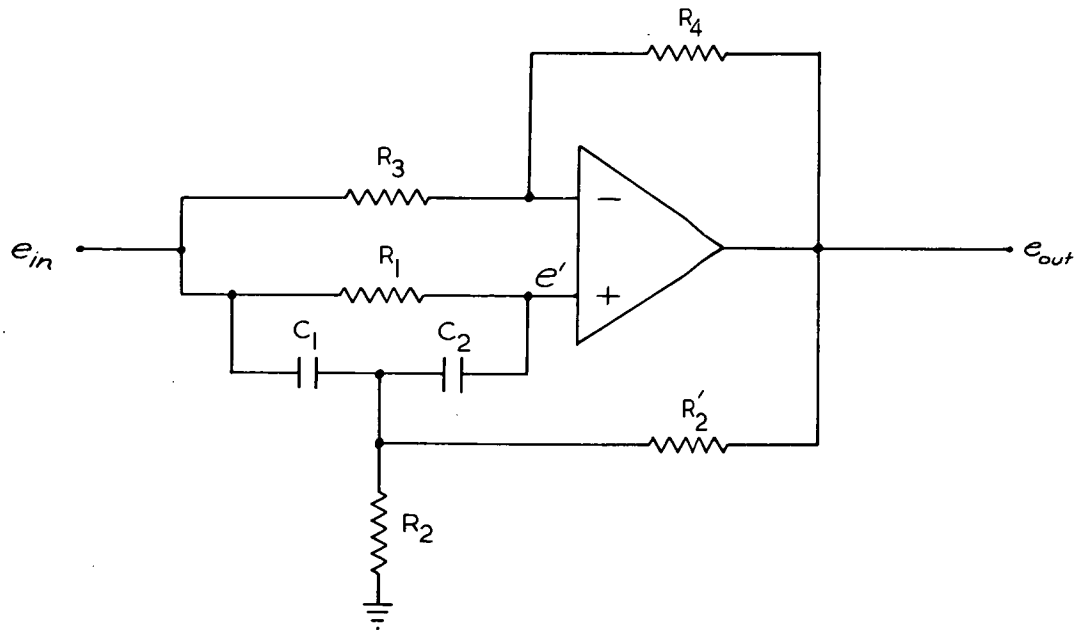

(b) ACTIVE DELAY CIRCUIT

FIG. B.8 DELAY CIRCUITS

This is based on the following approximation -

$$F(s) = \left[\frac{1 - \frac{s}{2n}}{1 + \frac{s}{2n}} \right]^n \qquad B.4$$

because

$$F(s) \rightarrow e^{-s} \qquad \text{for} \qquad n \rightarrow \infty$$

This transfer function is further approximated by the L C ladder circuit shown in fig. B.8(a). As a compromise between the accuracy and the complexity of the circuit the value chosen for n was four. The delay of the circuit is given by $\sqrt{LC}$ and the characteristic impedance by $\sqrt{\frac{L}{C}}$. The values of L and C required for a ten microsecond delay line with a characteristic impedance of 1 KΩ are 2.5 mH and 2500 pf.

With the frequency scaling of the experimental system altered to one thousandth of the television frequency, the increase in the values of L and C required to provide the increased time delay (100 microseconds) made such a circuit impractical.

An active delay line, based on the suggestions proposed by Potter[32], was chosen. The active circuit has two definite advantages -

1. From the practical point of view it is easier to realise.
2. It has no impedance matching problems whereas the LC ladder network is sensitive to impedance mismatches.

Potter has shown that a network with the normalised pole and zero positions given by -

$$s = -1.6 \pm j1.0$$

and $$s = 1.6 \pm j1.0$$

gives a delay equal to $\frac{1}{2}T$ within an accuracy of 0.5% over the required frequency range. To provide each delay, T, two active circuits must be used.

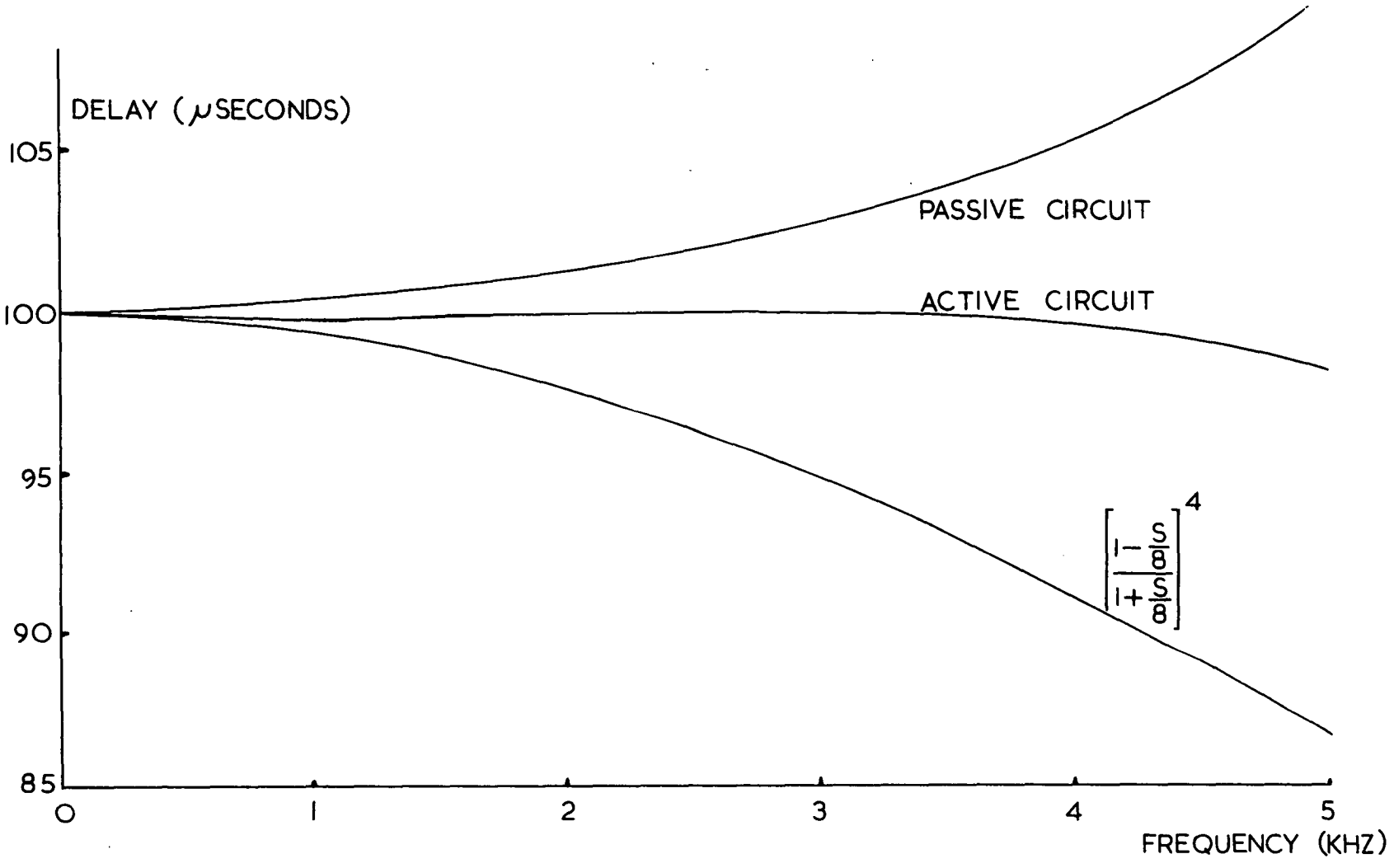

FIG. B.9 DELAY VERSUS FREQUENCY CHARACTERISTIC OF DELAY CIRCUITS

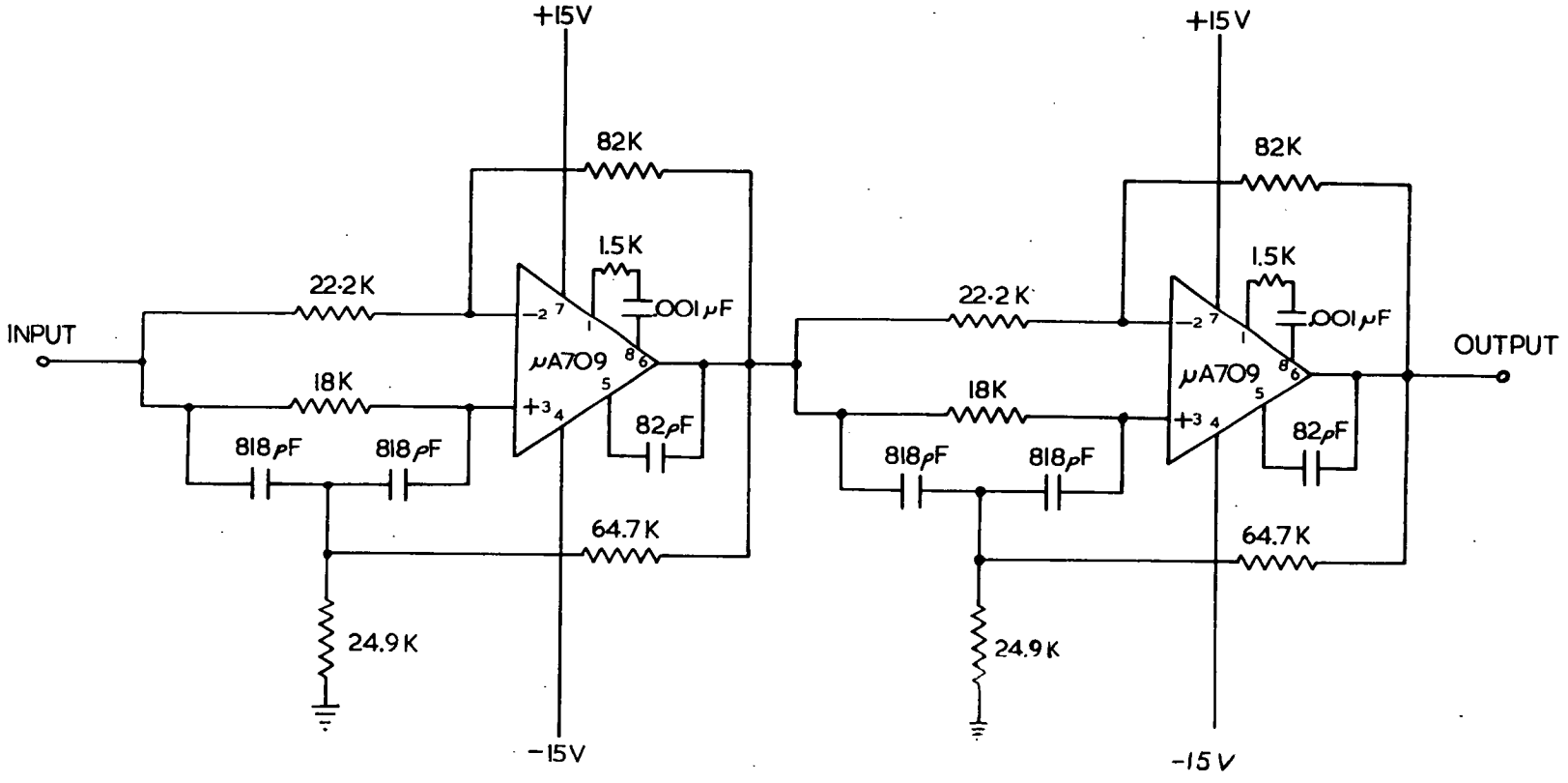

FIG. B. 10 100 MICROSECOND DELAY CIRCUIT

The accuracy of both the active and passive delay circuits is compared in fig. B.9 together with the ideal characteristic, as proposed by Mason and Zimmerman, for n = 4. These graphs were calculated using a circuit analysis computer programme [33]. They indicate that the use of the active circuit also provides a more accurate delay line than the other functions. It can be seen from this figure that the 0.5% indicated by Potter is not achieved. This is due to the fact that the calculations were based on the actual circuits with each component value chosen to within a practical tolerance, rather than the theoretical transfer functions.

The active circuits used by Potter contained one inductor each. In an attempt to further simplify the physical realisation of the delay line another circuit containing only resistors and capacitors was developed and is shown in fig. B.10.

Considering one section of the delay line (fig. B.8(b)) and assuming that the amplifier has a high gain, high input impedance and low output impedance, the resultant transfer characteristic is -

$$e_o(s) = e'(s)\left(1 + \frac{R_4}{R_3}\right) - e_{in}(s)\,\frac{R_4}{R_3} \qquad \text{B.5}$$

From a nodal analysis of the positive input circuit to the amplifier it can be shown that e'(s) is given by the following equation -

$$e'(s) = \frac{R_1}{R_1 + \frac{1}{C_2 s}}\left[\frac{\frac{1}{C_1 s}\left(R_1 + \frac{1}{C_2 s}\right)}{\frac{1}{C_1 s} + R_1 + \frac{1}{C_2 s}}\right]\left[\frac{\frac{1}{C_1 s}\left(R_1 + \frac{1}{C_2 s}\right)}{\frac{1}{C_1 s} + R_1 + \frac{1}{C_2 s}} + R''_2\right]^{-1}\left[\gamma e_o(s) - e_{in}(s)\right] \qquad \text{B.6}$$

where

$$\gamma = \frac{R_2}{R_2 + R'_2} \qquad \text{and} \qquad R''_2 = R_2 // R'_2$$

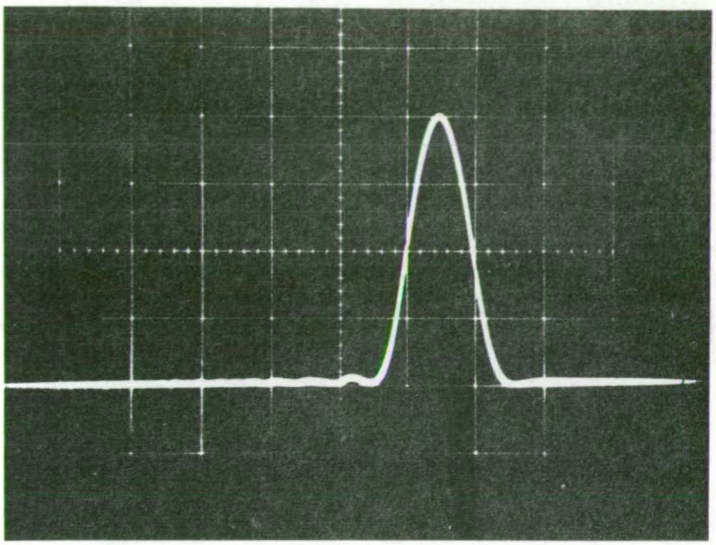

FIG. B.11 2T PULSE RESPONSE OF DELAY LINE

For

$$\omega_o^2 = [R_1 R''_2 C_1 C_2]^{-1} \quad ; \quad K_1 = \frac{R''_2}{R_1 C_1 C_2}(C_1 + C_2) \text{ and } K_2 = \frac{R_1 C_2}{R''_2 C_1}$$

equation B.6 reduces to -

$$e'(s) = \frac{(\frac{s^2}{\omega_o^2} + K_1 \frac{s}{\omega_o} + 1)\, e_{in}(s) + K_2 \gamma e_o(s) \frac{s}{\omega_o}}{\frac{s^2}{\omega_o^2} + (K_1 + K_2)\frac{s}{\omega_o} + 1} \qquad \text{B.7}$$

Substituting this equation into equation B.5 -

$$\frac{e_o(s)}{e_{in}(s)} = \frac{\frac{s^2}{\omega_o^2} + (K_1 - K_2 \frac{R_4}{R_3})\frac{s}{\omega_o} + 1}{\frac{s^2}{\omega_o^2} + (K_1 + K_2(1-\gamma(\frac{R_4}{R_3} + 1)))\frac{s}{\omega_o} + 1} \qquad \text{B.8}$$

The required equation is of the form -

$$\frac{e_o(s)}{e_{in}(s)} = \frac{\frac{s^2}{\omega_o^2} - 2\zeta\frac{s}{\omega_o} + 1}{\frac{s^2}{\omega_o^2} + 2\zeta\frac{s}{\omega_o} + 1} \qquad \text{B.9}$$

For ease of calculation the component values were chosen such that $C_1 = C_2$ and $R_1 = R''_2$, to give $K_1 = 2$ and $K_2 = 1$.

Therefore

$$\frac{R_4}{R_3} = 2(\zeta + 1) \qquad \text{B.10}$$

and

$$\gamma = \frac{3 - 2\zeta}{3 + 2\zeta} \qquad \text{B.11}$$

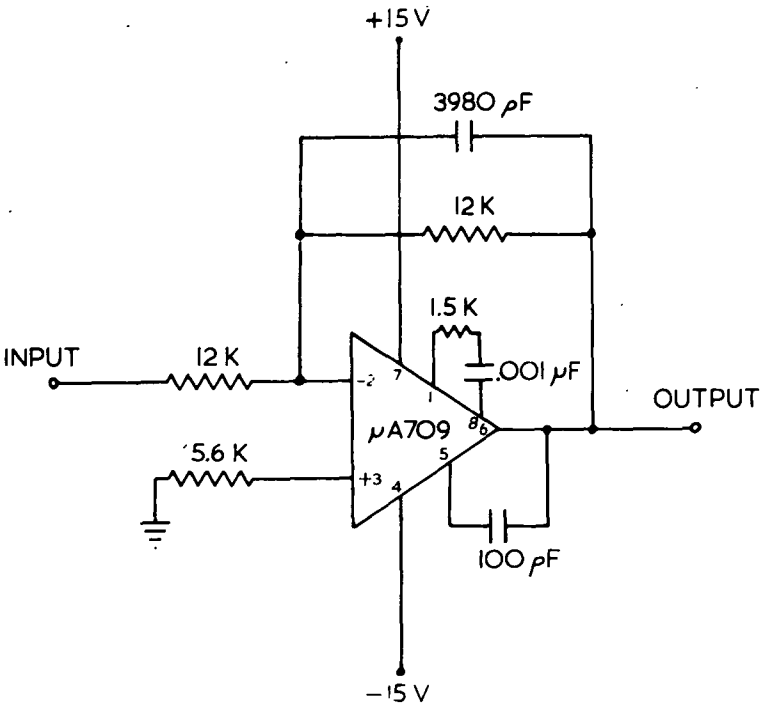

(a) TRANSFER FUNCTION $\frac{\alpha}{S+\alpha}$

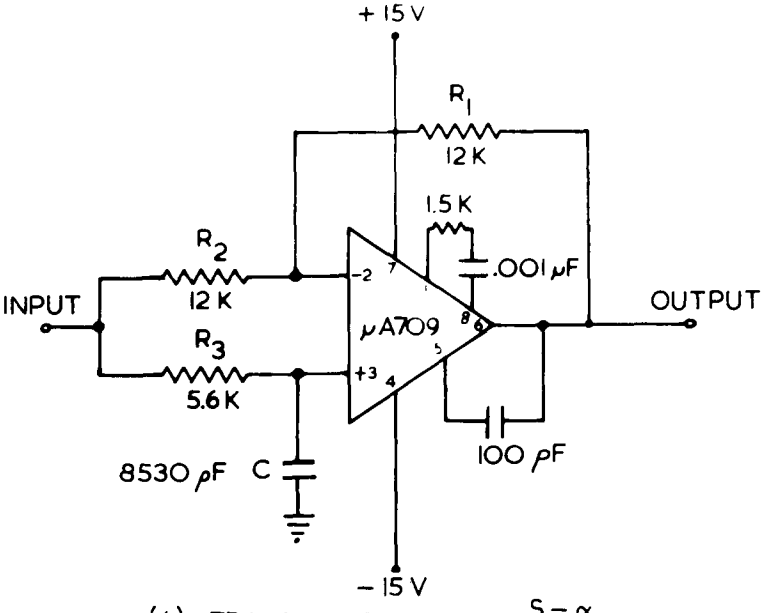

(b) TRANSFER FUNCTION $\frac{S-\alpha}{S+\alpha}$

FIG. B.12 LAGUERRE NETWORKS

The transfer function required for a 0.05 millisecond delay from each circuit is -

$$\frac{s^2 - 1.152_{10}5\, s + 4.61_{10}9}{s^2 + 1.152_{10}5\, s + 4.61_{10}9}$$

Thus $\gamma = 0.2779$ and $\frac{R_4}{R_3} = 3.698$. The component values shown in fig. B.10 were chosen to satisfy both these conditions and the bias conditions required for the amplifier.

All component values critical for obtaining the correct transfer function were measured to within a tolerance of 1% before placing in the circuit.

Fig. B.11 illustrates the performance achieved by the delay line. This figure shows the output of the tenth tap with the input of the delay line connected directly to the sine squared pulse generator. The total delay of the pulse was 0.9 milliseconds.

B.4.2 The Laguerre Functions

The transfer functions of Laguerre's orthogonal network are given by -

$$F_n(s) = \frac{\alpha}{s + \alpha} \left(\frac{\alpha - s}{\alpha + s} \right)^n \qquad \text{B.12}$$

These transfer functions may be synthesised with either passive or active circuits. The synthesis of the passive circuits is described by Lee [9].

For the experimental system, however, active circuits were used.

These are shown in fig. B.12. The circuit used to synthesise the transfer function $\frac{\alpha}{s + \alpha}$ (fig. B.12(a)) is a standard RC feedback circuit. The transfer function of fig. B.12(b) is calculated by assuming the amplifier characteristics as assumed for the delay line. Thus equation B.5 still applies.

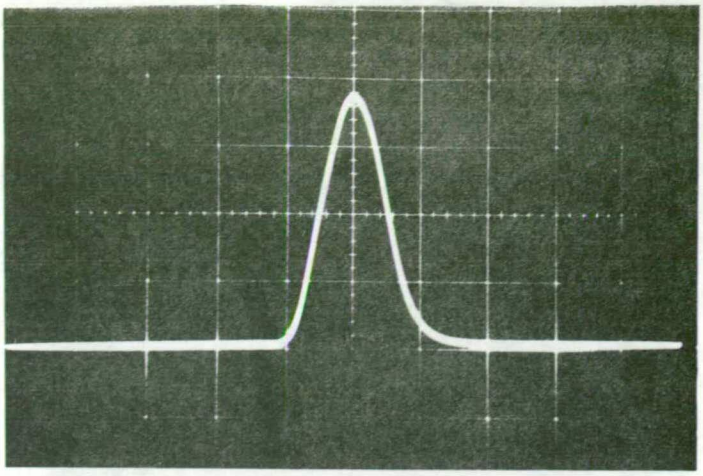

0.2 MS/DIV

(a) $\frac{\alpha}{S+\alpha}$

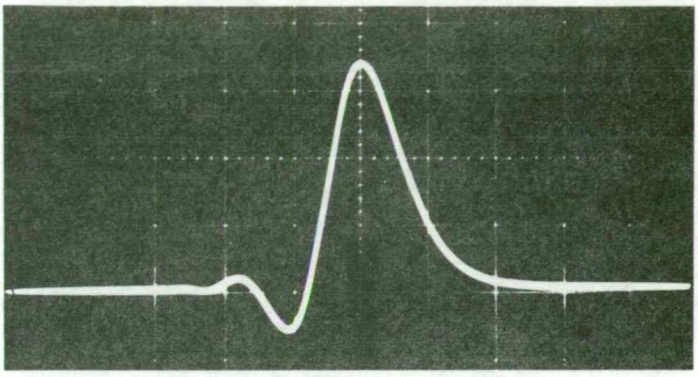

0.2 MS/DIV

(b) $\frac{\alpha}{S+\alpha}\left(\frac{S-\alpha}{S+\alpha}\right)^4$

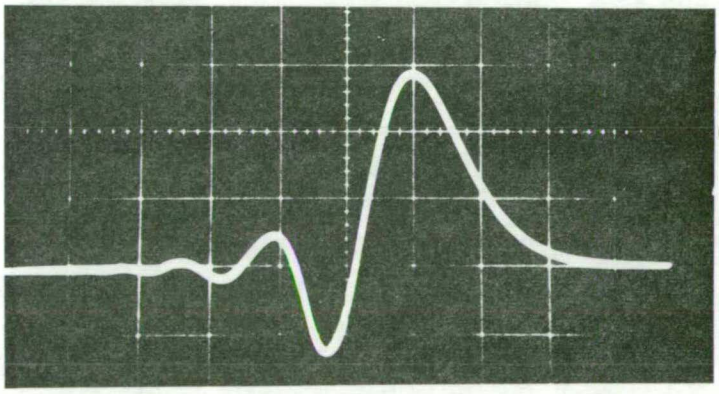

0.2 MS/DIV

(c) $\frac{\alpha}{S+\alpha}\left(\frac{S-\alpha}{S+\alpha}\right)^9$

FIG. B.13 2T PULSE RESPONSE OF LAGUERRE FUNCTIONS

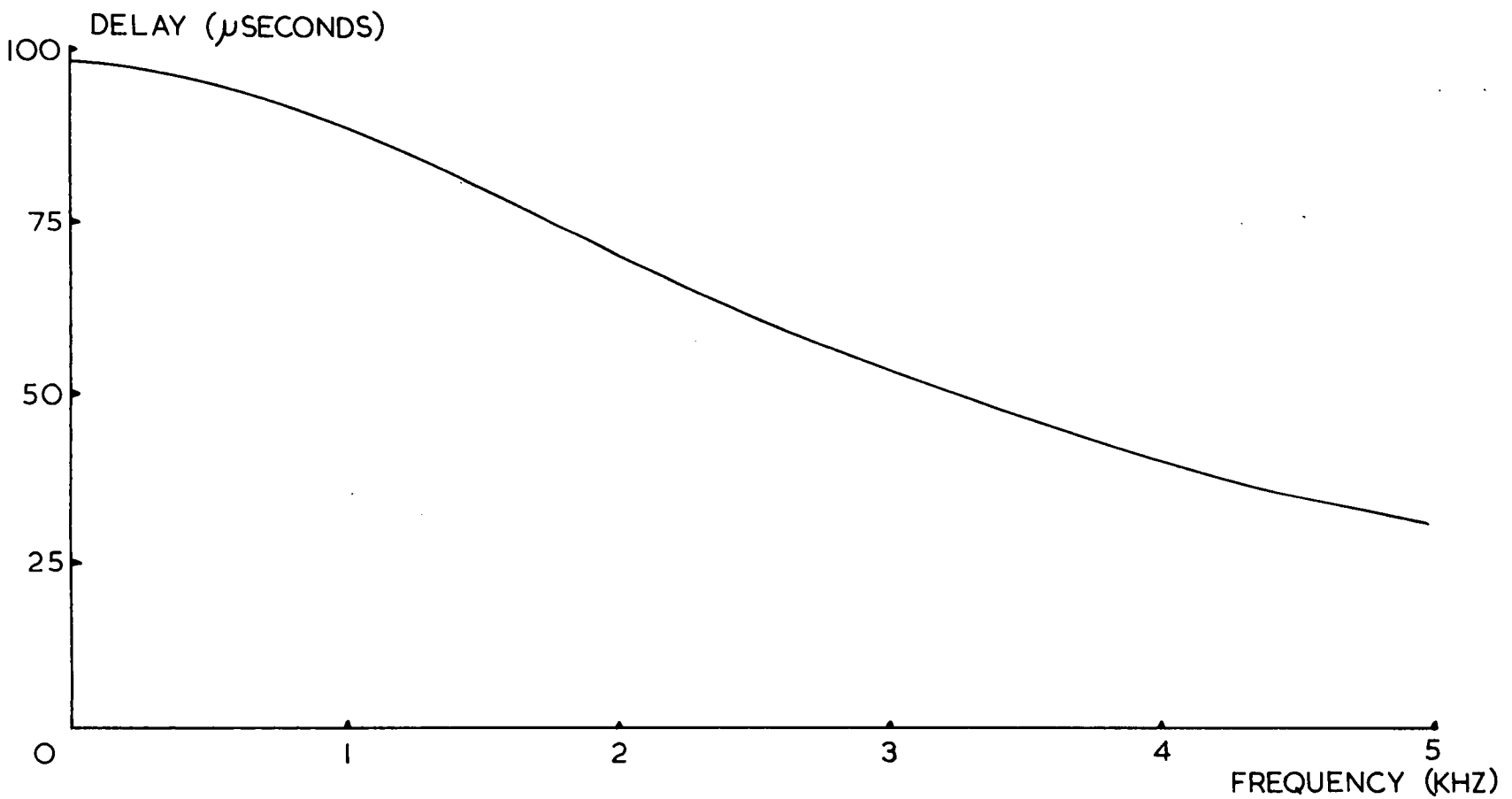

FIG. B.14 DELAY VERSUS FREQUENCY CHARACTERISTIC OF LAGUERRE NETWORKS

In this case e'(s) is given by -

$$e'(s) = \frac{\frac{1}{Cs}}{R_3 + \frac{1}{Cs}} \; e_{in}(s) \qquad \text{B.13}$$

Substituting this result into equation B.5 with $R_1 = R_2$ and $\alpha = \frac{1}{R_3 C}$, then -

$$\frac{e_o(s)}{e_{in}(s)} = \frac{\alpha - s}{\alpha + s} \qquad \text{B.14}$$

The choice of α was based on the value used by Sondhi. He chose a value of α equal to two-thirds the bandwidth of his system. For this particular system the corresponding value of α is $20.95_{10}{}^{3}$ radians per second. As for the previous active circuits, the component values were chosen to obtain both the desired transfer function and correct biasing conditions for the amplifier.

The relative simplicity of the circuits needed to synthesise the Laguerre functions, compared with the delay line, is readily appreciated by comparing the circuits used for this experimental system.

The sine squared waveform responses of three of the Laguerre functions are illustrated by figs. B.13(a), (b) and (c). Fig. B.13(a) is the output waveform of the first tap with the input connected directly to the sine squared pulse generator. The output of the fifth tap is shown in Fig. B.13(b) and the tenth tap in fig. B.13(c).

With the exception of the input transfer function, the Laguerre networks have a flat amplitude characteristic. Their waveform response is therefore determined by the delay characteristic of these networks. This characteristic is shown in fig. B.14.

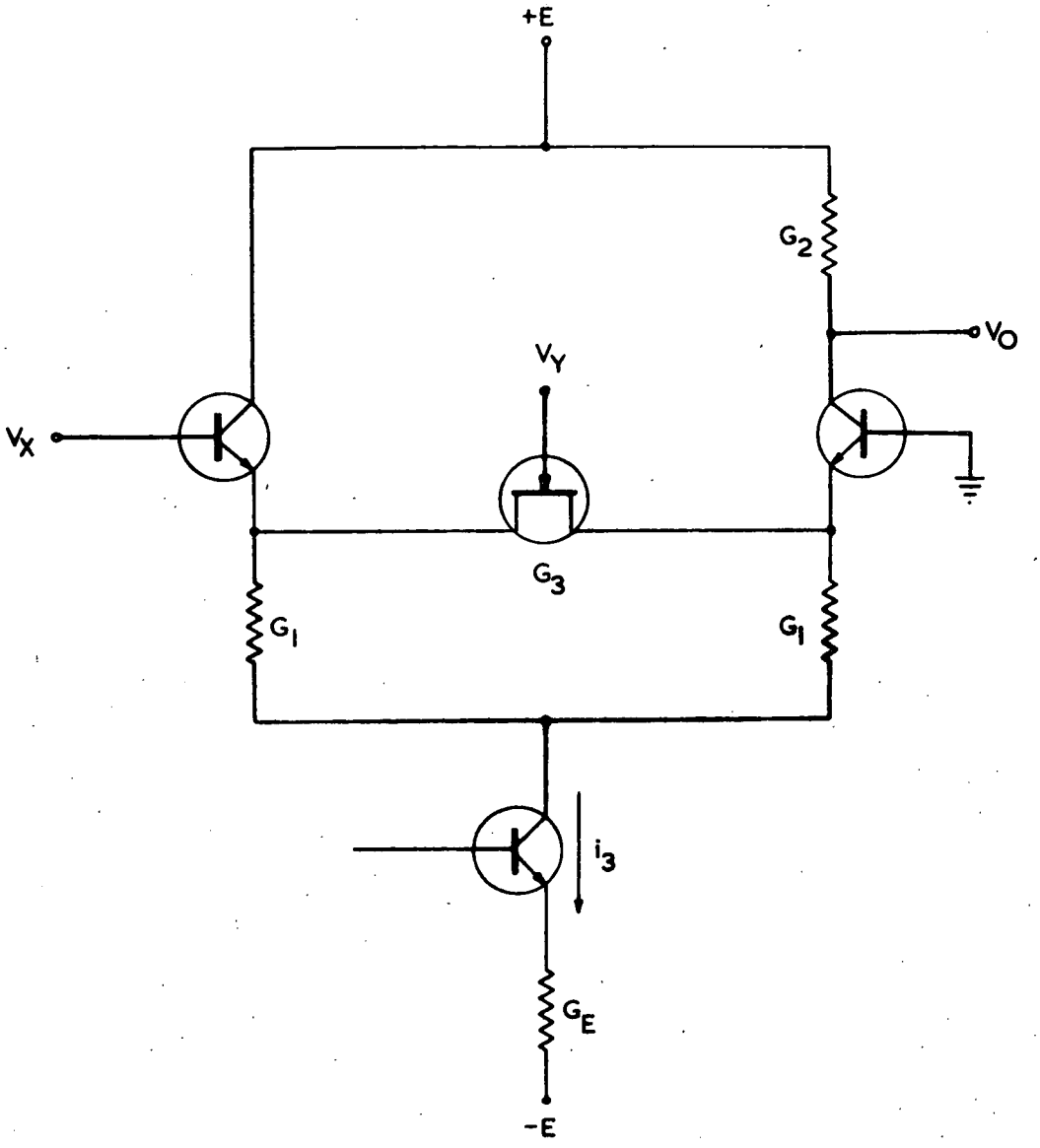

FIG. B.15 BASIC MULTIPLYING CIRCUIT

B.4.3 The Analogue Multipliers

The three major design factors which had to be considered for the analogue multipliers were the simplicity, cost and frequency response of the circuits. Because of the large number of analogue multipliers ultimately required (20) the simplicity and cost of the circuits had to be kept to a minimum. The initial frequency response required was 50 KHz.

Emerging indirectly from the development of modern solid state technology, analogue multipliers may be classified into two groups -

1. Circuits utilising the non-linear properties of bipolar transistors.
2. Circuits employing the f.e.t. as a voltage controlled conductance.

Circuits of group 1 generally have the advantage of a better frequency response but suffer from a higher degree of circuit complexity [19, 20, 34]. A multiplier of the second group was, therefore, designed and proved to be successful for the purposes required.

The actual approach to the multiplier design was suggested by Beene [35] and is shown in fig. B.15. Using nodal analysis it can be shown that

$$V_o = \frac{\frac{1}{2}G_1V_X + G_3V_X - \frac{1}{2}i_3}{G_2} + E \qquad \text{B.15}$$

for $h_{fe} >> 1$

Although Beene suggested zero bias on the f.e.t., it was found that for a given linearity figure a larger voltage swing could be applied at the X input if a small negative bias was employed. Generally the choice of bias is a compromise between the availability of a large output swing and the linearity of the circuit. For this particular application, a negative bias of approximately -3 volts gave the optimum result.

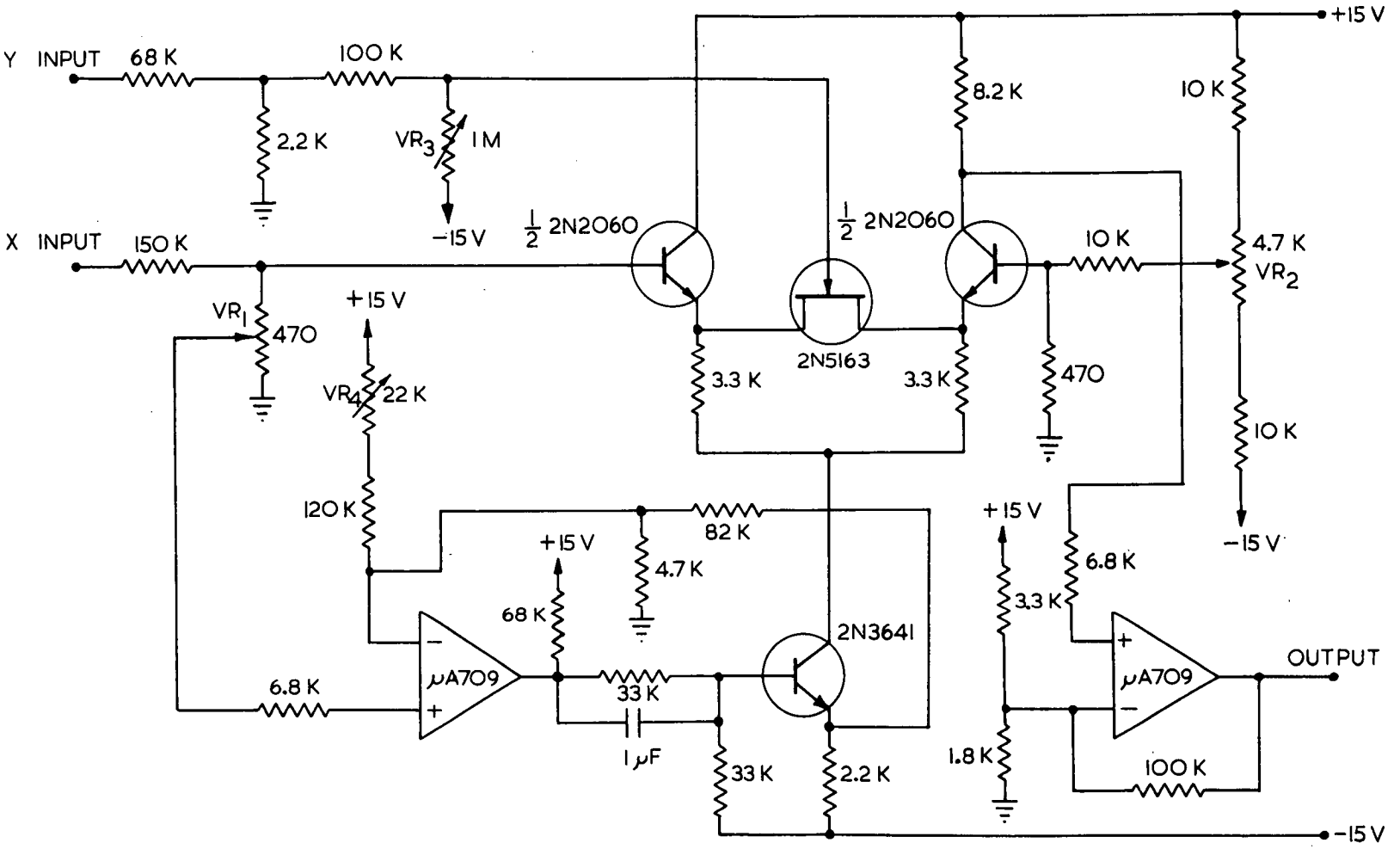

FIG. B.16 MULTIPLIER CIRCUIT

Rewriting Todd's original equation [36] -

$$G_3 = G_A \left[1 - \frac{V_Y + V_{bias}}{V_p} \right] \qquad B.16$$

where G_A is the f.e.t. conductance at zero bias

V_p is the f.e.t. pinch off voltage

V_Y is the input voltage to the f.e.t.

V_{bias} is the input bias voltage on the f.e.t.

If i_3 is controlled such that -

$$i_3 = \left[2G_A - 2G_A \frac{V_{bias}}{V_p} + G_1 \right] V_X + I \qquad B.17$$

where I is the d.c. bias current, then equation B.15 becomes -

$$V_o = \frac{-G_A}{V_p G} V_X V_Y + E - \frac{I}{2G_2} \qquad B.18$$

The multiplier circuit is shown in fig. B.16. It indicates four potentiometers which had to be adjusted for correct operation. Due to individual tolerances in the f.e.t. parameters VR3 was adjusted to provide optimum bias for the f.e.t. Once the bias was fixed the controlled current i_3 was set to give the correct ralationship between i_3 and V_X as given by equation B.17. This was achieved by adjusting VR1 so that there was no output when V_Y was zero. VR2 was then adjusted so that no output was produced for V_X equals zero. Finally the d.c. bias current, I, was set, by adjusting VR4, to null the d.c. output level.

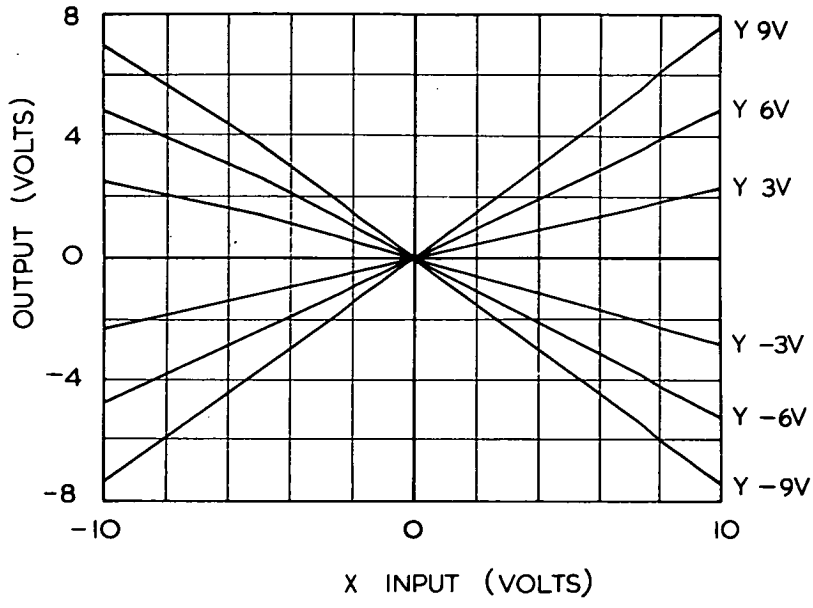

FIG. B.17 MULTIPLIER TRANSFER CHARACTERISTICS

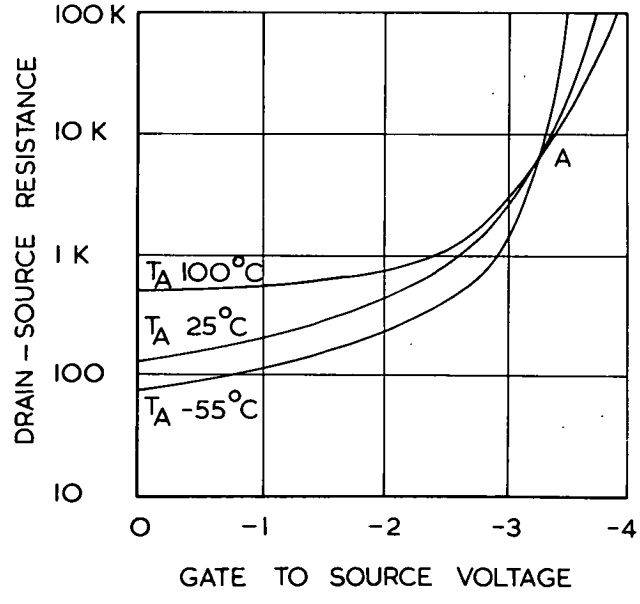

FIG. B.18 OPTIMUM BIAS POINT FOR TEMPERATURE COMPENSATION

The resistance values used with the differential pair were obtained experimentally to achieve the maximum linearity available from the circuit. The input attenuation circuits were then designed so that the multiplier was capable of handling input signal swings of ± 10 volts with a linearity of less than 5% relative to the maximum output. The resultant transfer characteristic of the circuit as drawn by an X-Y plotter is shown in fig. B.17.

In order to maintain a linearity of 5% the use of the multiplier was limited to approximately 20 KHz for the X input and 50 KHz for the Y input. The lower frequency limit on the X input was due to a slight phase shift being produced between the input voltage and i_3. This frequency limit could be raised to 50 KHz by placing a compensating capacitor across the 2.2KΩ current controlling resistor, for a very slight decrease in the linearity figure.

As the multiplier was to be used for experimental purposes only, no attempt was made to provide comprehensive temperature compensation. However, two simple circuit techniques were applied to minimise the effect of temperature variation. These were:

1. The dual amplifier used for the differential network, and
2. The feedback across the i_3 current controlling operational amplifier taken from the emitter of the regulating transistor.

The effects of temperature variation may appear as -

1. An incorrect multiplying action.
2. A d.c. output drift.

From equations B.17 and B.18 it can be seen that the f.e.t. parameters are critical for obtaining the correct multiplying action. Variation with temperature causes both a drift of the zero position of the Y input and a change in the value of the scale factor. Temperature compensation would, therefore, be required in the i_3 current controlling network to track the f.e.t. characteristic over the temperature range of interest. This drift may be minimised by biasing the f.e.t. at point A as indicated in Fig. B.18. Usual circuit design techniques similar to those required in the design of d.c. amplifiers may be used to limit the d.c. output drift.

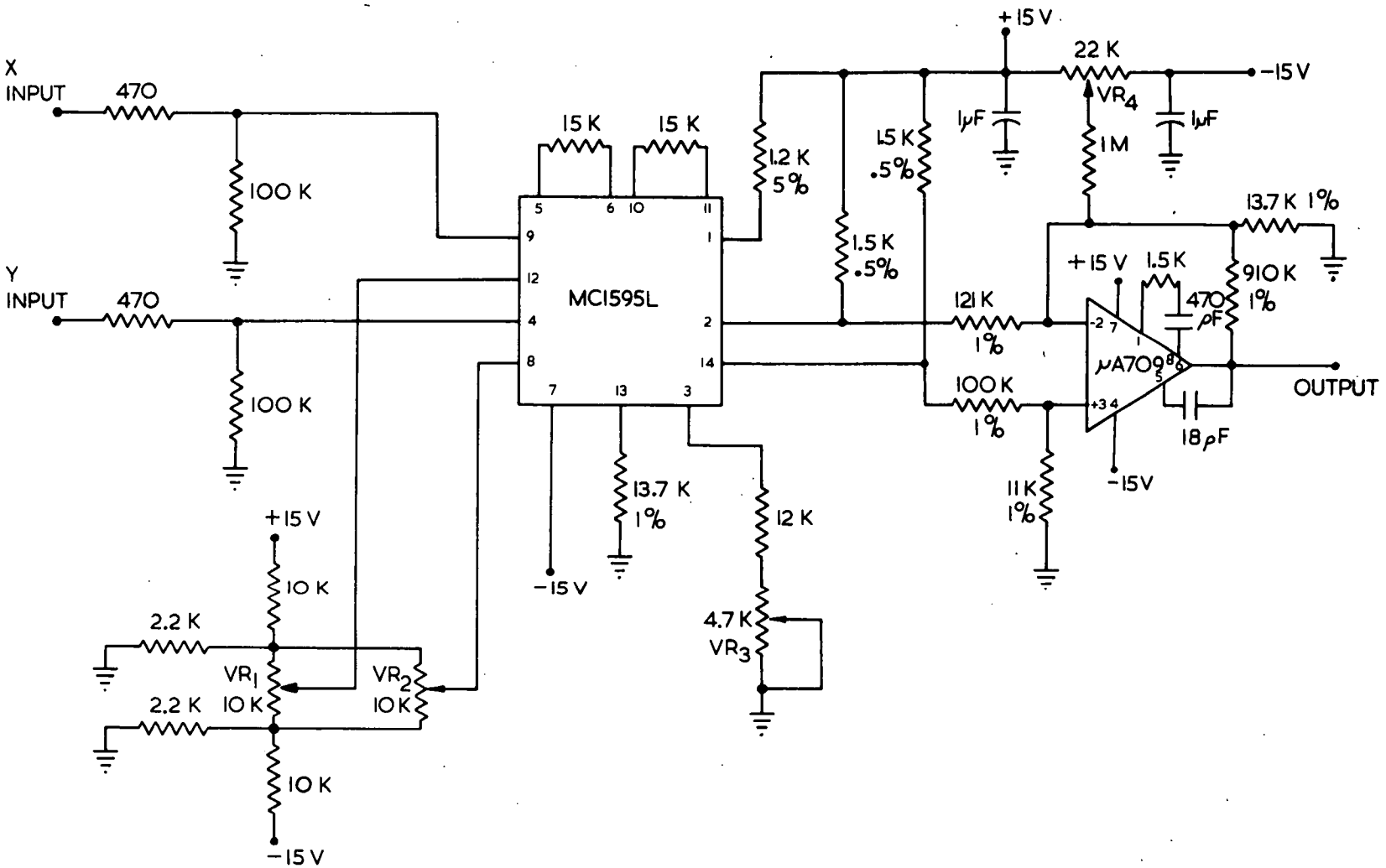

FIG. B.19 INTEGRATED CIRCUIT MULTIPLIER

The multiplier achieved the requirements for which it was designed. In particular it is a relatively simple and economic circuit.

After this analogue multiplier had been developed it became known that an integrated circuit multiplier was commercially available. As a number of these were also required by another research student, a total of twenty were purchased. These multipliers were ultimately used within the experimental system because of their superior static accuracy (within 1% and 2% of the maximum output for the X and Y inputs respectively), higher frequency response and higher input impedance. The circuit used is shown in fig. B.19.

The potentiometers VR1 and VR2 shown in the circuit are for adjusting the zeros of the X and Y inputs. VR3 adjusts the scale factor of the multiplier and VR4 the d.c. output. For economic reasons, trimmer potentiometers were used. The limited fine adjustment provided by these potentiometers made precise zeroing of the d.c. output level difficult.

With four adjustments per multiplier and a total of twenty multipliers, eighty adjustments were required each time the multipliers were calibrated. To enable these adjustments to be carried out in the shortest possible time a special unit for mounting the multipliers was constructed. This unit was complete with testing facilities and power supplies. The external circuit connections of the multipliers were provided by means of plug in connectors on the front panel, similar to those in the analogue computer.

B.4.4 The Infinite Clipper

Because the frequency response of the analogue multipliers used extended well beyond the ultimate bandwidth chosen for the system, the output of the clipper could be fed directly into the correlation multipliers with an insignificant loss in accuracy. This enabled the same circuitry, with the exception of the clipper, to be used for both linear and non-linear operation of the experimental system. For a practical nonlinear system, however, switched modulators would be used instead of analogue multipliers. For this system therefore, the magnitudes of the positive and negative output voltages of the clipper had to be equal.

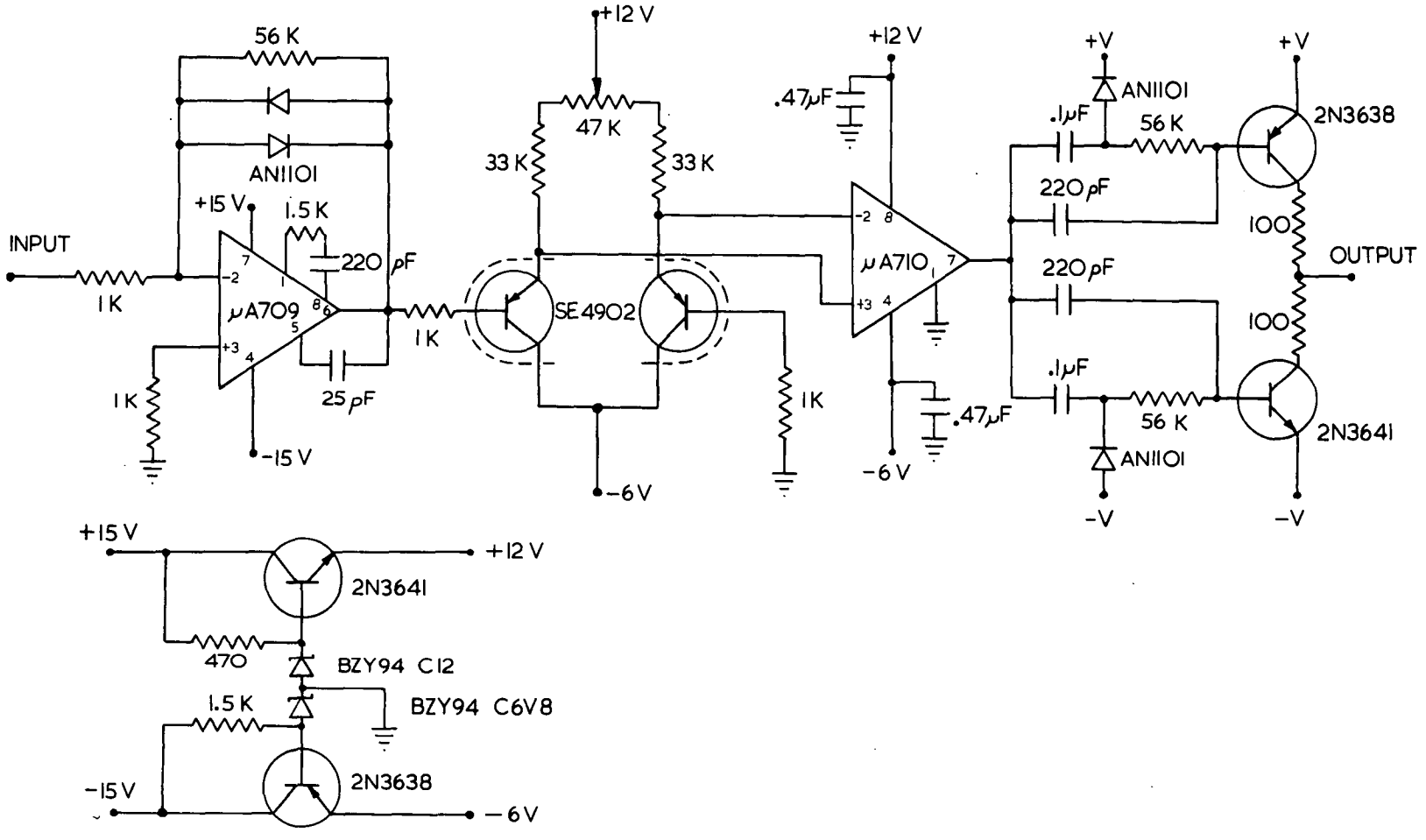

FIG. B.20 CLIPPER CIRCUIT

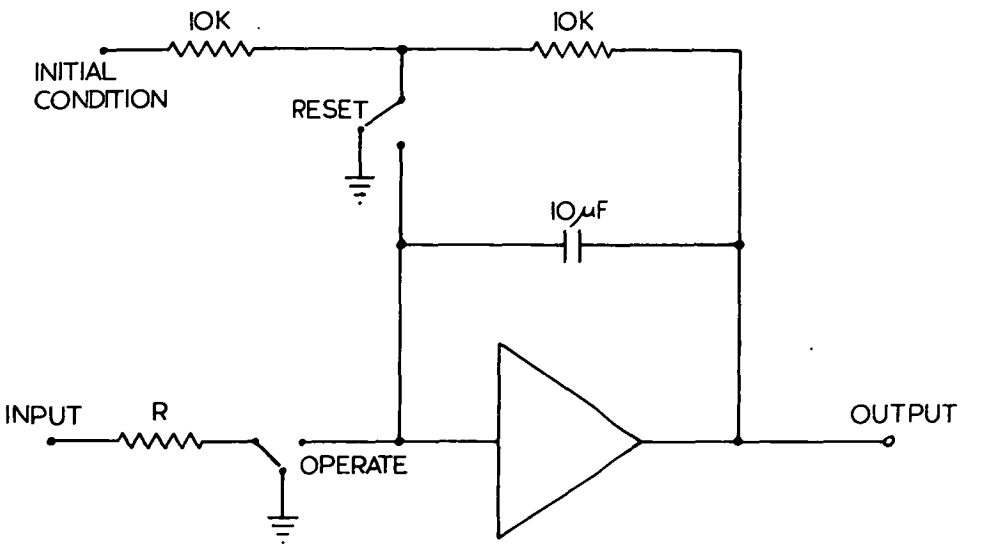

(a) INTEGRATOR

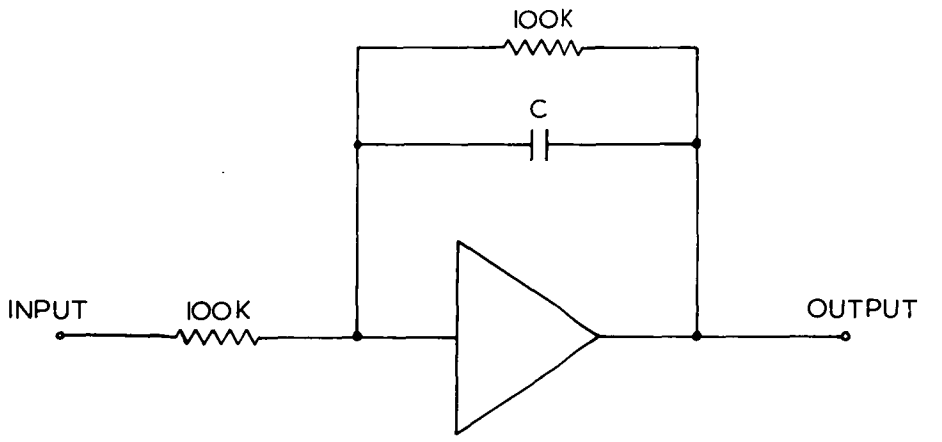

(b) LOW PASS FILTER

FIG. B.21 CORRELATION AVERAGING CIRCUITS

A μA710 comparator, with the negative input connected to earth, was used as the infinite clipper. A number of circuit additions were required for the following reasons -

1. The μA710 comparator does not provide a symmetrical output voltage swing (3.2 and -0.5 volts).
2. The maximum differential input voltage of the comparator is ± 5 volts, whereas the system was using signals with amplitudes up to ± 10 volts.
3. Initial experiments indicated that the gain provided by the μA710 alone was not sufficient to provide positive switching characteristics when the system had settled.
4. As an accurate switching characteristic was required, some adjustment of the negative input to the comparator was needed to allow for any bias offsets within the circuit.

The completed circuit is shown in fig. B.20.

The output circuit of the infinite clipper was supplied from an independent adjustable laboratory power supply to minimise power supply transients within the system. The μA710 was supplied by the simple regulation circuits shown in fig. B.20.

B.4.5 The Integrators

The integrators in the analogue computer were used for the correlation circuits. This enabled the circuits to be built quickly and also provided the system with the useful reset, hold and operate modes. This facility was necessary for measuring the accuracy of the equalisation. After settling the integrators were switched to the hold mode. The accuracy of the equalisation could then be measured by replacing the pseudo random noise with the sine squared pulse.

The circuit of the integrators is shown in fig. B.21(a). To vary the gain of the feedback loops the input resistor, R, was varied, taking the values 1kΩ, 10kΩ, 100kΩ.

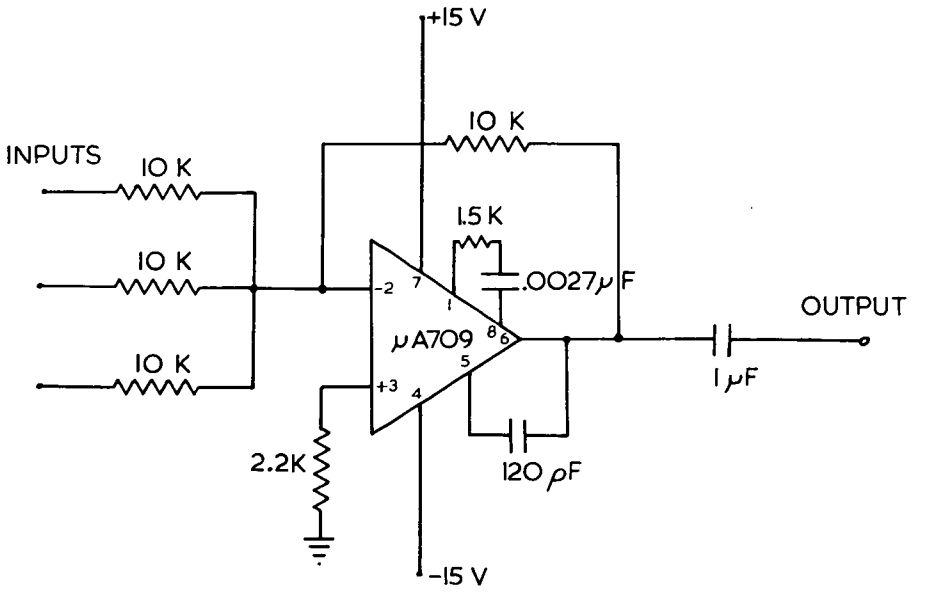

a) THREE INPUT

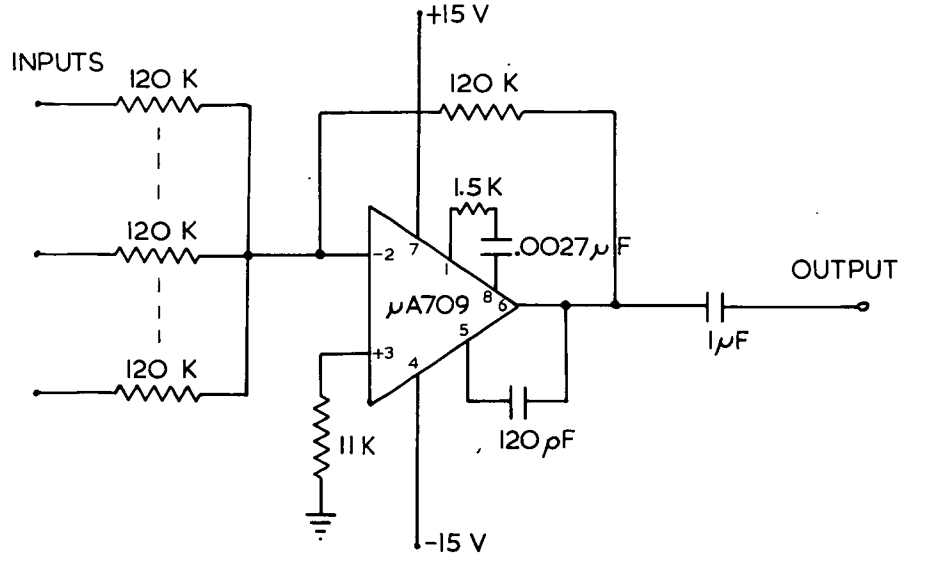

b) TEN INPUT

FIG. B.22 SUMMATION AMPLIFIERS

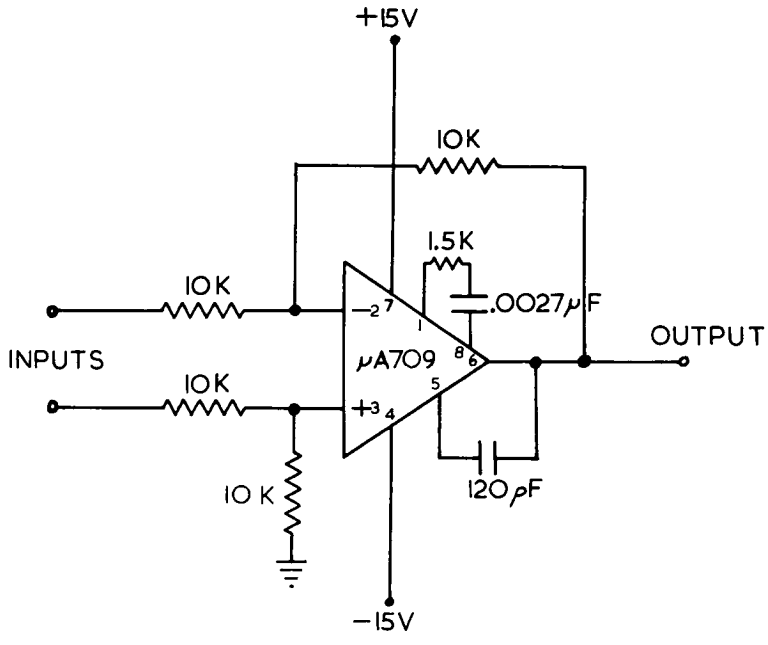

FIG. B.23 DIFFERENTIAL AMPLIFIER

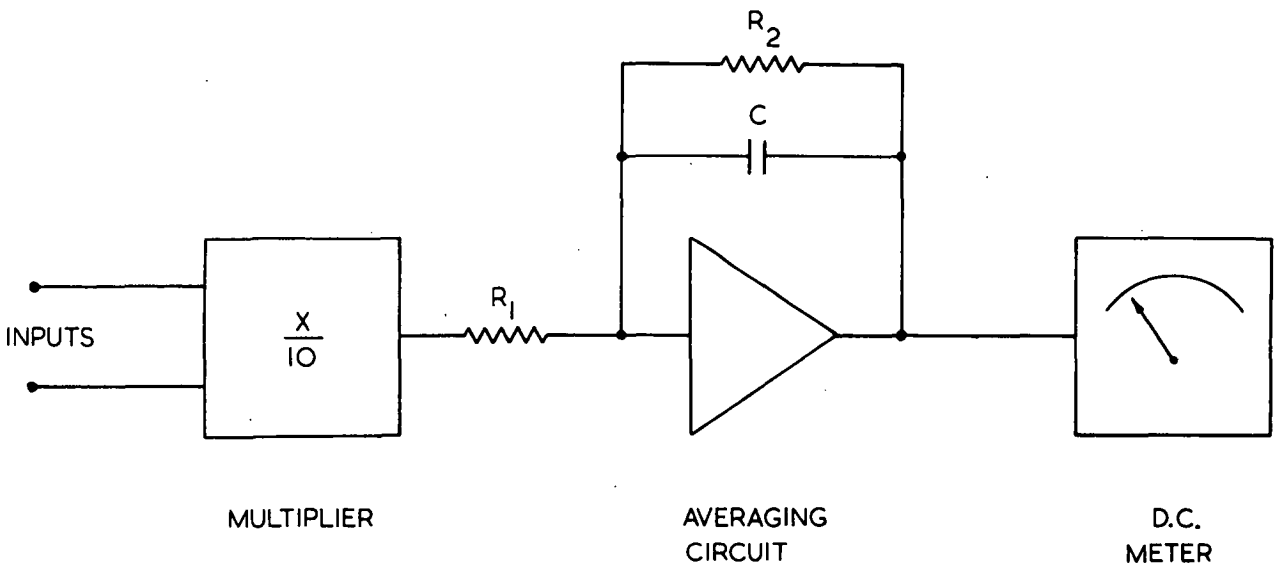

FIG. B.24 BLOCK DIAGRAM OF CORRELATION CIRCUIT

B.4.6 The Averaging Circuits

Simple low pass filters (fig. B.21(b)) were used to provide an extra time constant in the correlation circuits when required. The analogue computer was again used to provide the necessary circuitry. This enabled any change in the value of C to be made very easily. The capacitor was removed when the extra time constant was not required. The amplifier was retained in the tap control loop, however, to maintain the correct feedback polarity.

B.4.7 The Amplifiers

A number of amplifiers were used in the experimental system. Two summation amplifiers were required for summing the tap outputs, a three input amplifier, used for initial investigations, and a ten input amplifier. These were both conventional circuits (fig. B.22) employing μA709 operational amplifiers. The capacitors at the output of the amplifiers were employed to prevent any d.c. drift of the tap multipliers affecting the correlation circuits.

The differential amplifier shown in fig. B.23 was used to obtain the error between the equalised waveform and the reference waveform.

To enable any experiments requiring the loop gain of the system to be known accurately, the input and feedback resistors of these three amplifiers were measured to within a tolerance of 1%.

B.5 The Correlation Circuit

A number of auto-correlation and cross-correlation values of signals within the system were measured while investigating the experimental equaliser. A block diagram of the basic circuit used for these measurements is shown in fig. B.24.

B.6 The Power Supplies

The ± 15 volts required by the integrated circuits within the experimental system were supplied by the power supply built for the analogue multipliers. This was a stabilised power supply employing two μA723 precision voltage regulators.

APPENDIX C

Autocorrelation Function of Proposed Filter

The power density spectrum of the proposed filter is given by-

$$\Phi_{11}(\omega) = 1 \qquad \text{for } 0<\omega<\omega_1$$

$$= 0.5 + 0.5 \cos\left[\frac{(\omega - \omega_1)\pi}{\omega_2 - \omega_1}\right] \qquad \text{for } \omega_1<\omega<\omega_2$$

where

$$\omega_1 = 2\pi \times 4.5_{10}{}^{6} \quad \text{and} \quad \omega_2 = 2\pi \times 5.5_{10}{}^{6}$$

For an input signal of white noise the autocorrelation function of the output is given by -

$$\phi_{11}(\tau) = \frac{1}{2\pi} \int_{-\infty}^{\infty} \Phi_{11}(\omega) e^{j\omega\tau} d\omega$$

As $\Phi_{11}(\omega)$ is an even function then

$$\Phi_{11}(\tau) = \frac{1}{\pi} \int_{0}^{\omega_2} \Phi_{11}(\omega) \cos \omega\tau d\omega$$

$$= \frac{1}{\pi} \int_{0}^{\omega_1} \cos \omega\tau d\omega + \frac{1}{\pi} \int_{\omega_1}^{\omega_2} \left(0.5 + 0.5\cos\left(\frac{(\omega - \omega_1)\pi}{\omega_2 - \omega_1}\right)\right) \cos\omega\tau d\omega$$

$$= \frac{0.225_{10}{}^{-12}}{\pi\tau(0.225_{10}{}^{-12} - \tau^2)} \sin(\pi_{10}{}^{7}\tau) \cos(\pi_{10}{}^{6}\tau)$$

For $\tau = n_{10}{}^{-7}$ where n=1, 2, ... then $\phi_{11}(\tau) = 0$. Thus for a delay line equaliser with a tap spacing of 0.1 microseconds the above signal spectrum produces an orthogonal system.

REFERENCES

1. Macdiarmid, I.F. "Waveform Distortion in Television Links". P.O.E.E. Journal, No. 52, Pt. 1, July 1959 and Pt. 2, Oct. 1959.

2. Thiele, A.N. "Methods of Waveform Pulse and Bar Testing". Proc. I.R.E.E. Aust., Vol. 27, No. 12, Dec. 1966.

3. Thomson, W.E. "The Synthesis of a Network to have a Sine-Squared Impulse Response". Proc. I.E.E., Vol. 99, Pt. 3, No. 62, Nov. 1952.

4. Gouriet, G.G. "Spectrum Equalisation". Wireless Engineer, Vol. 30, No. 5, May 1953.

5. Linke, J.M. "A Variable Time Equaliser for Video-Frequency Waveform Correction". Proc. I.E.E., Vol. 99, Pt. 3A, No. 18, 1952.

6. Wheeler, H.A. "The Interpretation of Amplitude and Phase Distortion in Terms of Paired Echoes". Proc. I.R.E., June 1939.

7. Ellis, A.G., Harnath, R.W., Kitchenn, R.G. and Potter, J.B. "The Relaying of Television Programmes in Australia". I.E. Aust. Electrical Engineering Transactions, Vol. EE3, 1967.

8. Potter, J.B. "Pilot Waveform Insertion Unit for Use in the Australian T.V. Network". Proc. I.R.E.E. Aust., Vol. 27, No. 6, June 1966.

9. Lee, Y.W. "Statistical Theory of Communication". John Wiley, 1960.

10. Kitamori, T. "Applications of Orthogonal Functions to the Determination of Process Dynamic Characteristics and to the Construction of Self-Optimizing Control Systems". Proceedings of the First International Congress of the International Federation of Automatic Control, Vol. 2, Moscow 1960 (London Butterworths 1961).

11. Lucky, R.W. "Automatic Equalisation for Digital Communication". B.S.T.J., Vol. 44, April 1965.

12. Lucky, R.W. "Techniques for Adaptive Equalisation of Digital Communicatio B.S.T.J., Vol. 45, Feb. 1966. Systems".

13. Rudin, H.R. "Automatic Equalisation using Transversal Filters". I.E.E.E., Spectrum, Vol. 4, Jan. 1967.

14. Lucky, R.W. and Rudin, H.R. "An Automatic Equaliser for General Purpose Communication Channels". B.S.T.J., Vol. 46, Nov. 1967.

15. Lubbock, J.K. "Self-Optimizing Non-Linear Filter". Proc. I.E.E., Vol. 108, Pt. B, July 1961.

16. Sondhi, M.M. "An Adaptive Echo Canceller".
B.S.T.J., Vol. 46, March 1967.

17. Arnon, E. "An Adaptive Equaliser for Television Channels".
I.E.E.E. Trans. Comm. Technol., Vol. COM-17, No. 6, Dec. 1969.

18. Brueggemann, H. "New Feedback-Stabilised Analogue Multiplier".
Electronics Letters, Vol. 5, No. 5, March 1969.

19. Brueggemann, H. "Feedback Stabilised Four Quadrant Analogue Multiplier".
I.E.E.E. Journal Solid-State Circuits, Vol. SC-5, No. 4, Aug. 1970.

20. Morton, R.R.A. "A Simple d.c. to 10 Mc/s Analogue Multiplier".
Journal Scientific Instruments, Vol. 43, 1966.

21. Potter, J.B. "The Adaptive Equalisation of a Television Channel".
Proc. I.R.E.E. Aust., Vol. 29, No. 7, July 1968.

22. Hirsch, D. and Wolf, W.J. "A Simple Adaptive Equaliser for Efficient Data Transmission".
I.E.E.E. Trans. Comm. Technol., Vol. COM-18, No. 1, Feb. 1970.

23. Davies, W.D.T. "The Generation and Properties of Maximum Length Sequences".
Control, June 1966.

24. "Standards for the Australian Television Service".
Australian Broadcasting Control Board, (re-issued) Jan. 1962.

25. Rosenbloom, A. "Analysis of Linear Systems with Randomly Time-Varying Parameters".
Polytechnic Institute of Brooklyn, Proceedings of the Symposium on Information Networks, New York, April 1954.

26. Thé, G. "Theorem on Stieltjes Correlation".
Proc. I.E.E., Vol. 113, No. 6, June 1966.

27. Booton, R.C. "Nonlinear Control Systems with Random Inputs".
I.R.E. Trans. Comm. Technol., CT-1, 1954.

28. Narendra, K.S. and McBride, L.E. "Multiparameter Self-Optimizing Systems Using Correlation Techniques".
I.E.E.E. Trans. Automatic Control, Vol. AC-9, No. 1, Jan. 1964.

29. Lewis, N.W. "Waveform Responses of Television Links".
Proc. I.E.E., Vol. 101, Pt. 3, 1954.

30. E.A.I. Handbook of Analogue Computation.

31. Mason, S. and Zimmerman, H.J. "Electronic Circuits, Signals and Systems".
John Wiley & Sons, New York, 1960.

32. Potter, J.B. "A Laboratory V.S.B.S.C. Data Transmission Facility".
Research Report No. 1, 1968, Department of Electrical Engineering, University of Melbourne.

33. Brownell, R.A. "Use of the Digital Computer in the Analysis and Synthesis of Electrical Networks".
Ph.D. Thesis, University of Tasmania.

34. Giles, J.N. "Linear Integrated Circuits Applications Handbook". Fairchild Semiconductor, 1967.

35. Beene, G.W. "An Analogue Multiplier". Proc. I.E.E.E., Vol. 55, No. 7, July 1967.

36. Todd, C.D. "F.E.T. as Voltage Variable Resistors". Electronic Design, Vol. 13, No. 19, Sept. 1965.

37. Shinners, S.M. "Control System Design". John Wiley & Sons, New York 1964.

38. Bogner, R.E. "New Relay Correlation Method". Electronics Letters, Vol. 1, No. 3, May 1965.

39. Potter, J.B. "Use of Time Series Calculations in Investigation of Television Networks". Proc. I.R.E.E. Aust., Vol. 27, No. 8, Aug. 1966.

40. Thomson, W.E. "A Theory of Time Series for Waveform Transmission Systems". Proc. I.E.E., Vol. 99, Pt. 4, No. 4, Dec. 1952.

41. Lewis, N.W. "Waveform Computations by the Time Series Method". Proc. I.E.E., Vol. 99, Pt. 3, 1952.

42. Andrews, H. "A High Speed Algorithm for the Computer Generation of Fourier Transforms". I.E.E.E. Trans. Computers, Vol. C-17, April 1968.

43. Sperry, R.V. and Surenian, D. "A Transversal Equaliser for T.V. Circuits". B.S.T.J., Vol. 39, No. 2, March 1960.

44. Seyler, A.J. "An Experimental Time Equaliser for Television Signal Transmission". P.M.G. Research Laboratory Report, No. 4763, July 1958.

45. Roberts, P.D. and Davis, R.H. "Statistical Properties of Smoothed Maximal-Length Linear Binary Sequences". Proc. I.E.E., Vol. 113, No. 1, Jan. 1966.

46. Rappeport, M.A. "Automatic Equalisation of Data Transmission Facility Distortion Using Transversal Equalisers". I.E.E.E. Trans. Comm. Technol., Vol. COM-12, Sept. 1964.

47. Mackechnie, L.K. "Continuously Adaptive Echo Cancellers". Electronics Letters, Vol. 6, No. 3, 5th Feb. 1970.

48. Furmage, S.G. "A Simple Economic Analogue Multiplier". Proc. I.R.E.E. Aust., Vol. 31, No. 10, Oct. 1970.

Australian Electronics Communications is a section of the Proceedings devoted to the rapid publication of contributions containing new information on subjects of current interest.

Members of the Institution and other electronics and radio engineers are invited to take advantage of this section entitled Australian Electronics Communications to publish new and original work on any aspect of electronics and radio engineering and the application of these subjects in various branches of science, engineering and commerce.

Details concerning the preparation of contributions appear at the end of this section. Contributions may be sent to the Institution or to the Honorary Editor of this section, Professor R. E. Aitchison, Department of Electrical Engineering, The University of Sydney, Sydney, N.S.W., 2006.

A Simple Economic Analogue Multiplier

S. G. FURMAGE*

STUDENT, I.R.E.E.

Summary

A four quadrant analogue multiplier has been developed, based on the approach suggested by Beene. The multiplier has a bandwidth from d.c. to 20 kHz. Linearity figure is approximately 5% for input signals between ± 10 volts.

Introduction

The need for a four quadrant analogue multiplier often arises in the fields of signal processing and adaptive control systems. For example, the basic unit in a correlator for signal to noise optimisation is a multiplier. Similarly, an analogue multiplier is required in adaptive control systems using parameter perturbation methods.

A project on adaptive control was recently initiated which requires the use of a large number of analogue multipliers. Therefore, besides reasonable steady state and dynamic accuracy, two design factors which must be considered are economy and simplicity. Emerging indirectly from the development of modern solid state technology, analogue multipliers may be classified into two groups :

(i) circuits utilising the non-linear properties of bipolar transistors,

(ii) circuits employing the f.e.t. as a voltage controlled conductance.

Circuits of group (i) generally have the advantage of a better frequency response but suffer from a higher degree of circuit complexity.[1, 2] For the particular application for which the multipliers are required, the signals to be processed have a bandwidth of only 50 kHz. A multiplier of the second group has therefore been designed and proved to be highly satisfactory for the purposes required, as it is technically simple and also economic.

The Multiplier Circuit

The actual approach to the multiplier design was suggested by Beene[3] and is shown in fig. 1. Using nodal analysis it can be shown that

$$V_0 = \frac{\frac{1}{2} G_1 V_x + G_3 V_x - \frac{1}{2} i_3}{G_2} + E \qquad (1)$$

for $h_{fe} \gg 1$.

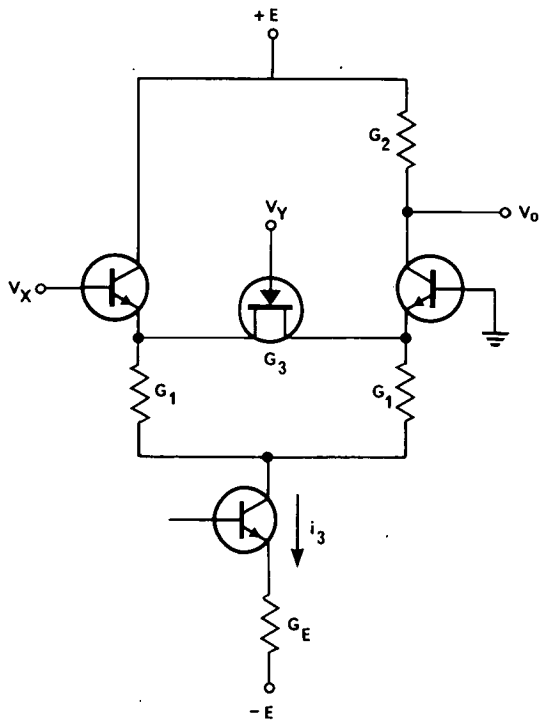

Figure 1.—Basic multiplying circuit.

*Department of Electrical Engineering, University of Tasmania, Hobart.

Manuscript received by The Institution January 1, 1970.
U.D.C. number 681.333 : 621.374.4.

1. Giles, J. N., " Linear Integrated Circuits Applications Handbook ", Fairchild Semiconductor, (1967), p. 152.
2. Morton, R. R. A., " Simple D.C. to 10 Mc/s Analogue Multiplier ", *J. Sci. Instruments*, Vol. 32, No. 3, March 1966, p. 65.
3. Beene, G. W., " An Analogue Multiplier ", *Proc. I.E.E.E.*, Vol. 55, No. 7, July 1967, p. 1206.

Although Beene suggested zero bias on the f.e.t., it is found that for a given linearity figure a larger voltage swing can be applied at the X input if a small negative bias is employed. Generally the choice of bias is a compromise between the availability of a large output swing and linearity. In the particular application envisaged a negative bias of approximately − 3 volts gives the optimum result.

Rewriting Todd's original equation[4]

$$G_3 = G_A \left[1 - \frac{V_Y + V_{bias}}{V_p}\right] \qquad (2)$$

where G_A is the f.e.t. conductance at zero bias,
V_p is the pinch-off voltage,
V_Y is the input voltage to the f.e.t.,
V_{bias} is the bias voltage on the f.e.t.

Performance

The input attenuation networks were designed so that the multiplier is capable of handling input signal swings of ± 10 volts with a linearity of less than 5% relative to the maximum output. The transfer characteristic of the circuit as drawn by an XY plotter is shown in fig. 3.

In order to maintain a linearity of 5%, the use of the multiplier is limited to approximately 20 kHz for the X input and 50 kHz for the Y input. The lower frequency limit on the X input is due to a slight phase shift produced between the input voltage and i_3. This frequency limit may be raised to 50 kHz by placing a compensating capacitor across the 2.2 kΩ resistor if a slight decrease in linearity can be tolerated. The multiplier achieves the requirements for which it was designed.

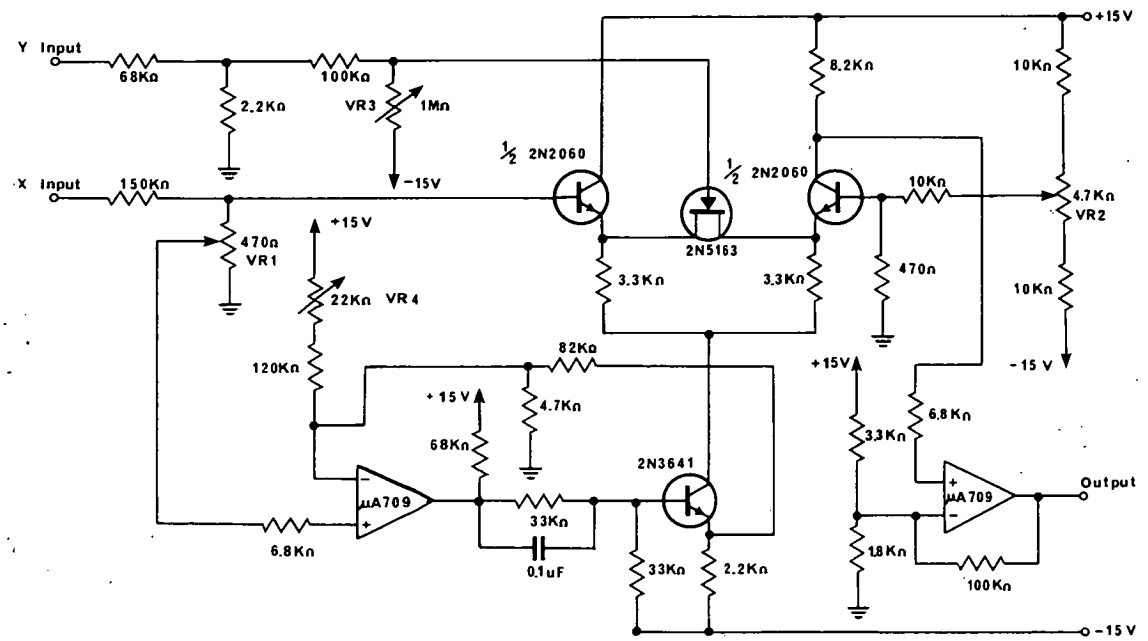

Figure 2.—Multiplier circuit.

If i_3 is controlled such that

$$i_3 = \left[2G_A - 2G_A \frac{V_{bias}}{V_p} + G_1\right] V_X + I \qquad (3)$$

where I is the d.c. bias current, then equation 1 becomes

$$V_0 = \frac{-G_A}{V_p G_2} V_X V_Y + E - \frac{I}{2G_2} \qquad (4)$$

The multiplier circuit as shown in fig. 2 has four potentiometers which must be adjusted for correct operation. Due to individual tolerances in the f.e.t. parameters, VR3 is adjusted to provide optimum bias for the f.e.t. Once the bias is fixed, the controlled current, i_3, must be set for the correct relationship between i_3 and V_X as given by equation 3.

This is achieved by adjusting VR1 so that there is no output when V_Y is zero. VR2 is then adjusted so that no output is produced when V_X equals zero. Finally the d.c. bias current, I, is set, by adjusting VR4, to null the d.c. output level.

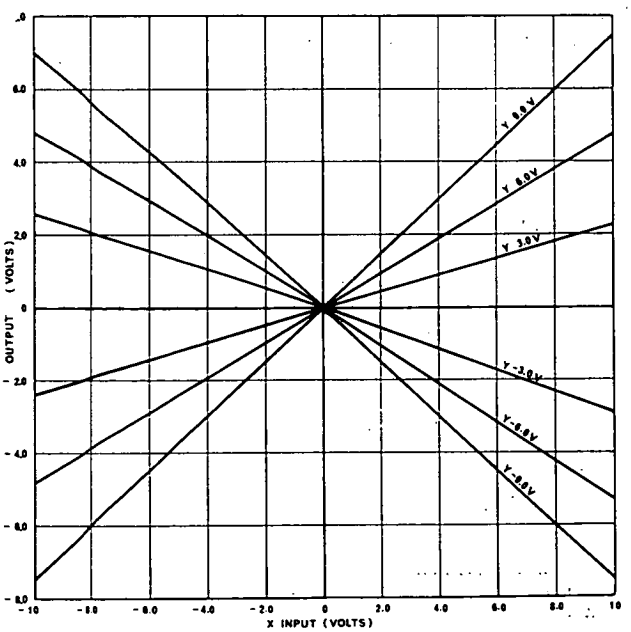

Figure 3.—Multiplier transfer characteristics.

4. Todd, C. D., "FET as Voltage Variable Resistors", *Electronic Design*, Vol. 13. No. 19, September 13, 1965, p. 66.

Discussion

As the multiplier is to be used for laboratory experiments only, no attempt was made to provide comprehensive temperature compensation. The effects of temperature variation may appear as :

(i) an incorrect multiplying action,

(ii) a d.c. output drift.

From equations 3 and 4 it can be seen that the f.e.t. parameters are critical for obtaining the correct multiplying action. Variation with temperature causes both a drift of the zero position of the Y input and a change in the value of the scale factor. To prevent any drift of the zero position of the Y input, temperature compensation must be applied to the current controlling network to track the f.e.t. characteristic over the temperature range of interest. This drift may be minimised by biassing the f.e.t. at point A as indicated in fig. 4. Concerning the problem of d.c. output drift, the usual circuit design techniques may be employed similar to those required in the design of d.c. amplifiers.

Acknowledgment

The author wishes to thank Mr. G. Thé for his helpful discussions and valuable suggestions relating to this project. The use of the facilities provided by the Electrical Engineering Department, University of Tasmania, is also gratefully acknowledged.

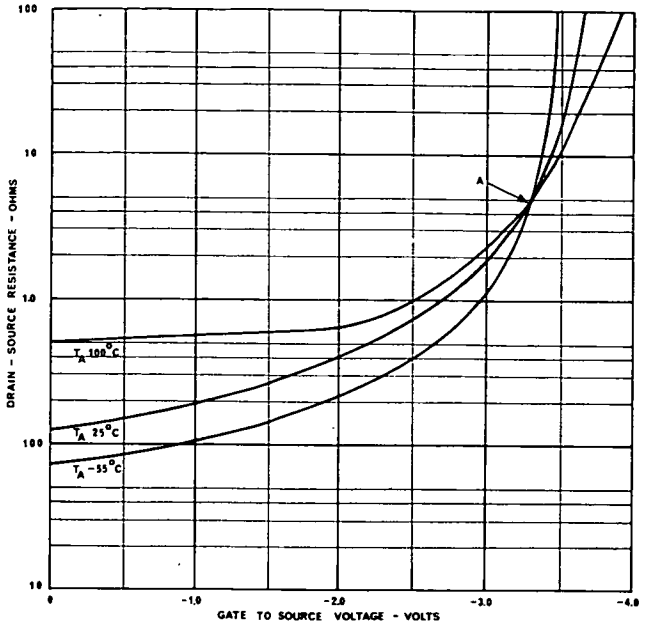

Figure 4.—Optimum bias point for temperature compensation.

Efficiency of Direct Radiator Loudspeaker Systems

R. H. SMALL*

MEMBER, I.R.E.E.

Summary

The low-frequency efficiency of direct-radiator loudspeaker systems is directly related to system cut-off frequency and to enclosure type and size. Plots are presented which show the efficiency of vented and sealed-box loudspeaker systems as a function of enclosure volume and cut-off frequency. Vented systems are found to possess a significant performance advantage.

The design of loudspeaker systems is usually based on three important specifications : size, efficiency and frequency response. Engineers have long been aware of the apparent interdependence of these specifications.

A. N. Thiele has shown[1] that the basic efficiency of a direct-radiator loudspeaker can be calculated from three basic parameters of the loudspeaker driver and that these same parameters also determine the low-frequency response of the driver in a vented box of a given size. The same analytical methods can be used to derive a relationship between the basic driver parameters and the low-frequency response of the driver in a sealed box.

The above efficiency and response relationships confirm that for each type of system, specifications of size, reponse and efficiency are not independent ; if two are specified, the third is determined and may be calculated. They also reveal that system small-signal performance does not depend on the diameter of the driver. The choice of driver size may be decided on the basis of cost or large-signal performance specifications such as acoustic power output or distortion.

The basic efficiency of vented loudspeaker systems adjusted for a fourth order Butterworth (maximally flat) response is plotted in fig. 1 as a function of net internal box volume, V_B, and system cut off frequency, f_3. A corresponding plot of the basic efficiency of high-compliance-ratio (acoustic-

*School of Electrical Engineering, University of Sydney, Sydney.
Manuscript received by The Institution May 21, 1970.
Revised manuscript received by The Institution June 22, 1970.
U.D.C. number 621.395.623.7.

1. Thiele, A. N., "Loudspeakers in Vented Boxes", *Proc. I.R.E.E. (Aust.)*, Vol. 22, No. 8, August 1961, p. 487.

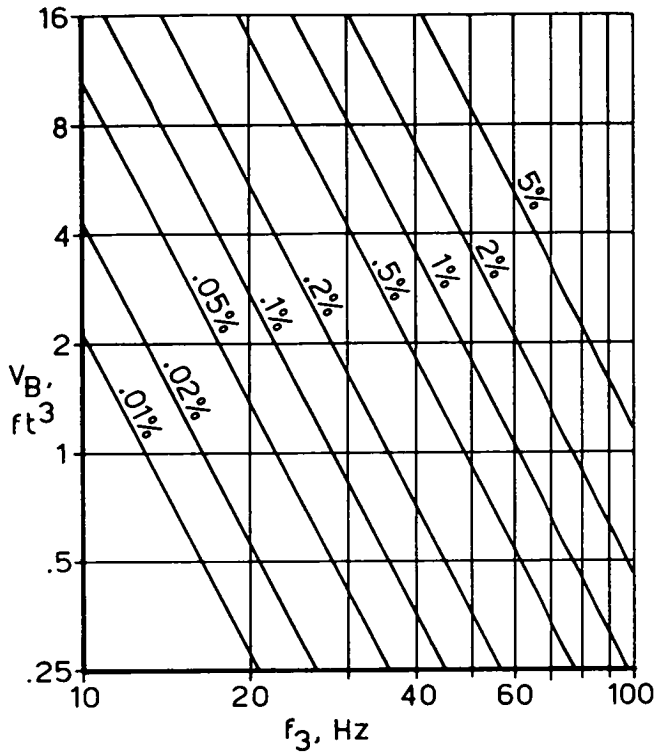

Figure 1.—Basic efficiency of vented loudspeaker systems as a function of net internal box volume, V_B, and system cut-off frequency, f_3.

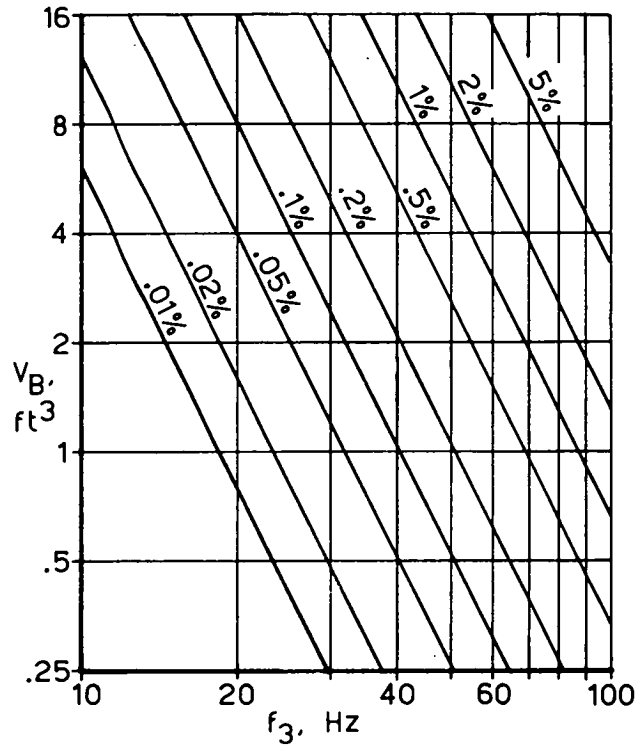

Figure 2.—Basic efficiency of acoustic-suspension loudspeaker systems as a function of net internal box volume, V_B, and system cut-off frequency, f_3.

suspension) sealed-box systems adjusted for a second order Butterworth response is presented in fig. 2.

In both figures, the cut off frequency, f_3, is the frequency at which the system response is 3 dB below pass-band level; this is the same as the vented system driver resonance or the sealed-box system resonance. Driver mechanical and acoustical losses of typical magnitude are allowed for and amplifier output resistance is assumed negligible compared to voice-coil resistance.

In each figure, the relationship determining basic efficiency is of the form $\eta = k_\eta f_3^3 V_B$, where η is the basic efficiency of the system and k_η is an efficiency constant. The value of k_η depends on the amount of electromagnetic damping in the loudspeaker driver; it is therefore determined in each case by the specifications of system type and response shape, because these specifications fix the amount of damping required. The efficiency values in the figures apply only to systems which have been adjusted for the specified response by manipulation of the driver parameters; they do not apply to systems using auxiliary filters or damping networks.

The figures indicate the limited efficiency available from typical compact enclosures: this is usually in the range of 0.2 to 0.4%. They also reveal that vented systems provide a performance advantage over sealed-box systems. This advantage, which results from a larger value of k_η, may be used to obtain $4\frac{1}{2}$ dB higher efficiency for the same size and bandwidth, half an octave greater bandwidth for the same size and efficiency or a size reduction of 2/3 for the same bandwidth and efficiency.

The efficiency relationships presented here provide a quantitative understanding of the interdependence of loudspeaker system size, efficiency and low-frequency response. This understanding should assist system designers, particularly those who have control over driver parameters in manufacture, to establish realistic loudspeaker and amplifier design goals.

The composite 8-8000 MHz spectrum of the Culgoora radiospectrograph is recorded on a continuously moving 70 mm film while the C.R.T. beam is swept in a direction perpendicular to the film movement in synchronisation with the swept receivers. The space available on this film for recording the 2-8 GHz spectrum allows about 200 separate resolution squares. Therefore, in order to make full use of the resolution available in the record, the receiver bandwidth should be not more than 6000/200 = 30 MHz, assuming that frequency changes linearly with time. As the C.R.T. beam is swept at the rate of four times per second the maximum effective time constant τ is $1/(4 \times 200)$ s or 1.25 ms.

4.5 *Radiometer Mode*

For routine noise figure measurements and aerial gain calibrations it is desirable that the microwave spectrograph be easily convertible to a radiometer operating at any desired frequency within the 2-8 GHz range. This is achieved by selecting a preset voltage with switch S_2 and locking the bistable multivibrator by setting S_3 or S_4 to the appropriate position. In this mode of operation the radiometer output can be integrated and fed to a pen recorder.

5. Calibrations and Tests

At the beginning of each day C.W. signals are transmitted to the parabolic reflector through standard gain horns placed at a convenient distance. These signals are recorded on the film and provide frequency calibration marks.

The output of a digital clock is photographed on the 70 mm film once every five minutes. The clock output includes the year, month, day and universal time.

As both the C.R.T. and film have non-linear characteristics a noise temperature versus film density calibration is needed. This is obtained by connecting the input of the mixer to a broad-band noise source and inserting a preset attenuator between the i.f. amplifiers. When the noise source is switched on the known noise temperature produces some level of density on the film. The attenuation is then decreased in 1 or 3 dB steps, thereby giving stepped calibration densities on the film. For this calibration the frequency range is restricted to the 2-4 GHz band so that only one noise source is needed.

5.1 *Quiet Sun*

Fig. 5 shows the variation of receiver output voltage with aerial declination when the microwave spectrograph was operated as a radiometer at fixed frequencies of 2.2, 3.9 and 6.4 GHz and the aerial scanned the quiet sun in declination. The aerial beamwidth is seen to be inversely proportional to frequency; the maximum heights of the three graphs are made equal by adjusting the relative gain of the receiver.

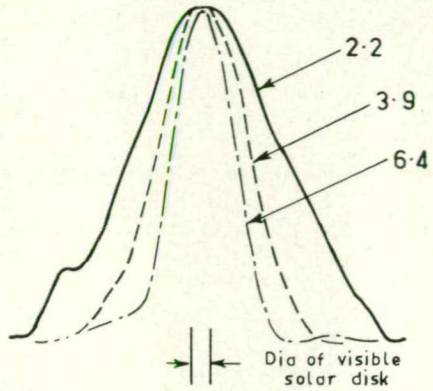

Figure 5.—Declination scans of the quiet sun when the microwave spectrograph was operated as a radiometer at 2.2, 3.9 and 6.4 GHz. The ordinate is a linear scale of the signal power.

6. Observations

The microwave spectrograph started operation in March 1970. Since then we have observed and reported several microwave bursts.

Fig. 6 illustrates two microwave solar radio bursts that occurred on November 16, 1970 and were associated with an optical flare that started at 00^h45^m U.T. and reached its maximum at 00^h52^m U.T. The first burst exhibits continuum-like broad-band characteristics and coincides with the flash phase of the flare; a short-wave fadeout is clearly visible in the low-frequency bands of the spectrograph. The second radio burst is a complex broad-band burst with impulsive onset at all wavelengths and very clear fine-structure features at the decimetre wavelengths. Reported radiometer observations indicate that the first maximum of 2200 s.f.u. at 2.7 GHz and 5600 s.f.u. at 5 GHz occurred at 00^h52^m U.T., while the second maximum of 1420 and 2110 s.f.u. respectively occurred at 01^h12^m U.T.

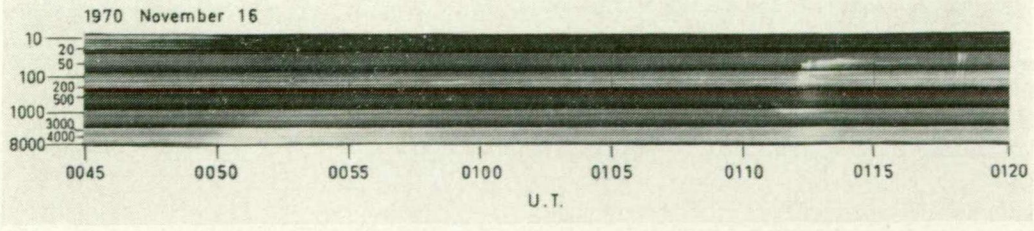

Figure 6.—The dynamic spectrum of radio outbursts on November 16, 1970. The lowest of the six bands in this figure (2000-8000 MHz) is produced by the spectrograph described here. The ordinate of the spectrum is frequency (MHz) and the abscissa is universal time.

7. Possible Developments

Future plans include the construction of a similar radio spectrograph to record the left-handed circularly polarised burst radiation of the Sun over the same frequency range, extension of the frequency coverage and improvement of the noise figure. A small decrease of the overall noise figure is now possible with the availability of new low-noise transistors.

Acknowledgments

It is a pleasure to acknowledge the help and encouragement I received from Dr. J. P. Wild, who initiated the project, and Dr. S. S. Suzuki; K. V. Sheridan's advice and help in testing techniques are appreciated. N. R. Labrum read the manuscript and made several valuable suggestions; K. R. McAlister designed both the aerial stand and drive mechanism and the workshop under the direction of E. C. Chenhall was responsible for the construction of all mechanical parts. J. Joisce carried out the observations and assisted in many experiments. P. W. Butler measured the radiation patterns of the aerial feed.

Subharmonic Instability in Pulse Width Modulated Feedback System

G. THÉ* and S. G. FURMAGE*
ASSOCIATE MEMBER, I.R.E.E. STUDENT, I.R.E.E.

Summary

When a pulse-width modulator is employed within a narrow-band closed loop system, the dynamic behaviour of the system can be analysed by replacing the modulator with a linear amplifier having an equivalent d.c. gain. However, this analysis method will fail if applied to a wide band system as it cannot predict the existence of oscillations at a subharmonic of the carrier frequency.

The general phenomena of subharmonic instability is investigated and a set of frequency-dependent describing functions are derived from the modulator. Based on these describing functions, a method is presented in which an accurate prediction of subharmonic instability and mode of oscillations can be made.

Apart from providing a better understanding of the concept of subharmonic oscillations, the describing function method is also a practical tool for measuring the relative degree of stability of pulse-width-modulated control systems. The whole of the theoretical work is supported by analogue-simulation studies.

1. Introduction

Although the principle of pulse width modulation (PWM) was primarily conceived for applications in communication systems, PWM has also entered the field of feedback control systems. In addition to its extensive applications for the altitude control of space vehicles, it is particularly attractive in industrial control and signal processing due to its ability to control large signal powers with high efficiency.

One of the important problems of PWM feedback systems which confronts the control engineer, is the stability problem. As the PWM feedback system is a special case of a non linear sampled data system, early researchers[1, 2] have investigated the criteria for absolute stability in the large through Liapunov's second method. This method however, yields conservative gain limits for stability as it depends on the appropriateness of the choice of a Liapunov function. Other investigators[3, 4] compared PWM systems in the state of limit cycles to finite pulsed systems with periodically varying sampling pattern and were able to use z-transformation to predict system stability. It is not clear however, how this method could be used to realize compensation in the linear plant so as to obtain a stable system. Instability in PWM feedback systems is characterised by the existence of subharmonic modes of oscillations. These are similar in nature to the problem of ripple instability inherent in closed loop systems employing thyristor amplifiers.

*Department of Electrical Engineering, University of Tasmania, Hobart.

Manuscript received by The Institution October 26, 1970.
Revised manuscript received January 27, 1971.
U.D.C. number 621.376.54.

1. Kadota, T. T. and Bourne Jr., H. C., "Stability Conditions of PWM Systems Through the Second Method of Liapunov", *Trans. I.R.E. on Automatic Control*, Vol. AC-6, pp. 266-276, Sept. 1961.
2. Murphy, G. J. and Wu, S. H., "A Stability Criterion for PWM Feedback Control Systems", *Trans. I.E.E.E. on Automatic Control*, Vol. AC-9, pp. 434-441, October 1964.
3. Jury, E. I. and Nishimura, T., "On the Periodic Modes of Oscillation in PWM Feedback Systems", *Trans. A.S.M.E. J.Basic Engineering*, Vol. 84, pp. 71-84, March 1962.
4. Jury, E. I. and Nishimura, T., "Stability Study of PWM Feedback Systems", *Trans. A.S.M.E. J.Basic Engineering*, Vol. 86, pp. 80-86, March 1964.

Fallside,[5] used the describing function analysis to predict instability in inverter-motor drives employing negative feedback. Although he outlined also, a similar approach which can be of use in the analysis of pulse modulated control systems,[6] no experimental results were reported to corroborate the accuracy of the method.

The purpose of this paper is to report on a method which can be employed to predict instability in wideband PWM feedback systems. This technique utilizes the envelope of a set of describing functions for the modulator which is then used to test system stability from a Nyquist criterion. In some way the procedure followed is similar to that used by West et al.[7]. However it should be pointed out that the dual input describing function method cannot be applied to a PWM system as the modulator input is operated on nonlinearly by the carrier signal.

This paper will illustrate how a clearer picture can be obtained as to the way subharmonic oscillations are generated in unstable PWM systems. More specifically, it will demonstrate how system stability can be improved through frequency compensation.

2. Pulse Width Modulating Characteristics

In pulse width modulation, constant amplitude rectangular pulses are generated whose widths are directly proportional to the modulating voltage. This modulation process may be performed by two different methods, depending on the type of sampling employed.

The first method consists of sampling the modulating signal at a constant rate as determined by the frequency of the carrier signal as shown in figure 1a. This form of sampling is known as periodic sampling.

The second method is carried out by comparing the modulating signal with a reference sawtooth waveform which runs at the carrier frequency. The output of the modulator consists of pulses whose polarity depends on whether the modulating signal is larger or smaller than the sawtooth waveform as illustrated in figure 1b. This form of sampling is known as natural sampling.

For modulators operating in the natural sampling mode, three types of reference signals may be used in the comparison process, i.e.

(i) sawtooth waveform with leading edges

(ii) sawtooth waveform with trailing edges

(iii) triangular waveform

As most practical realizations of pulse width modulators are of the type employing natural sampling, all investigations and discussions described in this paper including all the describing functions computed in section 5 refer to modulators which use this form of sampling and which utilize as a reference signal, a sawtooth waveform with leading edges, (as shown in figure 1b).

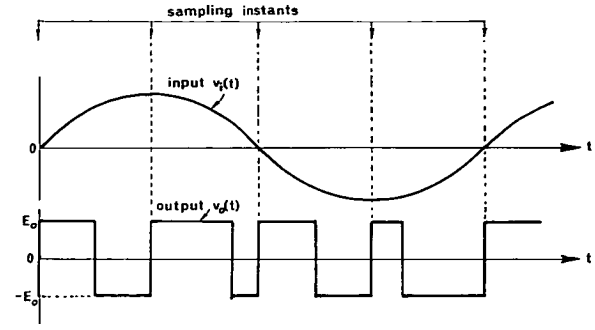

Figure 1a.—Pulse-width-modulation with periodic sampling.

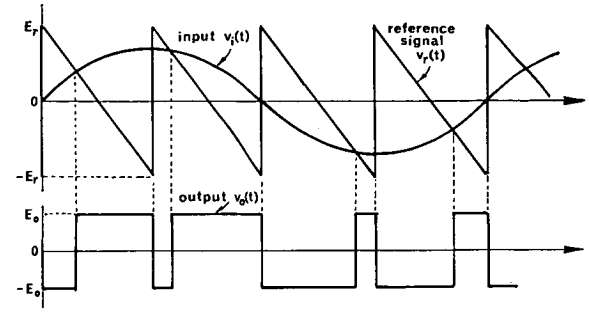

Figure 1b.—Pulse-width-modulation with natural sampling.

One of the major reasons for the frequent use of PWM in control applications stems from the fact that most control systems are of a low pass nature, and as demodulation of PWM signals requires time averaging, this can be carried out by the system itself.

3. The Describing Function Method

The describing function concept is a linearisation procedure which attempts to extend the very powerful transfer function approach of linear systems to nonlinear systems. As the describing function method is well established,[8, 9] it will be dealt with only briefly here.

If the input $v_i(t)$ of a nonlinear device is a pure sine wave

$$v_i(t) = E_i \sin \omega t$$

then in general, the output of the device, $v_0(t)$, is also a periodic signal having the same fundamental period as that of the input signal. Therefore, the steady-state output of the nonlinear device can be expressed by the Fourier series :

$$v_0(t) = \tfrac{1}{2}A_0 + \sum_{n=1}^{\infty} A_n \cos(n\omega t) + \sum_{n=1}^{\infty} B_n \sin(n\omega t)$$

where

$$A_n = \frac{2}{\pi}\int_0^{\pi} v_i(t)\cos(n\omega t).\,d(\omega t)$$

and

$$B_n = \frac{2}{\pi}\int_0^{\pi} v_i(t)\sin(n\omega t).\,d(\omega t)$$

5. Fallside, F. and Farmer, A. R., " Ripple Instability in Closed Loop Control Systems with Thyristor Amplifiers ", *I.E.E. Control & Science Record*, pp. 139-152, March, 1967.
6. Fallside, F., " Ripple Instability in Closed Loop Pulse Modulation Systems Including Invertor Drives ", *I.E.E. Control & Science Record*, pp. 218-228, March, 1968.
7. West, G. C., Douce, Y. L. and Livesley, R. K., " The Dual Input Describing Function and Its Use in the Analysis of Non-Linear Feedback Systems ", *Proc. I.E.E.*, Vol. 103, Part B, pp. 463-473, 1956.
8. Kochenburger, R. J., " A Frequency Response Method for Analysing and Synthesizing Contactor Servomechanism " *Trans. I.E.E.E.*, Vol. 69, pp. 270-284, 1950.
9. Shinners, S. M., " Control System Design ", Chapter 7, pp. 215-267, J. Wiley & Sons Inc. 1964.

The describing function, N, by definition, is an equation expressing the ratio of the amplitudes and the phase angle between the fundamental of the output and the input sinusoid, i.e.

$$N(E_i, \omega) = \frac{\sqrt{A_1^2 + B_1^2}}{E_i} \exp.[j . \arctan(A_1/B_1)]$$

Note that the describing function generally is a function of both the amplitude E_i and the frequency ω of the input sinusoid. In the case where an equation is not convenient, a curve or family of curves may be a satisfactory representation of the describing function.

All harmonics and any d.c. component are neglected. This assumption is reasonable since the harmonic terms are generally small compared to the fundamental term. In addition, a feedback control system usually provides additional attenuation of the harmonics terms because of its inherent low pass filtering action. Most nonlinear elements do not generate a d.c. term, since they are symmetrical.

The describing function can be utilized to determine the stability of a nonlinear feedback control system. Consider the system illustrated in figure 2. $G(j\omega)$ and $H(j\omega)$ are the transfer functions of the linear components

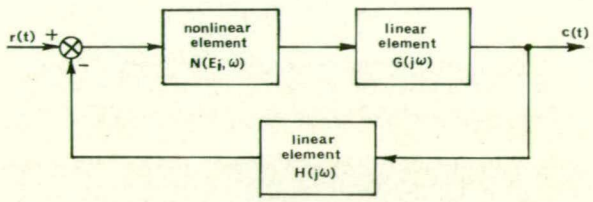

Figure 2.—Nonlinear feedback system.

and $N(E_i\ \omega)$ is the describing function of the nonlinear element. The transfer function of the feedback control system is then :

$$\frac{C(j\omega)}{R(j\omega)} = \frac{G(j\omega) . N(E_i, \omega)}{1 + G(j\omega) . N(E_i, \omega) . H(j\omega)}$$

and the Nyquist plot is based on the characteristic equation

$$1 + G(j\omega) . N(E_i, \omega) . H(j\omega) = 0 \quad \ldots\ldots\ldots\ldots\ldots\ldots (1)$$

The normal linear procedure is to obtain a polar plot of

$$[G(j\omega) . N(E_i, \omega) . H(j\omega)]$$

which makes the point $-1 + j0$ the critical point for stability analysis. However, a more satisfactory procedure is obtained by re-arranging equation (1) as follows :

$$G(j\omega) . H(j\omega) = -\frac{1}{N(E_i, \omega)} \quad \ldots\ldots\ldots\ldots\ldots\ldots (2)$$

Equation (2) separates the linear transfer function factors from the describing function factor. Therefore, $[G(j\omega)\ H(j\omega)]$ may be plotted as a polar transfer function curve. The term $[-1/N(E_i\ ,\ \omega)]$ may also be plotted on the same sheet to the same scale, except since it is generally a function of both signal amplitude and frequency, the plot may be a family of curves with the frequency as the parameter.

System stability can then be investigated by inspecting the relative location of a point on the $[G(j\omega)\ H(j\omega)]$ curve with respect to the corresponding $[-1/N(E_i\ ,\ \omega)]$ curve. The system is stable if for all frequencies the points on the $[G(j\omega)\ H(j\omega)]$ curve lie outside the corresponding $[-1/N(E_i\ ,\ \omega)]$ curves.

4. Subharmonic Instability

In general, the configuration of a PWM feedback system is as illustrated in figure 2, where the nonlinear element is the modulator. When analysing such a system, the simplest procedure commonly used consists of representing the modulator by a linear gain element, whose gain is equivalent to the d.c. gain of the modulator. This method may be applied successfully provided the system's cross over frequency is much smaller than the carrier frequency. Under this condition, the ripple feedback to the input of the modulator is negligible. However, if the system is to have a fast response, then the bandwidth must be increased and application of this simple linear stability analysis will give erroneous results. This is to be expected because the analysis method neglects the phase- and amplitude-characteristics of the modulator at the frequency band in the proximity of the carrier frequency.

When some of the high frequency components of the modulator output are fed back into the input with sufficient amplitude and correct phasing, self oscillation may result. Such oscillations always occur at a subharmonic of the carrier frequency. Investigations have established that the most common instability in PWM feedback systems is that occurring at the $\frac{1}{2}$-subharmonic of the carrier frequency. Figure 3a is a photograph of an oscilloscope display showing the input and output waveforms of the modulator in a system which suffers from $\frac{1}{2}$-subharmonic instability. The onset of $\frac{1}{2}$-subharmonic instability is always distinct, that is, if a system is poten-

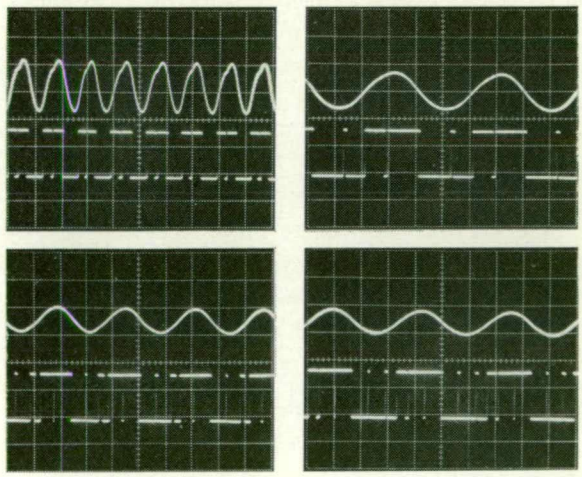

Figure 3.—Modulator input and output waveforms in unstable pulse-width-modulated feedback systems.
(a) 1/2 subharmonic instability
(b) 1/3 subharmonic instability
(c) 1/4 subharmonic instability
(d) 1/5 subharmonic instability
vertical scale : 5 volts/division
horizontal scale for (a) & (b) : 1 ms/division
horizontal scale for (c) & (d) : 2 ms/division

tially unstable at the $\frac{1}{2}$-subharmonic of the carrier frequency, then this instability will occur at a fixed value of the loop gain. This critical loop gain can be experimentally determined either by gradually increasing the gain of a stable system and noting the value of the gain when oscillations start, or else by gradually decreasing the gain of the unstable system and noting the gain value when the oscillations cease. In either case, the values of the critical loop gain thus obtained, are identical. In certain conditions, a PWM feedback system can be unstable at either $\frac{1}{3}$-, $\frac{1}{4}$- or even $\frac{1}{5}$-subharmonic of the carrier frequency. Figures 3b, 3c and 3d show the input and output waveforms of the modulator when the system is unstable at $\frac{1}{3}$-, $\frac{1}{4}$- and $\frac{1}{5}$-subharmonic frequencies respectively. However, in contrast to the case of $\frac{1}{2}$-subharmonic instability, systems which are potentially unstable at these lower subharmonic frequencies exhibit a certain degree of backlash during the experimental measurement of the critical loop gain. This is graphically shown in figure 4, where K_1 and K_2 are the lower and

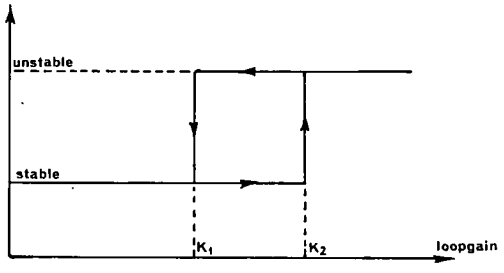

Figure 4.—Illustrating the backlash in critical loopgain measurement.

higher critical loop gain values respectively. If the loop gain lies somewhere between K_1 and K_2, then instability could be produced by causing a disturbance within the loop. This can be achieved by applying a step input to the system which then will cause the system to oscillate at the appropriate subharmonic frequency.

5. Describing Function for the Modulator

As instability in PWM systems occur at a subharmonic of the carrier frequency, the describing function of the modulator must be calculated at these subharmonic frequencies. There are two obvious methods for obtaining a solution for these describing functions. The first method relies on the generalised expression for the output frequency spectrum of the modulator. Although such a spectrum has been derived however, it is very difficult to determine the effects of signal saturation quantitatively. Signal saturation refers to the case when the amplitude of the modulator input signal exceeds the sawtooth reference signal over one or more periods of the carrier frequency. Most PWM systems are not safeguarded against this type of operation and therefore it is desirable to have describing functions which include the effects of signal saturation as well.

The second method is the direct method of obtaining the fundamental Fourier Component of the output waveform. Apart from the fact that this method lends itself to easy programming on the digital computer, signal saturation can be included in the general program.

An Elliot 503 computer was used to derive the describing functions for a pulse width modulator, in which the reference signal was a sawtooth waveform with leading edges as shown in figure 1b. On this program, the input at the modulator is the $(1/n)^{th}$ subharmonic sinewave :

$$v_i(t) = E_i \sin\left(\frac{\omega_c t}{n} + \alpha\right)$$

for n = 2, 3, 4 and 5

where ω_c is the carrier (sawtooth signal) frequency

$1/n$ is the order of the subharmonic frequency

α is the relative phase of the input signal with respect to the sawtooth reference waveform

Referring to figure 1b, normalisation is achieved by making $E_r = E_0$ so that the d.c. gain of the modulator is unity. For a given value of n, the value of E_i is fixed and α is varied from 0 to 2π radians while the intersections of the input signal and the sawtooth reference waveform is noted. The fundamental Fourier component is then calculated and the describing function computed which is a single curve with α as the variable, while k is a constant where

$$k = E_i/E_r$$

This process was repeated for different values of k so that the $(1/n)^{th}$ order describing function consists of a family of curves with k as the parameter. As required in section 3, the negative inverse describing functions were then plotted as shown in figures 5, 6, 7 and 8 for n equals 2, 3, 4 and 5 respectively.

6. Stability Analysis

As outlined in section 3, for any given PWM feedback system, the linear part of the loop transfer function should be combined and plotted as the Nyquist plot in the polar diagram. In doing so, the d.c. gain of the modulator must be included in the linear transfer function as all the describing functions derived are normalised to have unity gain. The describing functions computed apply only for the subharmonic frequencies. Therefore the negative inverse describing function should be compared with the point on the Nyquist plot corresponding to the subharmonic frequency of interest. If the corresponding Nyquist plot lies outside the negative inverse describing functions, the system is absolutely stable.

When comparing the negative inverse describing functions of figures 5, 6, 7 and 8, it is noticed that for the $\frac{1}{3}$, $\frac{1}{4}$ and $\frac{1}{5}$-subharmonic frequencies, the curve of the negative inverse describing function corresponding to $k \to 0$ are encircled by curves corresponding to larger values of k. Therefore it is always possible to construct a Nyquist plot which will intersect the curve corresponding to $k = 1$, but which will still lie outside the curve corresponding to $k \to 0$. It can therefore be deduced that such a system can be unstable for $k = 1$ and yet be stable for a smaller value of k. As k is a measure of the amplitude of the modulator input, this implies that

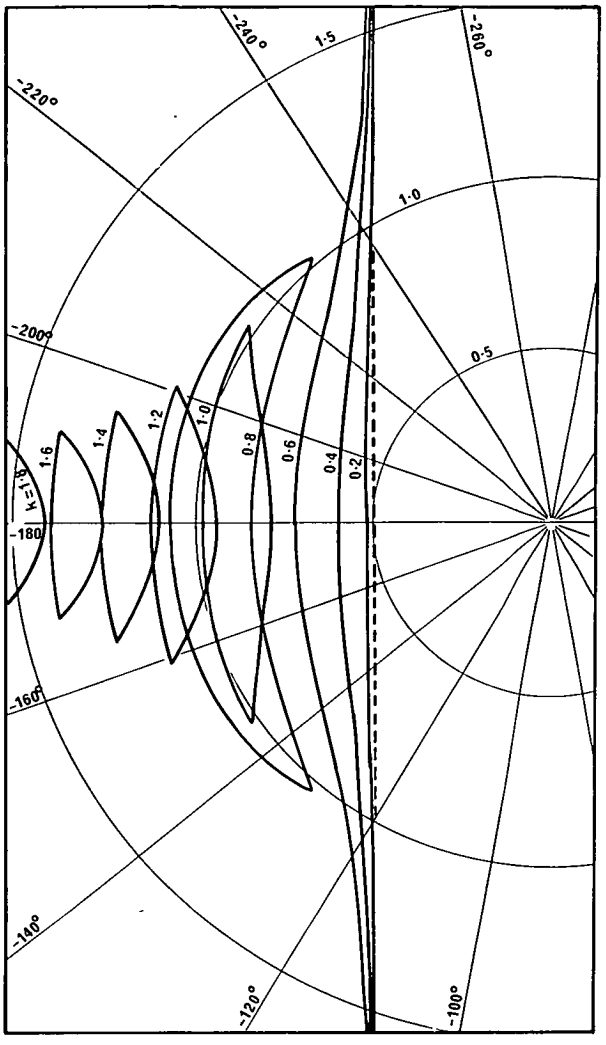

Figure 5.—Negative inverse describing function for 1/2 subharmonic frequency.

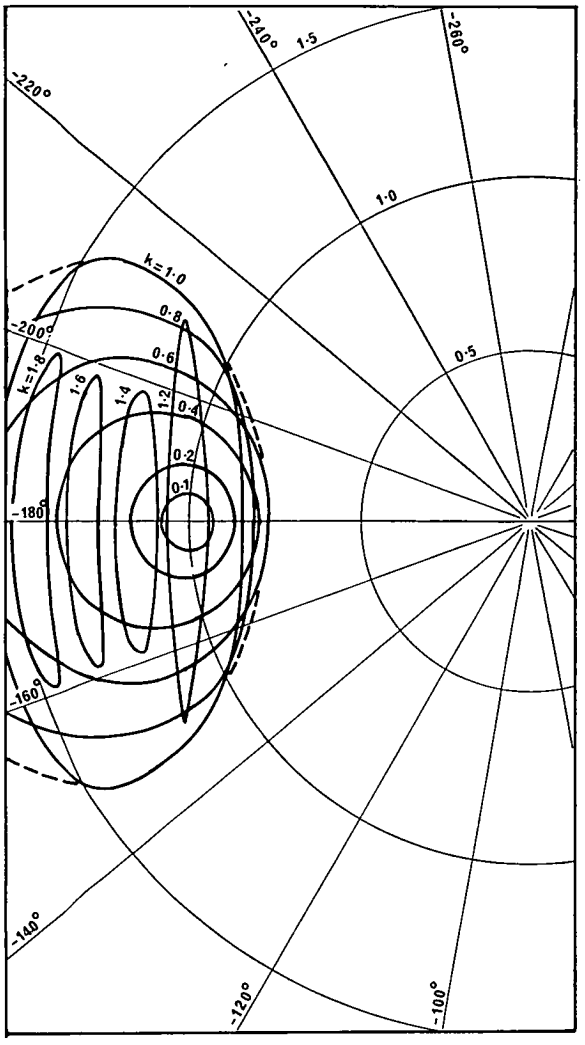

Figure 6.—Negative inverse describing function for 1/3 subharmonic frequency.

although the system is stable with no input, it is potentially unstable and merely requires a disturbance large enough to initiate subharmonic oscillations. This condition does not exist in the $\frac{1}{2}$-subharmonic frequency negative inverse describing function (figure 5), where it is clearly seen that any Nyquist plot must always intersect the curve corresponding to k = 0 first. This clearly explains the backlash phenomena which is described in section 4.

To enable good practical design of PWM feedback systems, it is sufficient to use the envelope of the negative inverse describing functions as shown dotted in figures 5, 6, 7 and 8. The absolute stability of the system can then be ascertained by comparing these envelopes with the corresponding subharmonic frequencies in the Nyquist plot.

7. Experimental Results

A large number of systems were simulated on the analogue computer, with the object of obtaining as broad a knowledge as possible into the behaviour of different systems under different conditions. In all cases without exception, the describing function method not only succeeds in detecting subharmonic instability, but it also predicts the order of subharmonic oscillations that the system will sustain.

For brevity, the results of four investigations will be reported here, as tabulated in table 1.

Table 1
Carrier Frequency = 800 Hz

Linear Transfer Function Including Modulator d.c. Gain	Nyquist Plot in Figure 9	Type of Instability
$\frac{70}{(0.003s+1)(0.004s+1)}$	curve A	$\frac{1}{2}$ subharmonic
$\frac{3260}{s(0.001s+1)(0.00015s+1)}$	curve B	$\frac{1}{3}$ subharmonic
$\frac{7}{(0.001s+1)^2(0.002s+1)}$	curve C	$\frac{1}{4}$ subharmonic
$\frac{9}{(0.001s+1)(0.003s+1)(0.0015s+1)}$	curve D	$\frac{1}{5}$ subharmonic

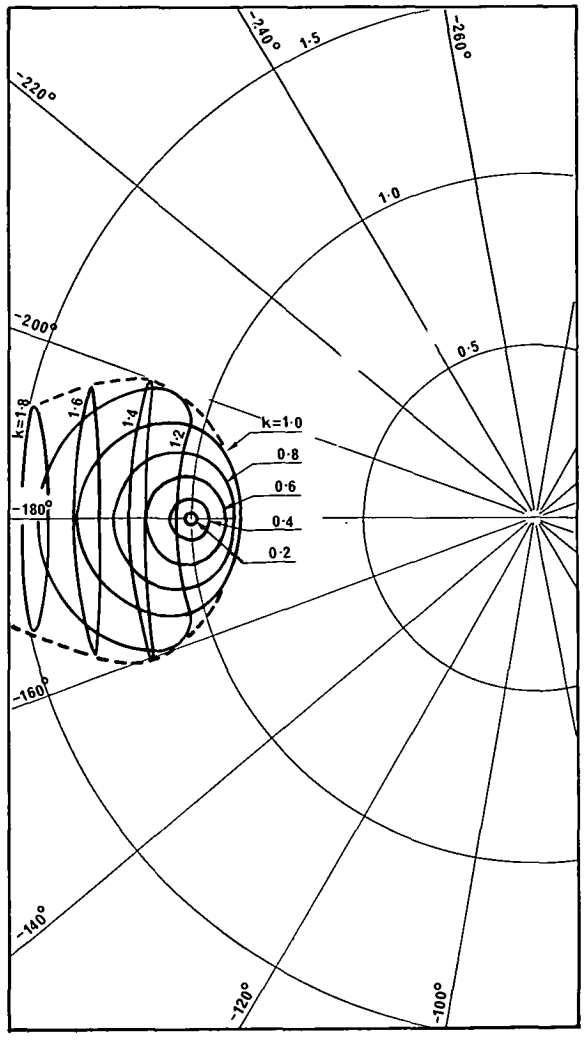

Figure 7.—Negative inverse describing function for 1/4 subharmonic frequency.

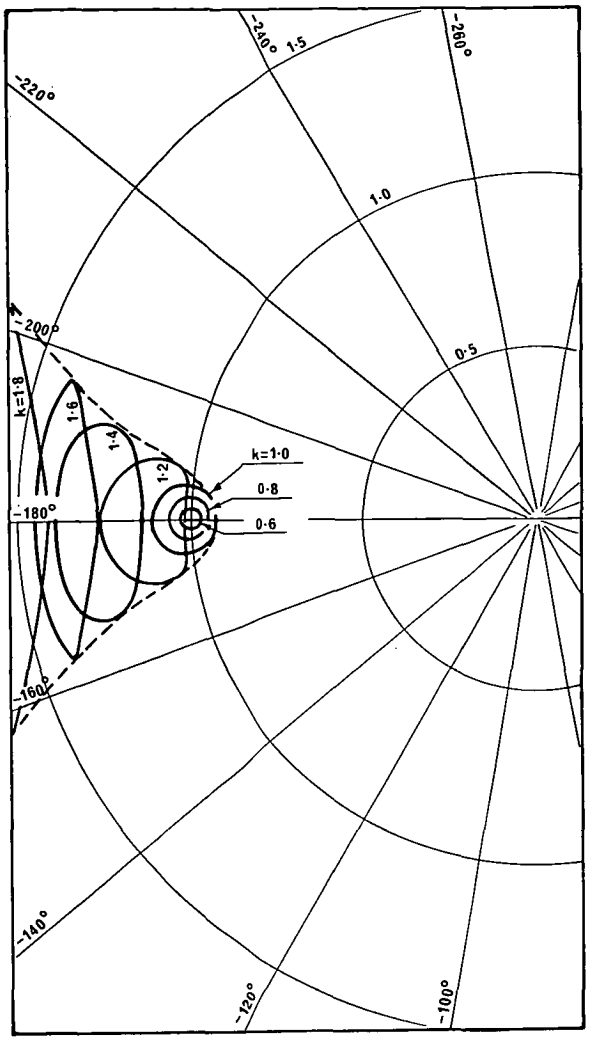

Figure 8.—Negative inverse describing function for 1/5 subharmonic frequency.

The describing function method can also be used as a graphical procedure in the design of effective series compensation network to give the PWM feedback system the necessary degree of stability. Just like the phase- and gain-margins are used as a measure of degree of stability in linear systems, in the analysis of PWM feedback systems the separations of the negative inverse describing function envelopes from the corresponding points on the Nyquist plot provide a measure of the degree of stability achieved.

The unstable system corresponding to curve B in figure 9 can be compensated by means of a series lag network as tabulated in table II.

Table II

Carrier Frequency = 800 Hz

Linear Transfer Function	Series Compensation	Nyquist Plot in Figure 10
$\frac{3260}{s(0.001s+1)(0.00015s+1)}$	uncompensated	curve A $\frac{1}{5}$ subharmonic instability
$\frac{3260}{s(0.001s+1)(0.00015s+1)}$	$\frac{0.005s+1}{0.01s+1}$	curve B (Stable system)

8. Accuracy

The describing function methods are based on the following two assumptions :—

(i) The fundamental component is the dominant output component of the nonlinear device.

(ii) The linear part of the system acts as an efficient low pass filter.

As these two conditions are generally not fully satisfied, the describing function method cannot be expected to yield a high degree of accuracy in system analysis.

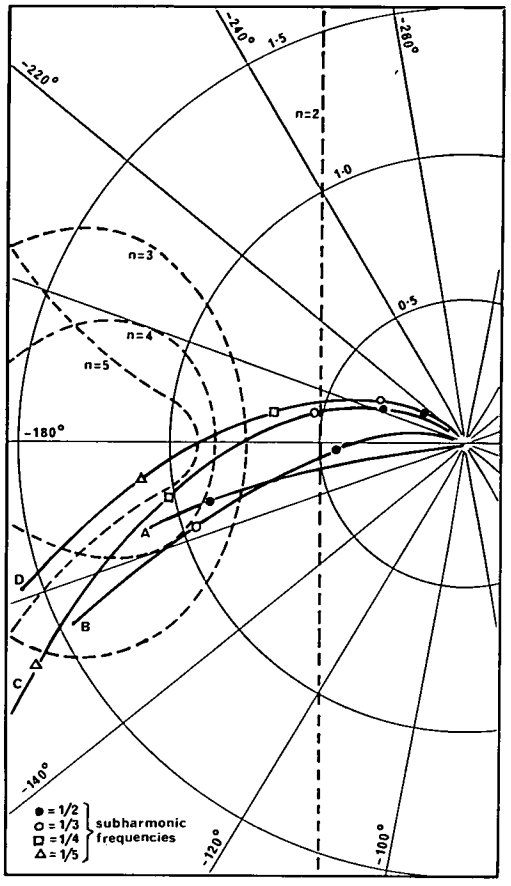

Figure 9.—Nyquist diagrams for unstable systems.

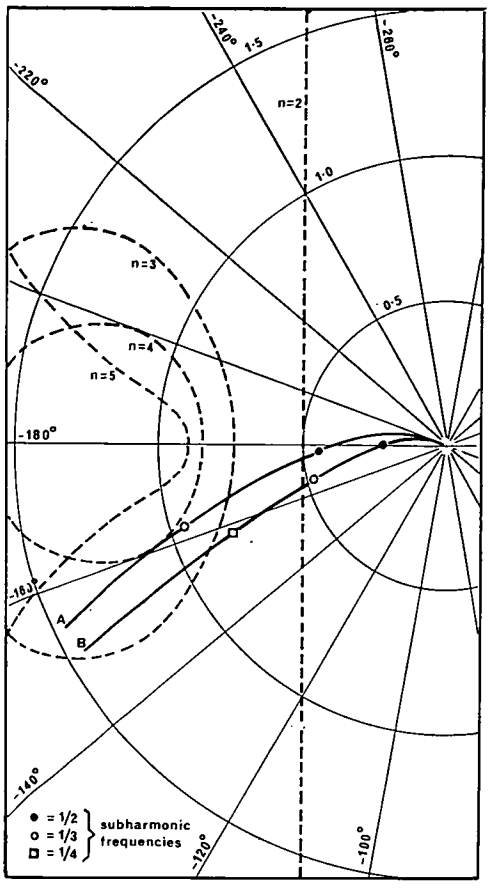

Figure 10.—Nyquist diagrams for uncompensated and compensated systems.

The results of experimental simulations indicate that in the case of $\frac{1}{3}$-, $\frac{1}{4}$- and $\frac{1}{5}$-subharmonic instability, the calculated value for the critical gain is to within 15 per cent of the actual measured value. In the case of $\frac{1}{2}$-subharmonic oscillations however, accurate error analysis is difficult to perform, because the onset of instability is very gradual. It can be seen from figure 3a that there is a high percentage of harmonic content in the $\frac{1}{2}$-subharmonic oscillations and therefore $\frac{1}{2}$-subharmonic instability analysis would not be very accurate. It appears, however, that from the results obtained, accuracy of better than 30% can be achieved.

In all cases of subharmonic instability analysis, the critical gain values obtained using the describing function method are always lower than the measured values. Therefore synthesis using the describing function method will always result in a conservative and safe design.

9. Conclusions

The problems of subharmonic instability in PWM feedback systems have been discussed. In particular, the basic difference between instability at the $\frac{1}{2}$-subharmonic frequency and instability at the other lower subharmonic frequencies is stressed. The describing functions for the modulator as computed, have been analysed and the results clearly give a qualitative explanation as to the manner in which subharmonic oscillations are generated.

As an analytical tool, the describing function method not only predicts system instability, but it also succeeds in determining the order of subharmonic oscillations.

As a graphical design procedure, the describing function always yields an absolute stable system. Furthermore, the method can be extended to give the system the necessary stability margins by series compensation.

Acknowledgment

The authors wish to acknowledge the Department of Electrical Engineering, University of Tasmania, for providing the facilities for carrying out these investigations.